INFORMATION TO USERS

This manuscript has been reproduced from the microfilm master. UMI films the text directly from the original or copy submitted. Thus, some thesis and dissertation copies are in typewriter face, while others may be from any type of computer printer.

The quality of this reproduction is dependent upon the quality of the copy submitted. Broken or indistinct print, colored or poor quality illustrations and photographs, print bleedthrough, substandard margins, and improper alignment can adversely affect reproduction.

In the unlikely event that the author did not send UMI a complete manuscript and there are missing pages, these will be noted. Also, if unauthorized copyright material had to be removed, a note will indicate the deletion.

Oversize materials (e.g., maps, drawings, charts) are reproduced by sectioning the original, beginning at the upper left-hand corner and continuing from left to right in equal sections with small overlaps.

Photographs included in the original manuscript have been reproduced xerographically in this copy. Higher quality 6" x 9" black and white photographic prints are available for any photographs or illustrations appearing in this copy for an additional charge. Contact UMI directly to order.

Bell & Howell Information and Learning
300 North Zeeb Road, Ann Arbor, MI 48106-1346 USA
800-521-0600

NOTE TO USERS

This reproduction is the best copy available.

UMI®

THE FLORIDA STATE UNIVERSITY

COLLEGE OF ARTS AND SCIENCES

MESOSCALE VARIABILITY ALONG THE SOUTHWEST COAST OF MEXICO INDUCED BY OCEANIC AND ATMOSPHERIC REMOTE FORCINGS

By

LUIS-FERNANDO ZAMUDIO-LOPEZ

A Dissertation submitted to the
Department of Oceanography
in partial fulfillment of the
requirements for the degree of
Doctor of Philosophy

Degree Awarded:
Spring Semester, 2001

UMI Number: 3005636

UMI Microform 3005636
Copyright 2001 by Bell & Howell Information and Learning Company.
All rights reserved. This microform edition is protected against
unauthorized copying under Title 17, United States Code.

Bell & Howell Information and Learning Company
300 North Zeeb Road
P.O. Box 1346
Ann Arbor, MI 48106-1346

The members of the Committee approve the dissertation of Luis-Fernando Zamudio-López defended on February 23, 2001.

James J. O'Brien
Professor Directing Dissertation

Eutiquio Young
Outside Committee Member

William C. Burnett
Committee Member

Doron Nof
Committee Member

Allan Clarke
Committee Member

To Lucia, Fernanda, and Gabriela

ACKNOWLEDGMENTS

I would like to thank the committee members, Dr. Eutiquio Young, Dr. William Burnett, Dr. Doron Nof, Dr. Allan Clarke, and Dr. James O'Brien for their time and helpful comments regarding the contents of this study. Special thanks to my major professor, Dr. James O'Brien, for his patience, for his support, for allowing me to work at COAPS, and especially for encouraging me to do independent research.

The numerical simulations discussed in this study were conducted at the Naval Research Laboratory, at the Stennis Space Center, by Drs. Harley Hurlburt and Joe Metzger. My knowledge about NLOM, satellite altimetry observations, and NSCAT winds has been benefited from insightful conversations with Alan Leonardi, Bulusu Subrahmanyam, and Mark Bourassa, respectively.

I would like to express my gratitude to my fellows at FSU (Charles Tilburg, Steven Morey, Jorge Zavala, Kenichi Mizoguchi, Francisco Sandoval, Ryan Sharp, and Rodrigo Nuñez) and at Ensenada (Rubén Castro, Rafael Walls, Toño Martinez, Gaby Montaño, and Manuel López) for their academic and non-academic support during the Ph.D. adventure.

I thank my parents, Hortencia and José Luis, and my sisters and brother for their support and faith in me. This study would not be possible without the encouragement and Love of my three beautiful Ladies: my daughters (Lucia, and Fernanda) and my wife (Gabriela).

During the first part of my studies I received a Fulbright-García Robles scholarship that was obtained through the Autonomous University of Baja California and the U.S.-Mexico Commission for Educational and Cultural Exchange and was administered by LASPAU. During the second part I received a scholarship/loan from CONACYT, Mexico.

TABLE OF CONTENTS

List of Figures.....vii

Abstract.....xii

1. Introduction.....1

2. Model and Data.....8

2.1 The Numerical Model.....8
2.1.1 Model Large-Scale Circulation.....11
2.2 The Data.....15

3. ENSO and Eddies on the Southwest Coast of Mexico.....18

3.1 Abstract.....18

3.2 Introduction.....18

3.3 Results.....21

3.3.1 Jet and eddies generation.....21
3.3.2 The CZ and the Gulf of Alaska Eddies.....30
3.4 Discussion.....38

3.5 Summary and Conclusions.....42

4. Tropical Waves Induce Ocean Eddies at Cabo Corrientes, Mexico.....43

4.1 Abstract.....43

4.2 Introduction.....43

4.3 Numerical Experiments.....48

4.4 Model results.....48

4.5 Discussion.....50

4.5.1 Comparison of the different numerical simulations.....50
4.5.2 Eddies' formation.....51
4.5.3 Observed and modeled eddies.....53
4.6 Summary and Conclusions.....54

5. On the Interannual Variability of the Tehuantepec Eddies.....58

5.1 Abstract.....58

5.2 Introduction.....58

5.3 Satellite observations.....63

5.4 The life cycle.....64

5.5 The strengthening and the weakening of the twin eddies.....66

5.6 The interannual variability.....68

5.7 The eddy train and the eddy kinetic energy.....74

5.8 Summary and Conclusions.....78

6. Summary and Concluding Remarks.....79

Appendix A. Model Parameters and Notation.....82

References.....86

Biographical Sketch.....93

LIST OF FIGURES

Figure 1. Latitude-time section of sea surface height anomaly (in centimeters) measured by TOPEX/Poseidon (T/P) along the 200 meters isobath along the North America West Coast. The latitudes of the T/P observations are indicated by the open circles. Note how the 1997-1998 El Niño event shows up as a coherent signal from the equator to the high latitudes, and how the signal starts to decay at the latitudes of the Baja California Peninsula (23° to 32° N).....**2**

Figure 2. Continental shelf bottom topography (color contours in meters) for the southwest coast of Mexico and part of the Gulf of Mexico. Note the narrow shelf from the west of the Gulf of Tehuantepec to Cabo Corrientes and how the María Islands work as an extension of the continental shelf. The position of Cabo San Lucas (CSL) at the tip of the Baja California Peninsula is indicated. The black continuous line represents the coastline.....**4**

Figure 3. Elevation contours in meters (dashed lines) for Central America and Mexico and sea level pressure in millibars (continuous lines) for November 13, 1996. After Bourassa et al., [1999].....**6**

Figure 4. Bottom topography (color contours in meters) used by NLOM. Depths shallower than 200 meters are indicated with white color. The arrows represent the NASA scatterometer (NSCAT) wind field on December 17, 1996. The length of each arrow is proportional to the wind speed. Note the offshore winds off the Gulf of Tehuantepec (GT) and the weak upwelling favorable winds along the coast just west of the Gulf.....**12**

Figure 5. NLOM upper layer currents for the time period indicated in the three different panels. The means were calculated from an 11-year climatology.....**13**

Figure 6. Principal seasonal circulation patterns of wind driven surface currents in the Eastern Tropical Pacific. After Badan-Dangon et al., [1989].....**14**

Figure 7. TOPEX/Poseidon ground tracks over the area of study. The positions of the Gulf of Tehuantepec (GT) and Cabo San Lucas (CSL) at the tip of the Baja California Peninsula are indicated.....**16**

Figure 8. Mean layer 1 thickness (color contours in meters) and mean currents (vectors) from NLOM for (a) March and (b) June. The contour interval is 5 meters and the vectors represent the currents at the arrowhead. The monthly means were calculated from an 11-year climatology. The solid black line represents the real coastline. The Gulf of Tehuantepec's location is indicated by GT **20**

Figure 9. The Japanese Meteorological Agency (JMA) index defines El Niño (La Niña) events based on sea surface temperature anomalies in the region 4°N–4°S and 150°–90°W. An El Niño (La Niña) event is observed when the 5-month running average of SST anomalies is greater (lower) than 0.5°C for at least 6 consecutive months. Furthermore, the series of 6 consecutive months must begin before September and must include October, November, and December. Years in black correspond to neutral events, in blue to La Niña events, and in red to El Niño events. Courtesy of J. Whalley, COAPS/FSU.....**22**

Figure 10. Magnitude of the vectorial velocity difference of NLOM layer 1 minus layer 2 (color contours in cm/s) and corresponding arrow vectors. The four different panels indicate: (a) The establishment of the strong, narrow and elongated jet, (b) the oscillating state, (c) the breaking of the jet, and (d) the CZ eddy formation. In addition, eddy activity in Cabo Corrientes and the Gulf of Tehuentepec (GT) is recognized, and is studied in sections 4 and 5 respectively.....**24**

Figure 11. Interannual mesoscale variability. NLOM upper layer thickness (color contours in meters) is displayed when mesoscale features are most evident.....**25**

Figure 12. Latitude-time section of sea surface height anomaly (in centimeters) measured by TOPEX/Poseidon (T/P) along the 200 meter isobath along the west coast of Mexico. The latitudes of the T/P observations are indicated by the open circles.....**29**

Figure 13. Sea surface height anomaly (color contours in centimeters) in November 1997 as determined from TOPEX/ERS 2 satellite altimeters. The reference level in this figure is a multiyear average. The position of the CZ anticyclonic eddy (CZE) is indicated. In addition, this picture includes cyclonic eddies offshore of the CZ and a Gulf of Tehuantepec (GT) anticyclonic eddy, which are due to different generation mechanisms. This map was obtained from the Colorado Center for Astrodynamics Res. publicly accessible web site (http://www-ccar.colorado.edu/~realtime/global-historical_ssh).....**31**

Figure 14. NLOM climatological mean currents (in m/s). The mean was calculated from an 11-year climatology. Note that only part of the southwest coast of Mexico and the Gulf of Alaska are characterized by coastally attached poleward-flowing currents.....**32**

Figure 15. NLOM monthly mean eddy kinetic energy (in log (m^2/s^2)) for: (a) August 1982, (b) September 1982, (c) October 1982, (d) November 1982, (e) December 1982, (f) January 1983, (g) February 1983, and (h) March 1983.....**34**

Figure 16. Baroclinic instability growth rate diagrams for the southwest coast of Mexico. (a) Only under the influence of the Costa Rica Coastal Current (CRCC). (b) Under the influence of the CRCC and the Coastal downwelling Kelvin waves associated with the 1982-83 El Niño event. The black vertical line indicates the location of wavelengths of approximately 350 km.....**40**

Figure 17. Sea surface height anomaly (color contours in centimeters) for four different dates in 1993 as determined from TOPEX/ERS-2 satellite altimeters. The most striking feature in the four different panels is the presence of the Cabo Corrientes eddy. These maps were designed to retain mesoscale sea surface height associated with fronts and eddies. They were obtained from the Colorado Center for Astrodynamics Research publicly accessible web site (http://www-ccar.colorado.edu/~realtime/global-historical_ssh).....**45**

Figure 18. Mean layer 1 thickness (color contours in meters) and mean currents (vectors) from NLOM. The contour interval is 2 meters and the vectors represent the currents at the arrowhead. The means were calculated from an 11-year climatology. The solid black line represents the real coastline. Note that the orientation of Cabo Corrientes and the María Islands forces the CRCC to separate from the coast. The layer 1 thickness is at maximum near the coast and decays northward and offshore.....**46**

Figure 19. Snapshots of layer 1 thickness (color contours in meters) from NLOM. The four different panels indicate: (a) the arriving of the coastally trapped waves to Cabo Corrientes and María Islands area, (b) the eddies formation, (c) the eddies separation from the coast, (d) and the eddies westward and southwestward drifting.....**47**

Figure 20. Latitude-depth sections of temperature (in °C) along the white line in Figure 21. (a) Climatology of the temperature for May. (b) Temperature field during May 1992. (c) Anomaly of the temperature for May 1992. From these transversal sections is not possible to conclude about a closed circulation. However, the downward bending of the isoterms in (b) (which reach a maximum depth between 20°N and 21°N) suggests the presence of an anticyclonic eddy in the area during May 1992. After Trasviña et al., [1999].....**55**

Figure 21. Snapshots of NLOM layer 1 thickness. The different panels indicate. (a) The arriving of the CTW to Cabo Corrientes and María Islands area. (b) The formation of anticyclonic eddies at the north sides of Cabo Corrientes and María Islands. (c) The two eddies have already fused and start the separation from the coast. (d)-(f) The eddy drifting westward. The white line represents the position of the hydrographic transect

where the temperature field in Figure 20 was measured on May 1992. Note that the modeled eddy crossed the white line during May 1992.....**56**

Figure 22. Conceptual portrayal of the jet stream's different positions during cold (blue), neutral (white) and warm (red) ENSO phases. After Green et al., [1997].....**60**

Figure 23. (a) Time series of European Center for Medium-Range Weather Forecasts (ECMWF) sea surface wind speed estimated at the center of the Gulf of Tehuantepec (GT). (b) Trajectory followed by an eddy generated at the GT as determined by the Topex/Poseidon (T/P) altimeter (magenta line). The yellow circles represent the position of the maximum altitude of the anticyclonic eddy shown in Figure 25. The white circle indicates the location of the minimum altitude of the cyclonic eddy shown in Figure 25a. Both eddies were generated during the wind event identified by the green shading in Figure 23a. The color contours (in 1×10^{-8} Pascals per meter) and the black arrows (in m/s) represent a 17 day average wind stress curl and wind field, respectively. Those 17 days (identified with yellow color in Figure 23a) are the period of time between the first and the second T/P measurement of the anticyclonic eddy. The red arrows represent the NLOM long term climatological mean ocean current. Black lines identify the satellite tracks along which T/P detected the Tehuantepec eddies. The position of the Gulf of Papagayo (GP) is also indicated.....**61**

Figure 24. Sea surface temperature (in °C) for the Gulf of Tehuantepec for January 22, 1996. Note the strong zonal sea surface temperature gradient in the area and the coastal cold tongue of water from 96°W to 98°W characterized by yellow-green colors. Image processed by Agustin Fernandez (UNAM, Mexico).....**62**

Figure 25. Sea surface height anomaly (in centimeters) measured by T/P along the different satellite tracks shown in Figure 22b. A southwestward migration of the anticyclonic eddy is evident in this example. The elevation and horizontal dimensions of this anticyclonic Tehuantepec eddy range from 21 to 36 cm and from 250 to 500 km, respectively. Note the presence of a cyclonic eddy in panel "a" (which is characterized by a SSH minimum of ~17 cm and a diameter of ~450 km) and how this eddy disappears in the rest of the panels.....**65**

Figure 26. TOPEX/Poseidon (T/P) sea surface height standard deviation (in meters) for the period October 1992-April 2000. Note the location of the maximum standard deviation, which lies on the trajectory of the Tehuantpec (white circles) and Papagayo (green circles) eddies. This Tehuantepec eddy is the same as the one presented in Figures 23b and 25. The Papagayo eddy was measured by T/P during 1992-1993. The period of time between two white circles is indicated in Figure 25 and the one between two green circles is 10 days.....**67**

Figure 27. TOPEX/Poseidon sea surface height (SSH) anomaly (color contours in meters) for four different periods. The arrow vectors are the 17-day average ECMWF wind stress curl of Figure 23a. Note the westward drifting of the cyclonic eddy (minimum negative SSH anomaly, which is identified with the letter "c") from panel (a) to panel (b) and how that eddy weakens (c) and disappears (d). In addition, the anticyclonic eddy (maximum positive SSH anomaly is clearly recognized in the four panels.....**69**

Figure 28. Longitude-time section of sea surface height anomaly (in meters) measured by T/P for the 10° N-15° N latitude band. The longitude of the center of the GT is indicated with a red arrow.....**70**

Figure 29. (a) TOPEX/Poseidon (T/P) sea surface height anomaly time series measured along the red portion of the T/P satellite track shown in panel (b). The red (blue) arrows indicate positive (negative) sea surface temperature anomaly in the Japanese Meteorological Agency El Niño-La Niña index (Figure 9).

Figure 30. (a)-(b) NLOM snapshots of layer 1 thickness (in meters). T/P tracks are indicated with a white line and the green circles represent the location of maximum elevation of the anticyclonic eddy shown in the (b) and (g) panels of Figure 25. (c) Magnitude of the vectorial velocity difference of layer 1 minus layer 2 (color contours in m/s). (d) Sea surface height anomaly (color contours in meters) as determined by T/P.....**75**

Figure 31. NLOM monthly mean eddy kinetic energy (in log (m^2/s^2)) for January 1993 for the shown region.....**77**

Figure 32. Conceptual portrayal including the equatorial return flow (the North Equatorial Counter Current (NECC) and the Costa Rica Coastal Current (CRCC)) and equatorially generated waves that travel eastward until the Americas west coast where they turn poleward and propagate as coastal trapped waves (CTW) passing by the southwest coast of Mexico. The positive combination of the CRCC and the currents generated by the CTW contributes to the formation of the Acapulco and Cabo Corrientes eddies (red circles), whereas, the Tehuantepec eddies (yellow circles) are generated by the strong, intermittent, and offshore blowing Gulf of Tehuantepec (GT) winds, which appear after the arrival of cold fronts at the Gulf of Mexico.....**80**

ABSTRACT

The mesoscale variability along the southwest coast of Mexico is studied using sea surface height satellite altimeter observations and the Naval Research Laboratory Layered Ocean Model. The study is divided into three parts: The formation and fate of El Niño/Southern Oscillation (ENSO) related eddies, the existence and genesis for anticyclonic eddies near Cabo Corrientes, and the life cycle of the Tehuantepec eddies.

Investigation of ENSO related eddies indicates that during strong warm ENSO events the upper ocean circulation along the southwest coast of Mexico is destabilized. The effect of ENSO appears as three distinct stages. First, a coastal jet characterized by strong vertical shear flow develops. Second, the shear flow strengthens, increasing both its horizontal dimension and the amplitude of its oscillations. Finally, the jet becomes unstable and breaks into anticyclonic eddies, which separate from the coast and drift southwestward. The genesis and strengthening of the jet is due to the simultaneous occurrence of the poleward-flowing currents along the southwest coast of Mexico and the poleward circulation associated with warm ENSO events.

Examination of the generation of anticyclonic eddies near Cabo Corrientes indicates that the arrival of downwelling coastally trapped waves at Cabo Corrientes corresponds to intensification of local currents. The interaction of these intensified currents with the coastline geometry generates anticyclonic eddies. Comparison of different numerical simulations suggests that the bottom topography and the local

wind are not responsible for the eddy generation. In contrast, the coastline geometry, most notably the cape at Cabo Corrientes, causes the formation of eddies. The existence and timing of the modeled eddies are validated with sea surface height altimeter observations and temperature hydrographic data.

Analysis of the life cycle of the anticyclonic eddies generated in the Gulf of Tehuantepec suggests that: The interannual variability of the number and strength of the Tehuantepec eddies is directly related to the El Niño-La Niña cycle. These eddies migrate ~5000 km, weakening (decreasing their maximum sea surface elevation) and disappearing when exposed to the cyclonic shear between the North Equatorial Current and the North Equatorial Counter Current. Outside of the equatorial region, the Tehuantepec eddies are the most energetic signal in the Eastern North Pacific Ocean.

1. INTRODUCTION

A peculiar characteristic of oceanography is that the locally observed processes are not always completely explained in terms of local factors. In fact, they are often elucidated in light of processes that originate far away in time and space, and have the ability of be transmitted through the ocean. Ocean waves are one of the better examples of this oceanic remote forcing.

Equatorial oceans are natural wave laboratories where waves in all frequencies and scales can be generated. Some of these equatorial waves propagate eastward until they reach the eastern boundary coast, which may be used as a new wave-guide to continue a freely coastally trapped poleward propagation. In some cases, the propagation can be of thousands of kilometers [Figure 1; Moore, 1968; Cane and Sarachik, 1977; Busalacchi and O'Brien, 1981; Clarke, 1992; Ripa, 1997]. In our particular case of the Northeastern Pacific Ocean, specifically the southwest coast of Mexico (12° N–23° N), there are several different topographic changes, coast-line variations, and ocean currents regimens that modify the characteristics of the freely poleward propagating coastally trapped waves.

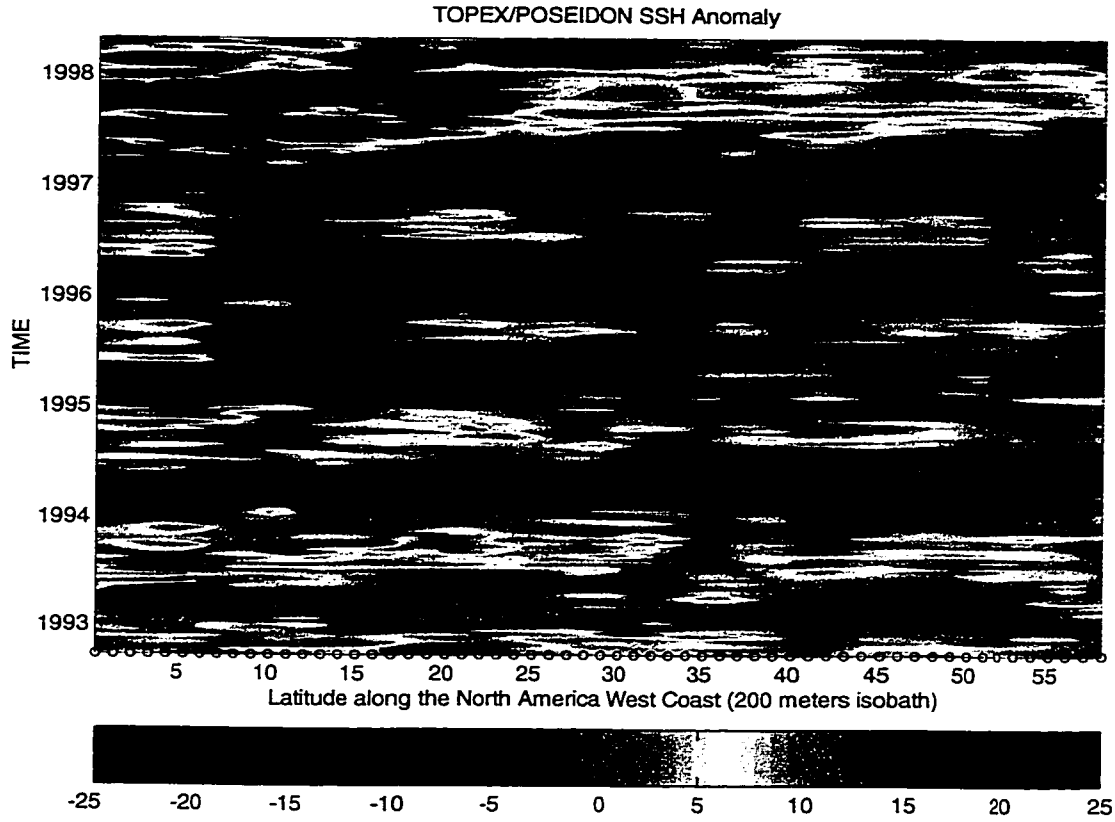

Figure 1. Latitude-time section of sea surface height anomaly (in centimeters) measured by TOPEX/Poseidon (T/P) along the 200 meters isobath along the North America West Coast. The latitudes of the T/P observations are indicated by the open circles. Note how the 1997-1998 El Niño event shows up as a coherent signal from the equator to the high latitudes, and how the signal starts to decay at the latitudes of the Baja California Peninsula (23° to 32° N).

The first obstacle (progressing northward from the equator and along the Pacific Coast) is found at the Gulf of Tehuantepec (with center close to 94.5°W–15.5°N). There, the continental shelf changes abruptly from a wide shelf to a narrow shelf (Figure 2). Thus, when the coastally trapped waves arrive to at Gulf of Tehuantepec topographic discontinuity, some of them will be transmitted through the narrow shelf and some will be reflected [Ripa and Carrasco, 1993]. Nevertheless, for low frequency waves (i.e., periods of few years) the Gulf of Tehuantepec topographic discontinuity poses no obstacle.

The next coastal area where the tropical waves can be altered is found from the northwest of the Gulf of Tehuantepec to the southeast of Cabo Corrientes (105.6°W–20.3°N) (Figure 2). In this case, the poleward-flowing local coastal currents can couple to the currents generated by the coastally trapped waves and produce a strong coastal vertical shear flow, which can destabilize and break into eddies (section 3). Continuing their northward propagation the waves interact with the topographic variation that starts close to Cabo Corrientes. There is a transition from a narrow to a wide shelf, the coastline changes its orientation from northwest to approximately eastward, and the Maria Islands Archipelago works as an extension of the continental shelf (Figure 2). The arrival of downwelling coastally trapped waves at Cabo Corrientes corresponds to the intensification of the local currents. The interaction of these currents with the coastline geometry generates anticyclonic eddies (section 4). The effect of the next coast-line-topographic obstacle, the Gulf of California, is not included in this study. Equatorial generated waves are evidence of

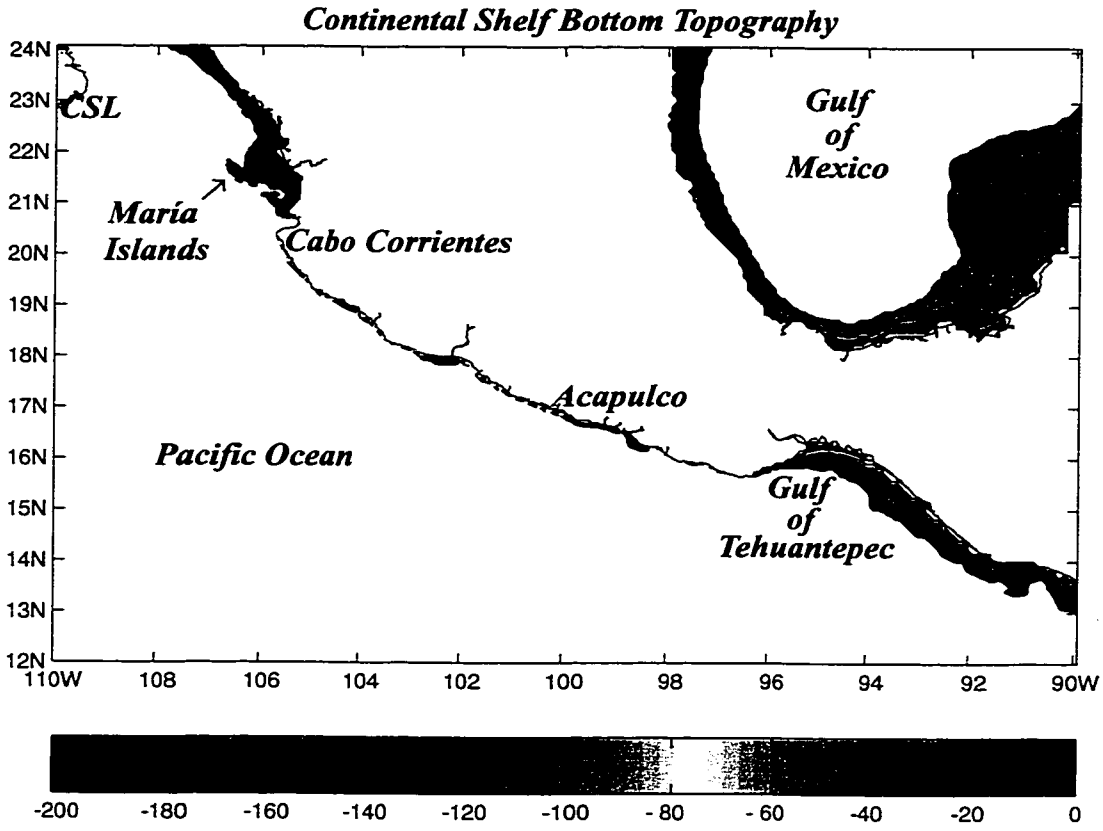

Figure 2. Continental shelf bottom topography (color contours in meters) for the southwest coast of Mexico and part of the Gulf of Mexico. Note the narrow shelf from the west of the Gulf of Tehuantepec to Cabo Corrientes and how the María Islands work as an extension of the continental shelf. The position of Cabo San Lucas (CSL) at the tip of the Baja California Peninsula is indicated. The black continuous line represents the coastline.

the existence of oceanic remote forcing that contributes to the mesoscale variability along the southwest Coast of Mexico. In contrast, the Gulf of Tehuantepec strong intermittent winds are an example of atmospheric remote forcing.

The processes that generate the Gulf of Tehuantepec winds are reasonably well understood. The North American cold season is characterized by cold fronts traveling southward, and the route of these fronts is sometimes determined by continental topography. For example, when the cold fronts arrive at the Gulf of Mexico they find that the Sierra Madre Mountains are a natural barrier. These mountains do not allow cold fronts to travel freely over the Mexican mainland. However, this barrier is broken by a low-altitude, narrow mountain gap, Chivela Pass, which runs north-south from the Gulf of Mexico's Bay of Campeche to the Pacific Ocean's Gulf of Tehuantepec (Figure 3). The resultant pressure gradient drives strong winds along the mountain pass. On the south side of the pass these winds can be intense, with maximum gusts around 60 m/s [Stumpf, 1975]. These winds are locally referred as "*Nortes*" (meaning northerly), but they are frequently referred to in scientific literature as "*Tehuantepecers*" or "*Tehuanos*". They blow offshore across the Gulf of Tehuantepec coast, favoring strong nearshore oceanic mixing, intense lowering of sea surface temperatures, and the generation of anticyclonic eddies [Hurd, 1929; Roden, 1961; Stumpf, 1975; Clarke, 1988; McCreary et al., 1989; Lavin et al., 1992; Fiedler, 1994; Trasviña et al., 1995]. Satellite altimetry observations reported in this study indicate that the anticyclonic eddies generated at the Gulf of Tehuantepec can travel approximately five thousand kilometers westward (section 5).

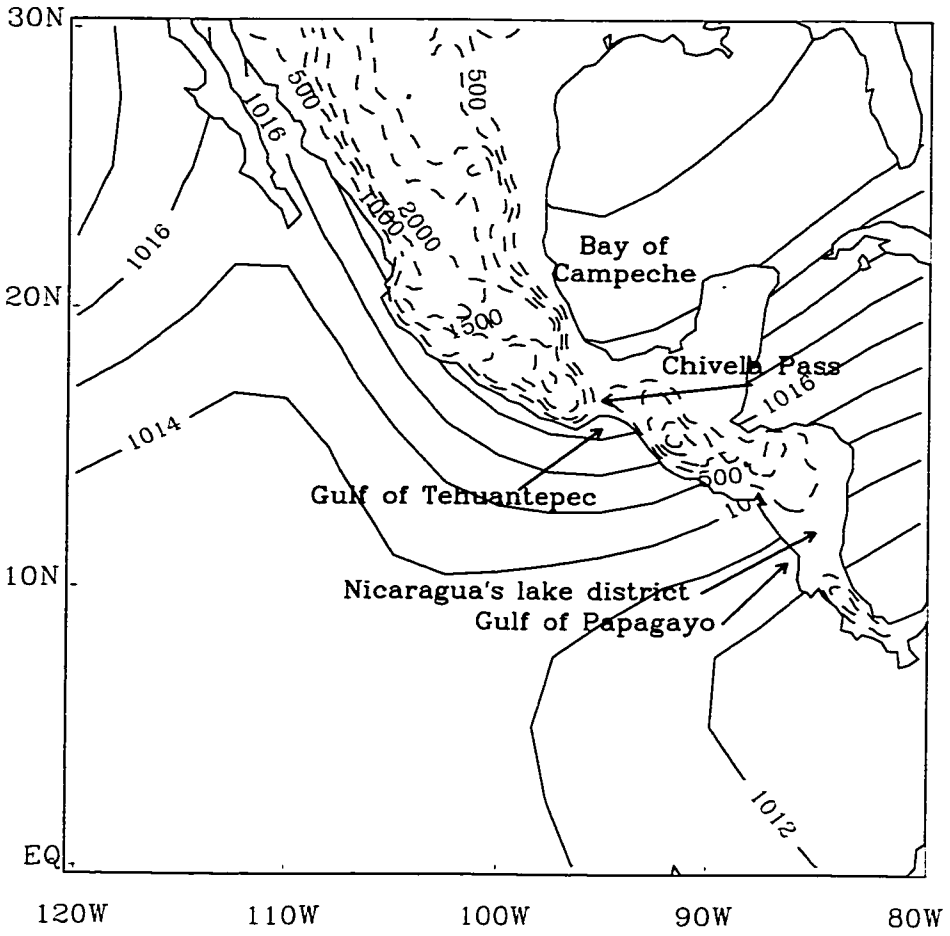

Figure 3. Elevation contours in meters (dashed lines) for Central America and Mexico and sea level pressure in millibars (continuous lines) for November 13, 1996. After Bourassa et al. [1999].

Ocean eddies can be extremely long lived marine systems that have the ability to migrate thousands of kilometers transporting water, heat and energy and playing an important role in the biota concentration and related fisheries. Thus, in addition to the physical intrigue of the problem by itself, it is interesting to study the generation and evolution of the southwest coast of Mexico eddies for fisheries and the related biological processes [Blackburn, 1962; Robles-Jarero and Lara-Lara, 1993; Färber-Lorda et al., 1994; Lukas and Santiago-Mandujano, 2001].

This work is devoted to the study of the oceanic and atmospheric remote forcing effects on the southwest coast of Mexico. The results presented in sections three and four are being reported for the first time. It is hoped that this piece of work contributes to initiate a new line of research dedicated to study the mesoscale variability off the southwest coast of Mexico.

This dissertation is organized as follows. Section 2 includes a description of the model and data utilized. In section 3 a generation hypothesis of a strong coastal jet and anticyclonic eddies is presented and validated using the results of a numerical ocean model and satellite altimetry observations. Section 4 includes observational and numerical evidence about the anticyclonic eddy generation on Cabo Corrientes. In section 5 the eddies generated in the Gulf of Tehuantepec are studied. A link between the interannual variability of the number and strength of the Tehuantepec eddies and El Niño-La Niña cycle is presented. Finally, the conclusion section draws together the results of this entire study. Sections 3, 4, and 5 are intended as stand-alone reports and thus contain their own introductions and conclusions.

2. THE MODEL AND DATA

2.1 The Numerical Model

The Navy Layered Ocean Model (NLOM) has been extensively documented by Wallcraft [1991], Hurlburt and Metzger [1998] and references therein. Here we give a brief description of the hydrodynamic version of the model used in this study. The equations solved for each of the n-layer in the model are:

$$\begin{aligned}&\frac{\partial \vec{V}_k}{\partial t}+\left(\vec{\nabla}\cdot\vec{V}_k+\vec{V}_k\cdot\vec{\nabla}\right)\vec{v}_k+\hat{k}\times f\vec{V}_k=-h_k\sum_{l=1}^{n}\left[G_{kl}\vec{\nabla}(h_l-H_l)\right]+(\vec{\tau}_{k-1}-\vec{\tau}_k)/\rho_o\\&+\max(0,-\omega_{k-1})\vec{v}_{k-1}-\left[\max(0,\omega_{k-1})+\max(0,\omega_k)\right]\vec{v}_k+\max(0,\omega_k)\vec{v}_{k+1}\\&+\max(0,-C_M\omega_{k-1})(\vec{v}_{k-1}-\vec{v}_k)+A_H\vec{\nabla}^2\vec{V}_k\end{aligned} \tag{1}$$

$$\frac{\partial h_k}{\partial t}+\vec{\nabla}\cdot\vec{V}_k=\omega_k-\omega_{k-1} \tag{2}$$

Where, $k=1.....n$ if it refers to layers, and $k=0.....n$ if it refers to interfaces between layers with $k=0$ at the surface. Details about the parameters and notation in (1) and (2) are provided in appendix A. Equations (1)-(2) are solved numerically in the Pacific Ocean model domain that extends from 20°S to 62°N and from 109.125°E to 77.2031°W. The eddy-resolving (1/16° resolution in latitude by 45/512° in longitude), non-linear model is characterized by a semi-implicit time scheme, Arakawa C grid, and a free surface. In addition, it includes six isopycnal layers, realistic bottom

topography and coastline geometry. The last two features are based on a modified version of the 1/12° ETOPO5 bottom topography [NOAA, 1986]. The ETOPO5 data set was interpolated to the model grid and twice smoothed using a 9-point smoother. The idea of smoothing is to reduce energy generation at smaller scales that are poorly resolved by the model [Leonardi et al., 1999]. The model geometry is determined by the 200 meters isobath, the minimum depth in the model, which represents the nominal shelf break. The amplitude of the topography above the maximum depth of 6500 meter was multiplied by 0.8 to confine it to the lowest layer. Layer thicknesses and densities where chosen in accordance with the Levitus' [1982] climatology. Another important characteristic of the model is isopycnal outcropping that is incorporated by entrainment from the layer below whenever a layer becomes thinner than a prescribed minimum thickness. Mass is conserved within the layers so that an accumulation of entrainment mass in one layer is balanced by an equal amount of detrained mass elsewhere in the model domain [Shriver and Hurlburt, 1997]. The model boundary conditions are kinematic and no slip.

The latitudinal extension of the model domain (20°S–62°N) has the purpose of allowing equatorially generated signals (i.e. coastally trapped Kelvin or related waves) to influence the northeast Pacific Ocean. The roles of these waves as eddy generation mechanisms are analyzed in two locations along the Mexican west coast (sections 3 and 4).

Wind stress is the only external forcing in the simulations reported here. Initial conditions were taken from an ocean state snapshot that corresponded to a 1/8° resolution previous simulation. Then, the model was spun up to statistical equilibrium

using Hellerman and Rosenstein [1983] (H/R) monthly wind stress climatology. Next, the integration already spun-up was forced by 12-hourly 1000 mbar winds from the European Center for Medium-Range Weather Forecasts (ECMWF) [ECMWF, 1994] from 1981 to 1996. Thus, interannual variability is also present in the numerical experiment. The 1981-1996 ECMWF temporal mean was replaced by the annual mean from H/R to produce a hybrid wind set (ECMWF/HR), as reported by Metzger et al. [1994]. The last authors determined that a more realistic mean state could be obtained in the ocean model by using the hybrid wind set. Consequently, the annual mean solution would still be driven primarily by the H/R data, but seasonal and interannual forcing would come from ECMWF.

Of particular importance in the study included in section 5, the eddy generation and migration (partially) depends on the accuracy of the wind used to force the model. The ECMWF/HR winds incorporate the seasonal strong intermittent Gulf of Tehuantepec winds, which permit the model to reproduce the observed eddies' generation and migration. The results reported in section 5 validate the use of the ECMWF/HR wind set to force the model to study the Gulf of Tehuantepec eddies generation and propagation. In the case of ENSO related and Cabo Corrientes eddies, their generation mechanics are explained in terms of tropically generated waves rather than local wind forcing. Consequently, precise ECMWF winds over the equatorial Pacific would generate the tropical waves that are crucial for the eddy generation mechanics discussed in sections 3 and 4.

The minimum depth in the model (200 meters) could be a questionable limitation for the application of the model on a broad continental shelf. However, that

is not the case for our area of study. For example, in the Gulf of Tehuantepec area the winds affect a region that consists mostly of deep waters [Figure 4; Trasviña, el al. 1995]. Moreover, the shelf is broad off Central America and up to the Gulf of Tehuantepec, but rather narrow off mainland Mexico [Figure 2; Badan, 1998]. In addition to this main simulation in section 4 we used several other different simulations (which are described there) to isolate the crucial elements on the Cabo Corrientes eddies generation.

2.1.1 Model Large-Scale Circulation

The large-scale circulation off Mexico's Pacific coast is mainly influenced by the North Pacific Anticyclonic Gyre and by the equatorial circulation system [Wyrtki, 1966; Badan-Dangon et al. 1989]. NLOM long term climatological seasonal mean currents (Figure 5) were generated to compare them with the observed wind-driven seasonal patterns (Figure 6). In general, the model reproduces all the major currents. From the north the California Current dominates the circulation off the Baja California Peninsula. It leaves the coast around 22°N, feeds the North Equatorial Current and usually reaches its maximum southward penetration in April. From the south the North Equatorial Counter Current feeds the Costa Rica Coastal Current, which flows poleward off mainland Mexico until around the mouth of the Gulf of California. More details about this coastal current are provided in sections 3 and 4. The model contains several different coastal circulation characteristics that are not included in the observations. Nevertheless, this is an expected result because "no direct measurements of the Costa Rica Coastal Current exist; the presence of the current is inferred mostly from the large-scale hydrography" [Badan, 1998]. In any case, this short model-data

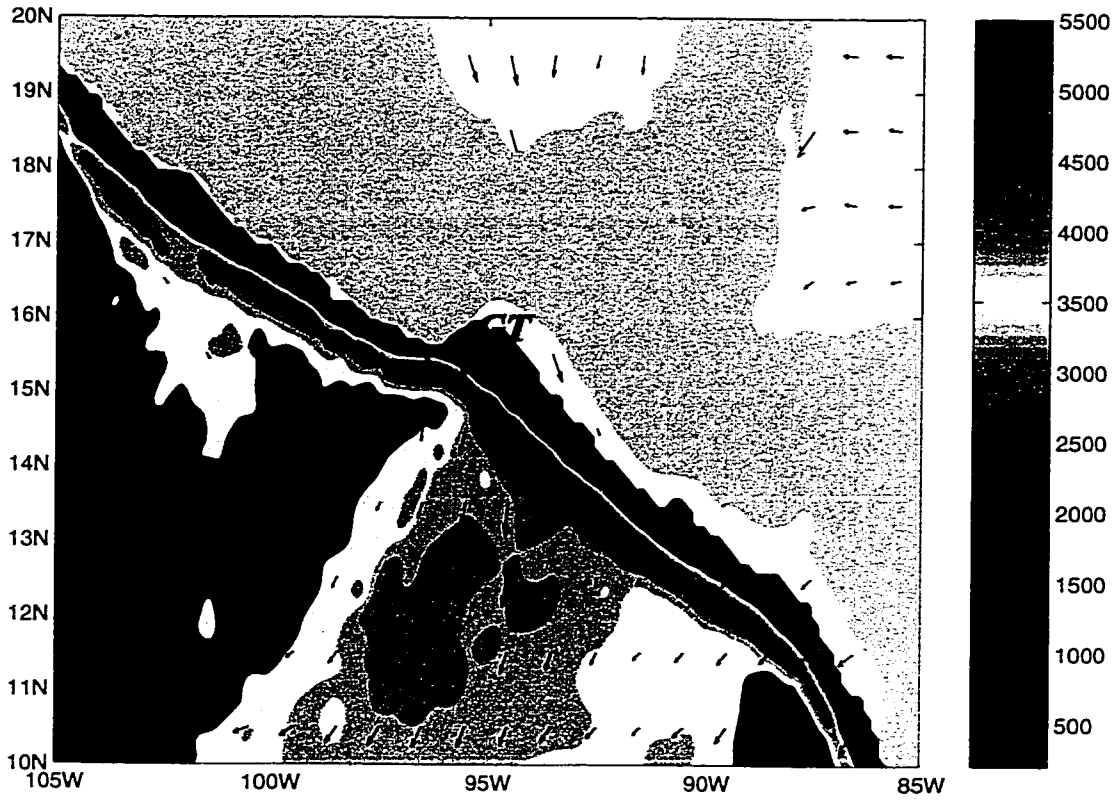

Figure 4. Bottom topography (color contours in meters) used by NLOM. Depths shallower than 200 meters are indicated with white color. The arrows represent the NASA scatterometer (NSCAT) wind field on December 17, 1996. The length of each arrow is proportional to the wind speed. Note the offshore winds off the Gulf of Tehuantepec (GT) and the weak upwelling favorable winds along the coast just west of the Gulf.

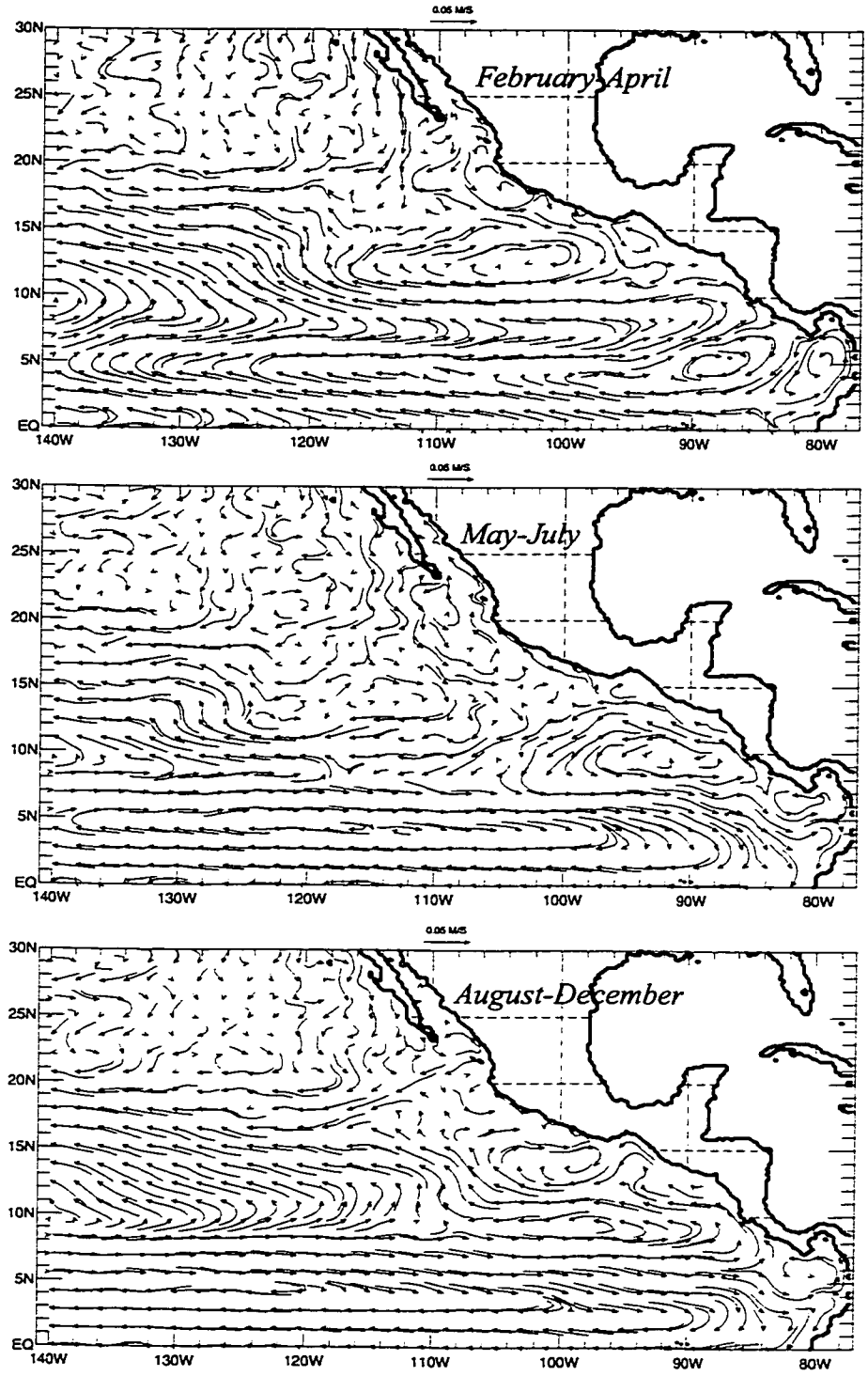

Figure 5. NLOM upper layer currents (in m/s) for the time period indicated in the three different panels. The means were calculated from an 11-year climatology.

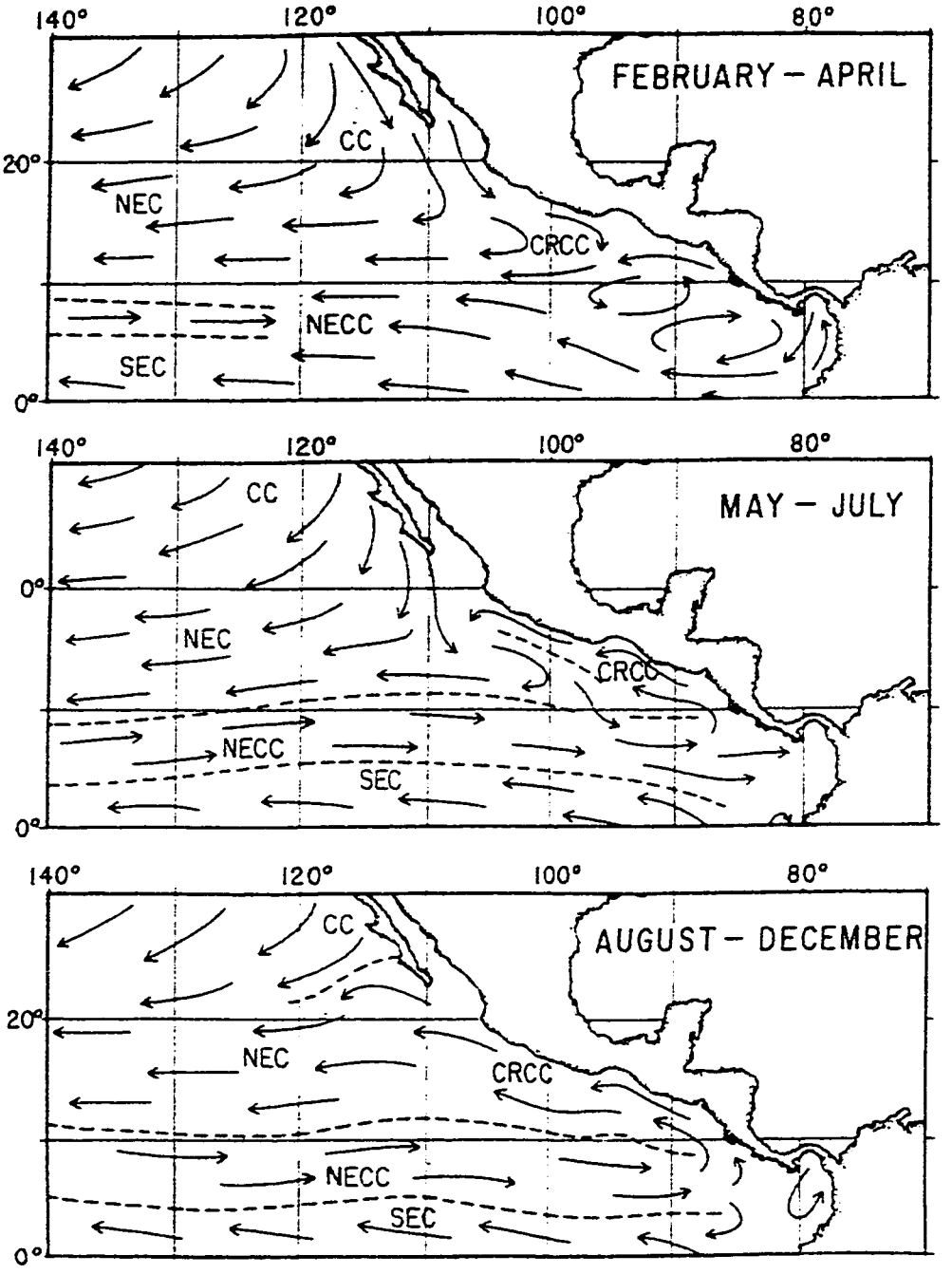

Figure 6. Principal seasonal circulation patterns of wind driven surface currents in the Eastern Tropical Pacific. After Badan-Dangon et al., [1989].

comparison ensures that the model incorporates the large-scale circulation features off Mexico's west coast. In fact, the application of NLOM to the north Pacific has been extensively validated [Hurlburt et al., 1992, 1996; Hogan et al., 1992; Donohue et al., 1994; Jacobs et al., 1994, 1996; Metzger et al., 1994; Kindle and Phoebus, 1995; Mitchum, 1995; Metzger and Hurlburt, 1996; Mitchell et al., 1996; Melsom, 1999].

2.2 The Data.

Two independent satellite altimeter sources were utilized. TOPEX/Poseidon (T/P) sea surface height (SSH) anomaly data span from October 1992 to April 2000 (T/P cycles 2-278 inclusive). The T/P altimeter measures SSH every 6.2 km along predetermined satellite tracks (Figure 7). The satellite time period to repeat an orbit (cycle) is 10 days. The distance between two continuous ascending or descending tracks is approximately 300 km in our area of study. This last characteristic usually is a major objection to track eddies using direct satellite altimeter observations. However, the diameter of the Gulf of Tehuantepec eddies (section 5) is bigger than 300 km and their lifetime is order one year. Thus, T/P along track observations can measure the dimensions and position of the Tehuantepec eddies.

In contrast, the eddies generated by the tropical waves near Acapulco and Cabo Corrientes (sections 3 and 4, respectively) are characterized by diameters of 100-200 km. Therefore, T/P wide tracks could have problems to detect those eddies. The European Remote Sensing Satellite Altimeter 2 (ERS-2) is a T/P contemporary. ERS-2 measures SSH every 6.2 km, has a track-to-track resolution of less than 60 km, and

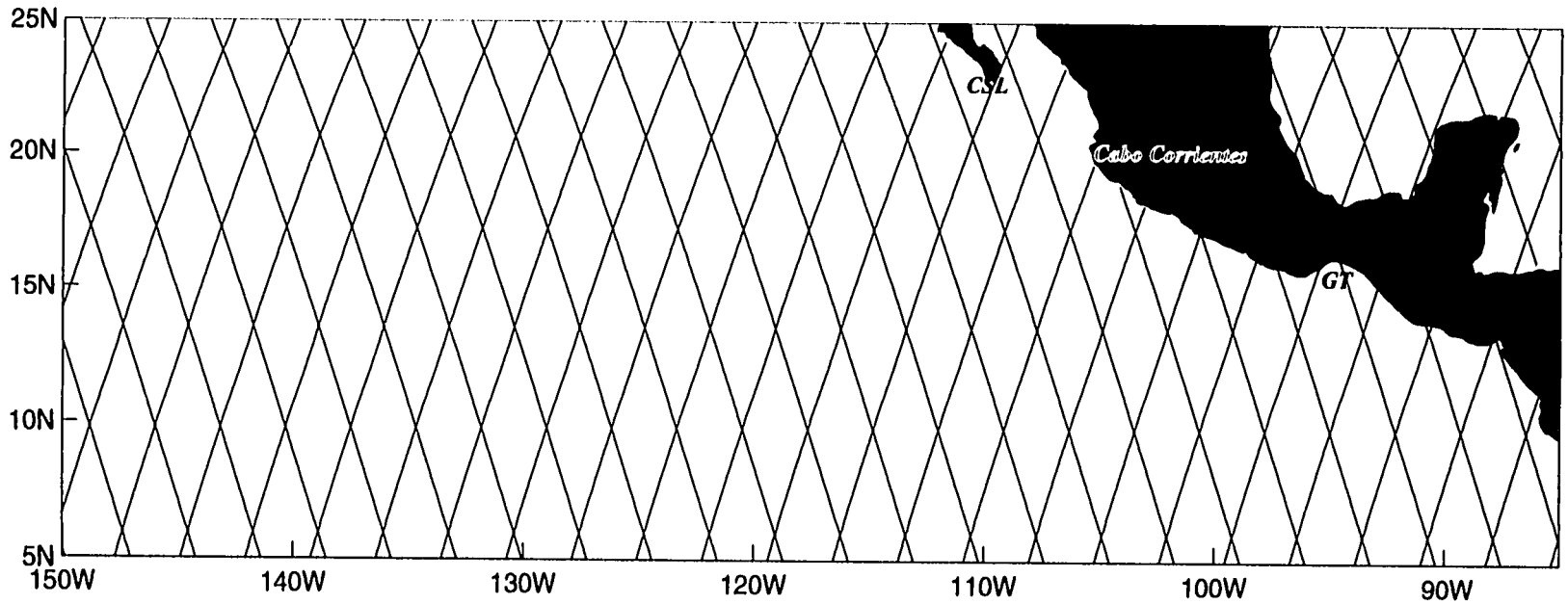

Figure 7. TOPEX/Poseidon ground tracks over the area of study. The positions of the Gulf of Tehuantepec (GT) and Cabo San Lucas (CSL) at the tip of the Baja California Peninsula are indicated.

it starts a new cycle every 35 days. Then, combining T/P and ERS-2 data sets the Colorado Center for Astrodynamics Research generated high-resolution images, which are designated to retain mesoscale SSH associated with fronts and eddies (web site http://www-ccar.colorado.edu/~realtime/global-historical_ssh). The T/P ERS-2 (T/ERS) maps provide evidence about the existence, position and altitude of the Acapulco and Cabo Corrientes eddies. Even though the eddies characteristics as reported in the SSH altimetry maps are not absolute (because the map generation implies an interpolation processes), they can be used as observational evidence to support the numerical results and the generation mechanism hypotheses presented in sections 3 and 4.

3. ENSO AND EDDIES ON THE SOUTHWEST COAST OF MEXICO

3.1 Abstract

TOPEX/Poseidon and ERS-2 (T/ERS) sea surface height altimeter observations and the Naval Research Laboratory Layered Ocean Model (NLOM) are used to study the circulation along the southwest coast of Mexico. The results of this research indicate that strong El Niño/Southern Oscillation (ENSO) warm phase Kelvin waves (KW) destabilize the upper ocean circulation. The effect of ENSO appears as three distinct stages. First, a coastal jet characterized by strong vertical shear flow develops. Second, the shear flow strengthens, increasing its horizontal dimension and the amplitude of its oscillations. Finally, the jet becomes unstable and breaks into anticyclonic eddies, which separate from the coast and drift southwestward. The genesis and strengthening of the jet is due to the simultaneous occurrence of the poleward-flowing currents along the southwest coast of Mexico and the poleward circulation associated with ENSO downwelling KW.

3.2 Introduction.

The Mexican West Coast (12°N–32°N) is subject to the influence of both mid-latitude and tropical ocean dynamics via the California Current (CC) and the Costa Rica Coastal Current (CRCC), respectively. The CC dominates the circulation off the

Baja California Peninsula (23°N–32°N) throughout the year. During its strengthening period (late winter to early spring), the CC penetrates southward to ~15°N (Figure 8a). The less documented CRCC originates from the branch of the North Equatorial Counter Current that turns northward near the western coast of the Americas. It shows up as a surface poleward flow from 5°N to 23°N from middle spring to early winter (Figure 8b), and plays an important role transporting subtropical subsurface waters to the northern latitudes [Badan et. al., 1989]. The CRCC reaches its maximum intensification and northward penetration in fall [Wyrtki, 1966].

The area located in the confluence of the two currents, from the northwest of the Gulf of Tehuantepec to Cabo Corrientes, is characterized by a poleward flow during most of the year. At the same time, the variability of the circulation on this confluence zone (CZ) is also influenced by interannual, intrasesonal (equatorially generated) and higher frequency (storm-induced) signals (e.g., coastally trapped KW) [Chelton and Davies, 1982; Christensen et al., 1983; Enfield and Allen, 1983; Spillane et al., 1987; Enfield, 1987; Ramp et al., 1997]. KW associated with ENSO warm (cold) phase are characterized by a substantial positive (negative) sea surface height (SSH) anomaly (Figure 1).

T/ERS altimeter observations and results from NLOM show that when downwelling KW arrive at the CZ, their induced circulation accelerates the already existent poleward coastal currents in the CZ producing a coastal baroclinic jet, which turns unstable and generates eddies. Similar mechanics have already been proposed to explain the presence of eddies in the Gulf of Alaska [Melsom et al., 1999].

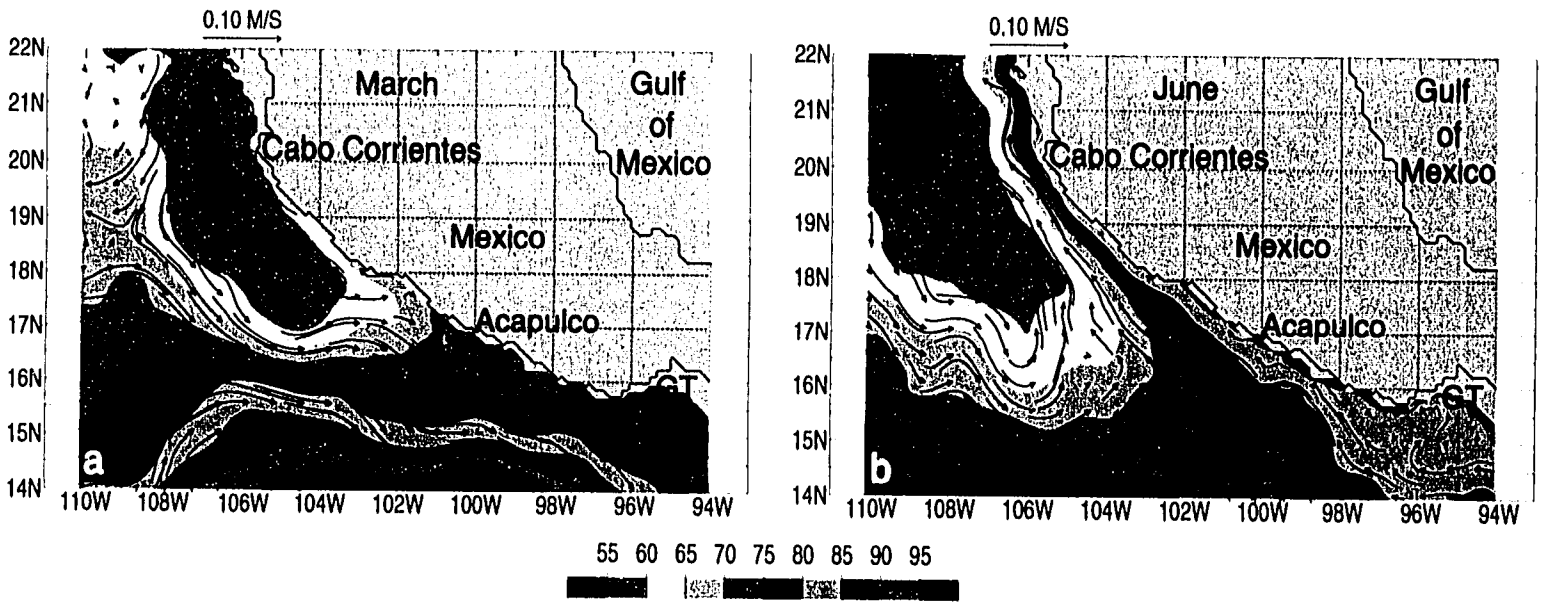

Figure 8. Mean layer 1 thickness (color contours in meters) and mean currents (vectors) from NLOM for (a) March and (b) June. The contour interval is 5 meters and the vectors represent the currents at the arrowhead. The monthly means were calculated from an 11-year climatology. The solid black line represents the real coastline. The Gulf of Tehuantepec's location is indicated by GT.

This section examines the nature and evolution of this newly recognized coastal jet and provides the evidence to support that only downwelling KW contribute to the generation of the jet. Our approach is via the analysis of 16 years of data (1981–1996) from the NLOM simulation described in section 2. The numerical results and the eddy generation hypothesis are validated with T/ERS observations.

3. 3 Results

The sixteen years (1981-1996) of the NLOM experiment allow us to compare three different scenarios: neutral years (1981, 1983-1985, 1989-1990, 1992-1996), ENSO warm phase (El Niño) years (1982, 1986-1987, 1991), and ENSO cold phase (La Niña) years (1988). ENSO phases were identified using the Japanese Meteorological Agency [1991] index (Figure 9). In subsection 3.3.1 the jet evolution and eddies generation are described. Subsection 3.3.2 includes a temporal sequence concerning with ENSO and eddies formation in the CZ and the Gulf of Alaska.

3.3.1 Jet and eddies generation

The upper ocean circulation is included in the two uppermost layers. Hence, results description and discussion (in section 3.4) are focused on the variability of layers 1 and 2. Examination of the interannual variability of the modeled layer thickness during La Niña and neutral years indicate that variations in layer 1 and 2 thickness are relatively small in the CZ. However, during strong El Niño years increases in layer 1 thickness exceed 100% and layer 2 thickness changes ~20%. The typical velocity difference magnitude between layers 1 and 2 during neutral and La Niña years is 10 cm/s, with intermittent maxima of ~25 cm/s. In contrast, during

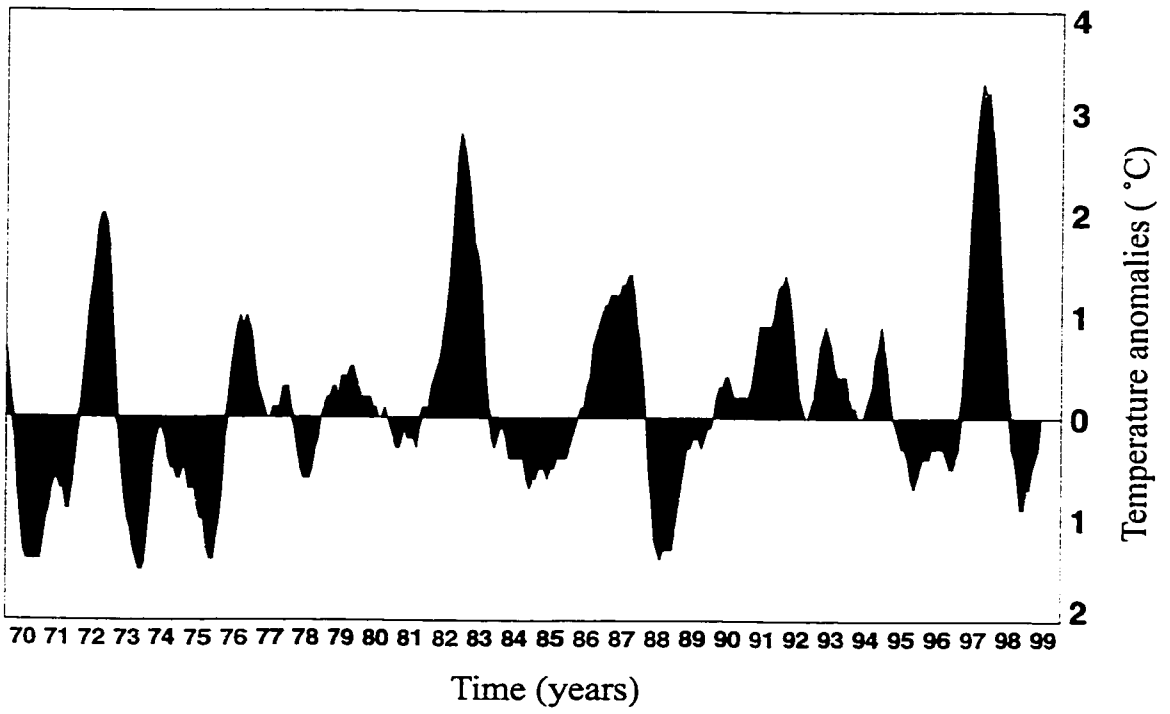

Figure 9. The Japanese Meteorological Agency (JMA) index defines El Niño (La Niña) events based on sea surface temperature anomalies in the region 4°N-4°S and 150°-90°W. An El Niño (La Niña) event is observed when the 5-month running average of SST anomalies is greater (lower) than 0.5°C for at least 6 consecutive months. Furthermore, the series of 6 consecutive months must begin before September and must include October, November, and December. Years in black correspond to neutral events, in blue to La Niña events and in red to El Niño events. Courtesy of J. Whalley, COAPS/FSU.

strong El Niño years the typical velocity difference magnitude is around 35 cm/s, with maxima exceeding 70 cm/s. This vertical shear is maintained for several months, generating a narrow and elongated jet of ~40 km in the cross-shore direction and more than 1000 km in the alongshore direction (Figure 10a). Later, the jet oscillates, at this time wave-like oscillations of ~500 km wavelength are recognized (Figure 10b); becomes unstable and breaks (Figure 10c); generating anticyclonic eddies (Figures 10d). An intrinsic characteristic of the modeled jets is that they destabilize when the wavelength of their oscillations is ~500 km (Figure 10b). The new eddies are characterized by a diameter of 110 km, a layer 1 thickness maximum of ~140 m at their core, a migration speed of ~10 cm/s, and a layer 1 swirl velocity of 65 cm/s. After four months they drift more than 1000 km to the southwest and remain characterized by a layer 1 thickness maximum of 110 m.

In general, the model results indicate that anticyclonic eddy formation in the CZ is not limited to strong El Niño years (Figure 11). However, the stronger eddies are only generated during strong El Niño years. In addition, the model includes some cyclonic eddy activity; nevertheless, the number of modeled anticyclonic eddies is much larger than the number of cyclonic ones. Also, as can be observed in Figure 11, the simulation results contain a significant amount of mesoscale variability in this region.

The T/P high-resolution characteristic enables it to measure interannual SSH variability along the Mexican west coast (Figure 12). The 1995-96 strong negative anomaly and the 1997-98 El Niño (positive anomaly) events are two of the most

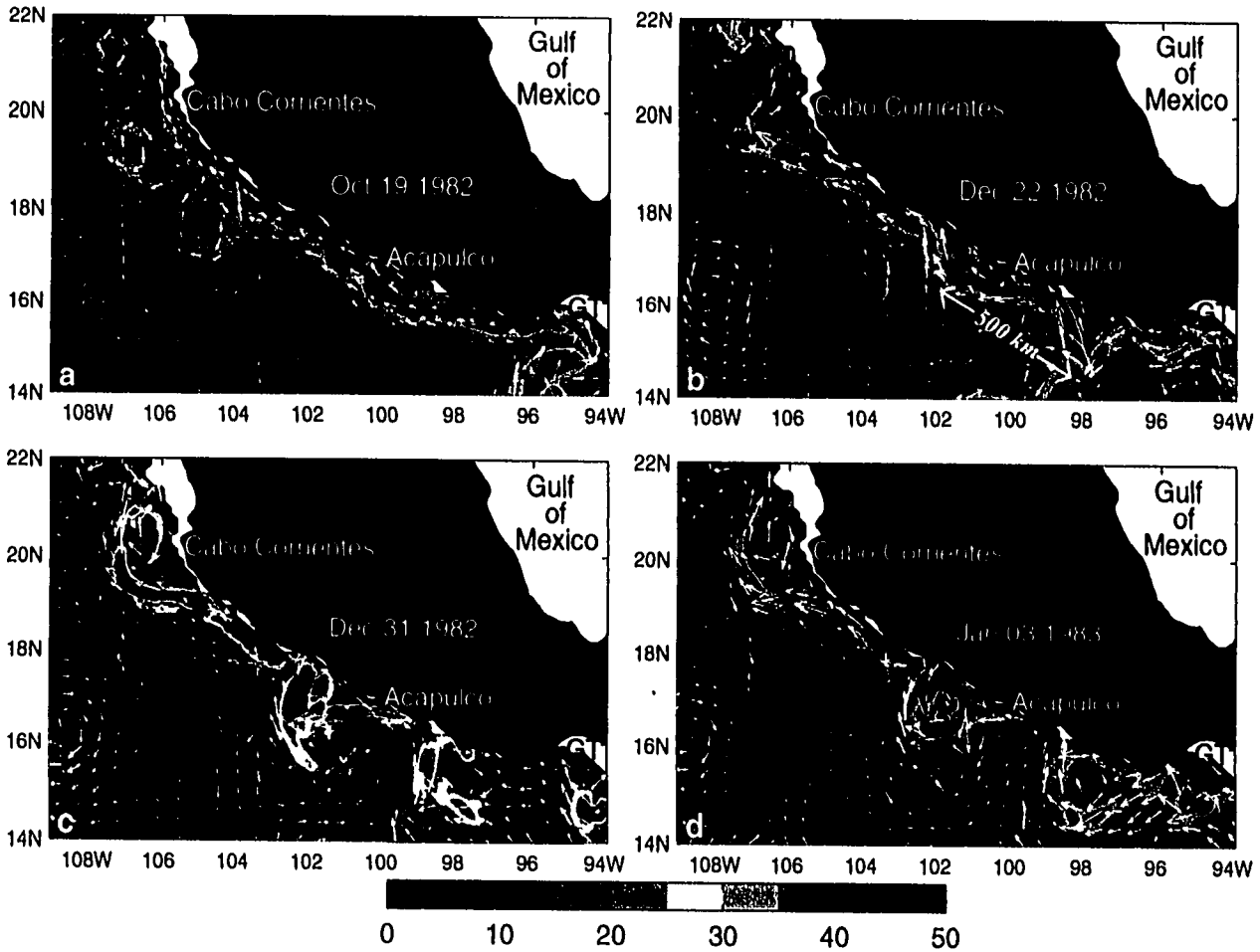

Figure 10. Magnitude of the vectorial velocity difference of NLOM layer 1 minus layer 2 (color contours in cm/s) and corresponding arrow vectors. The four different panels indicate: (a) The establishment of the strong, narrow and elongated jet, (b) the oscillating state, (c) the breaking of the jet, and (d) the CZ eddy formation. In addition, eddy activity in Cabo Corrientes and the Gulf of Tehuentepec (GT) is recognized, and is studied in sections 4 and 5, respectively.

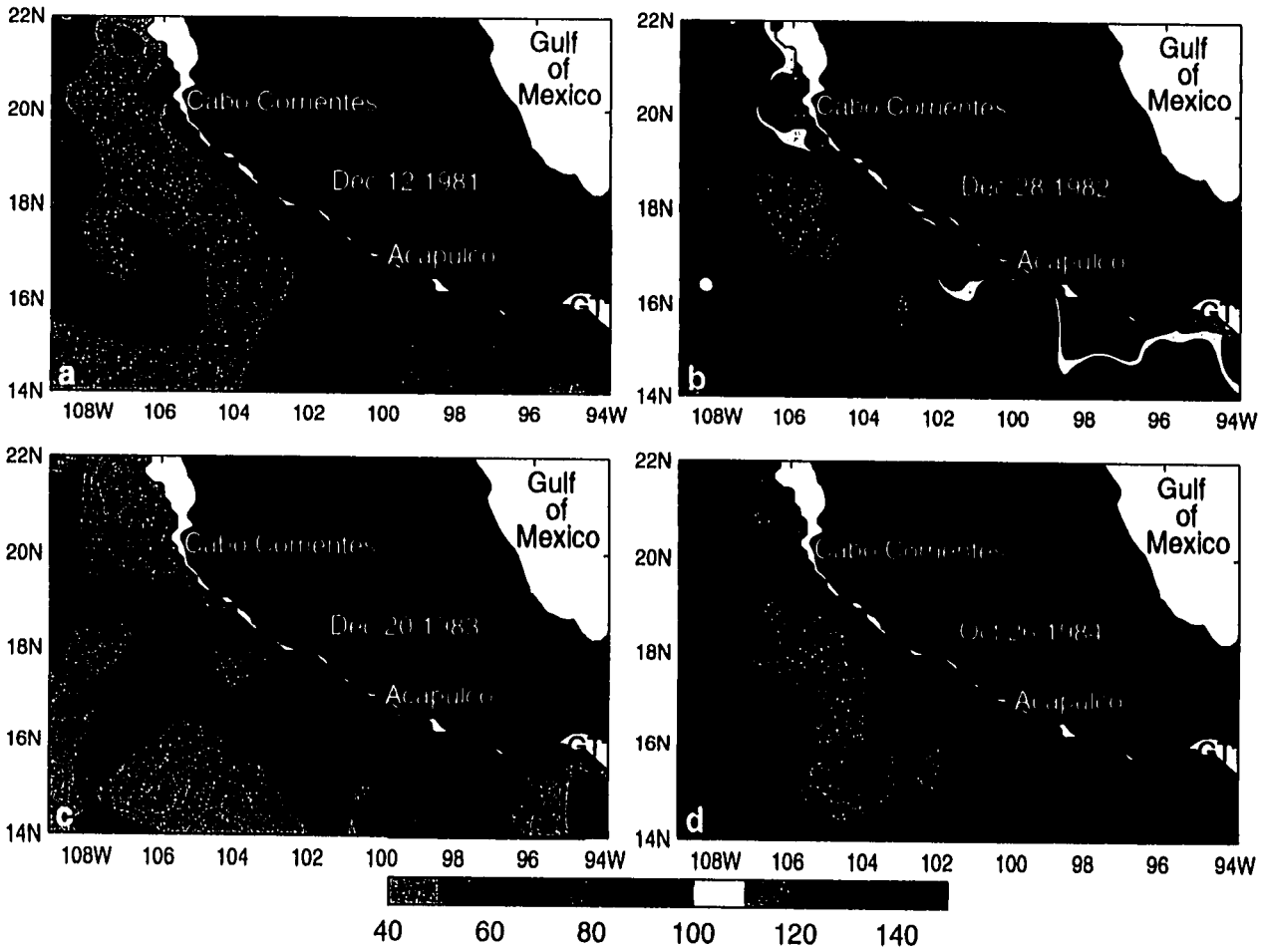

Figure 11. Interannual mesoscale variability. NLOM upper layer thickness (color contours in meters) is displayed when mesoscale features are most evident.

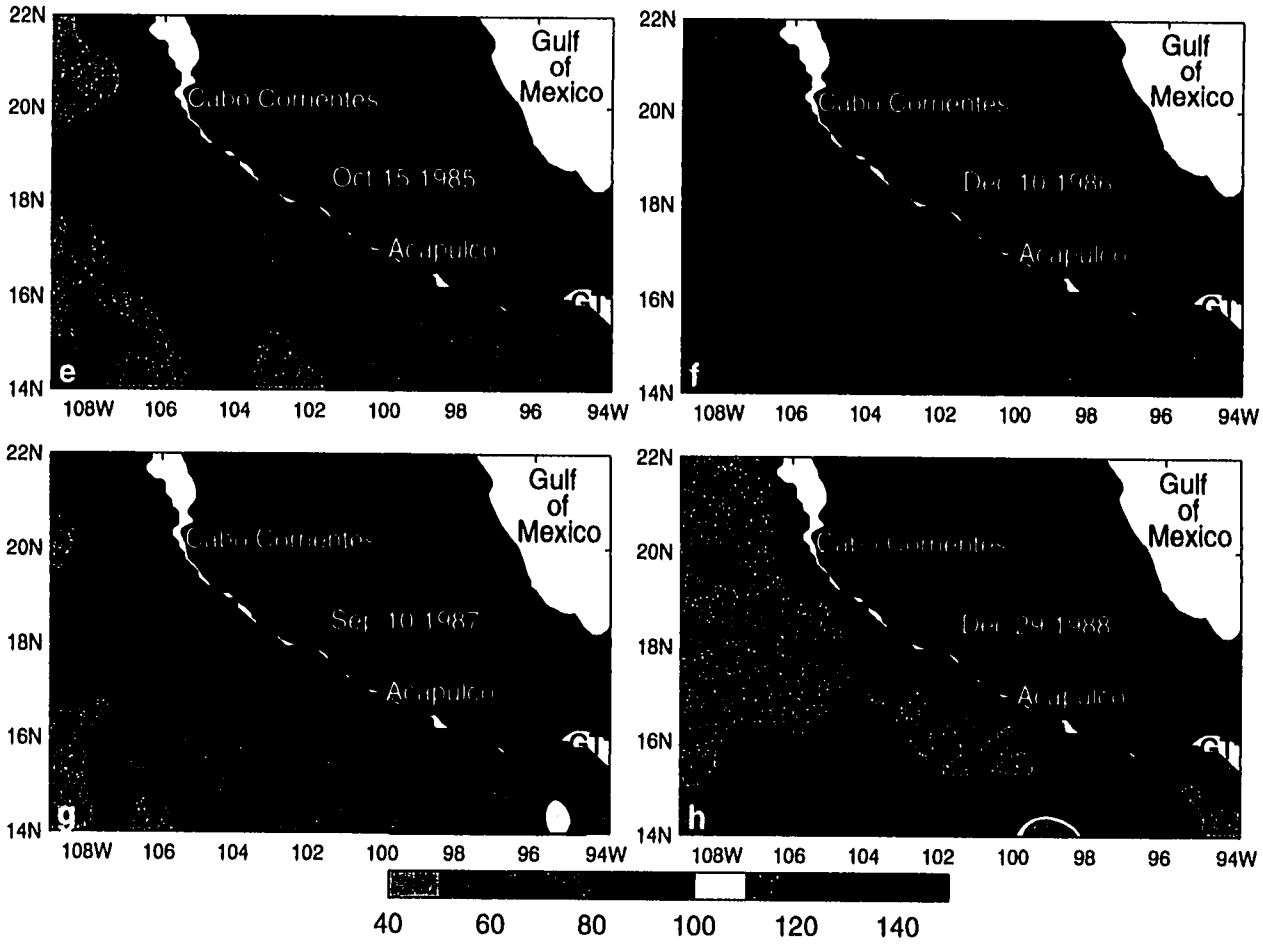

Figure 11. -continued

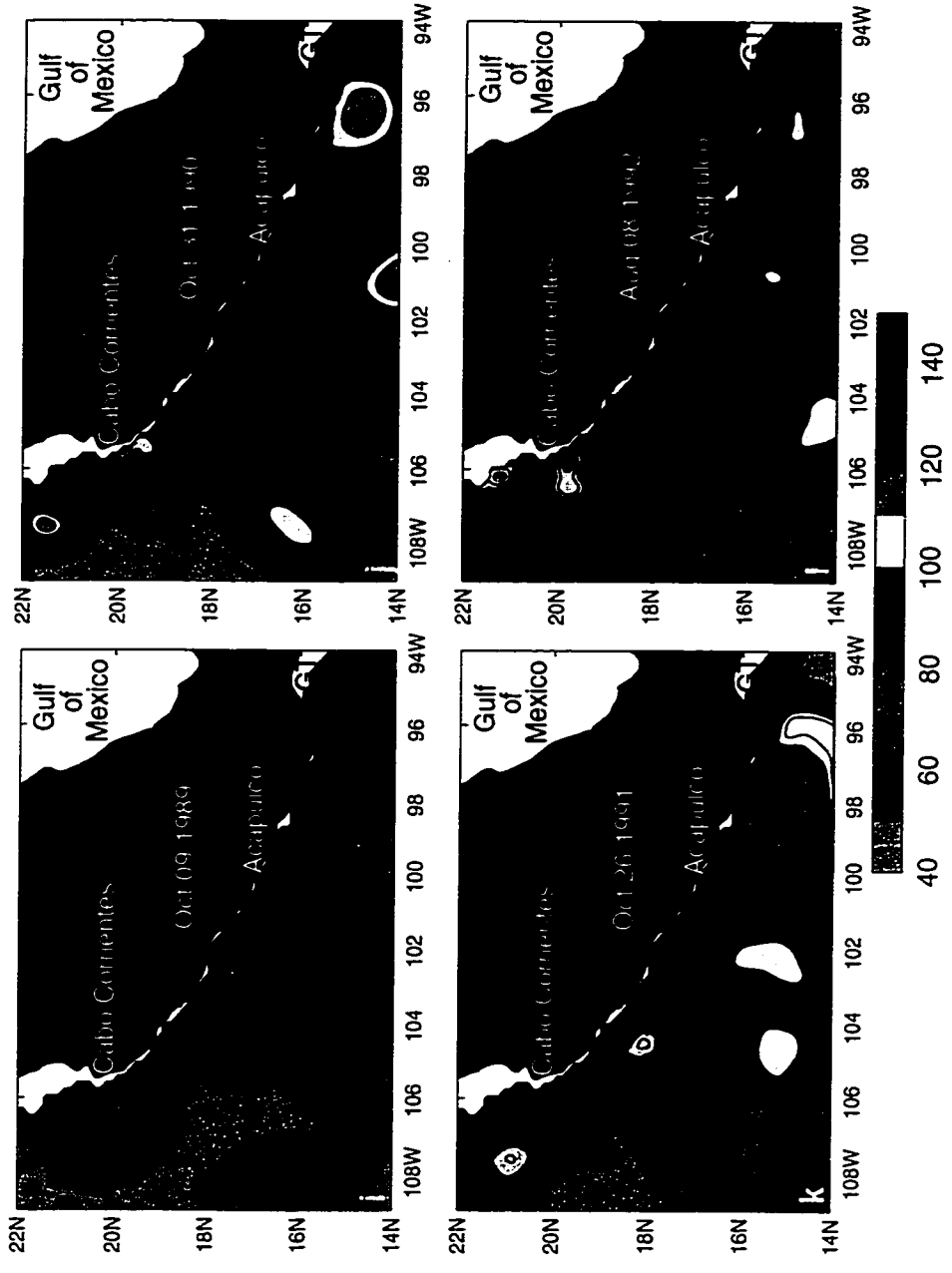

Figure 11. continued

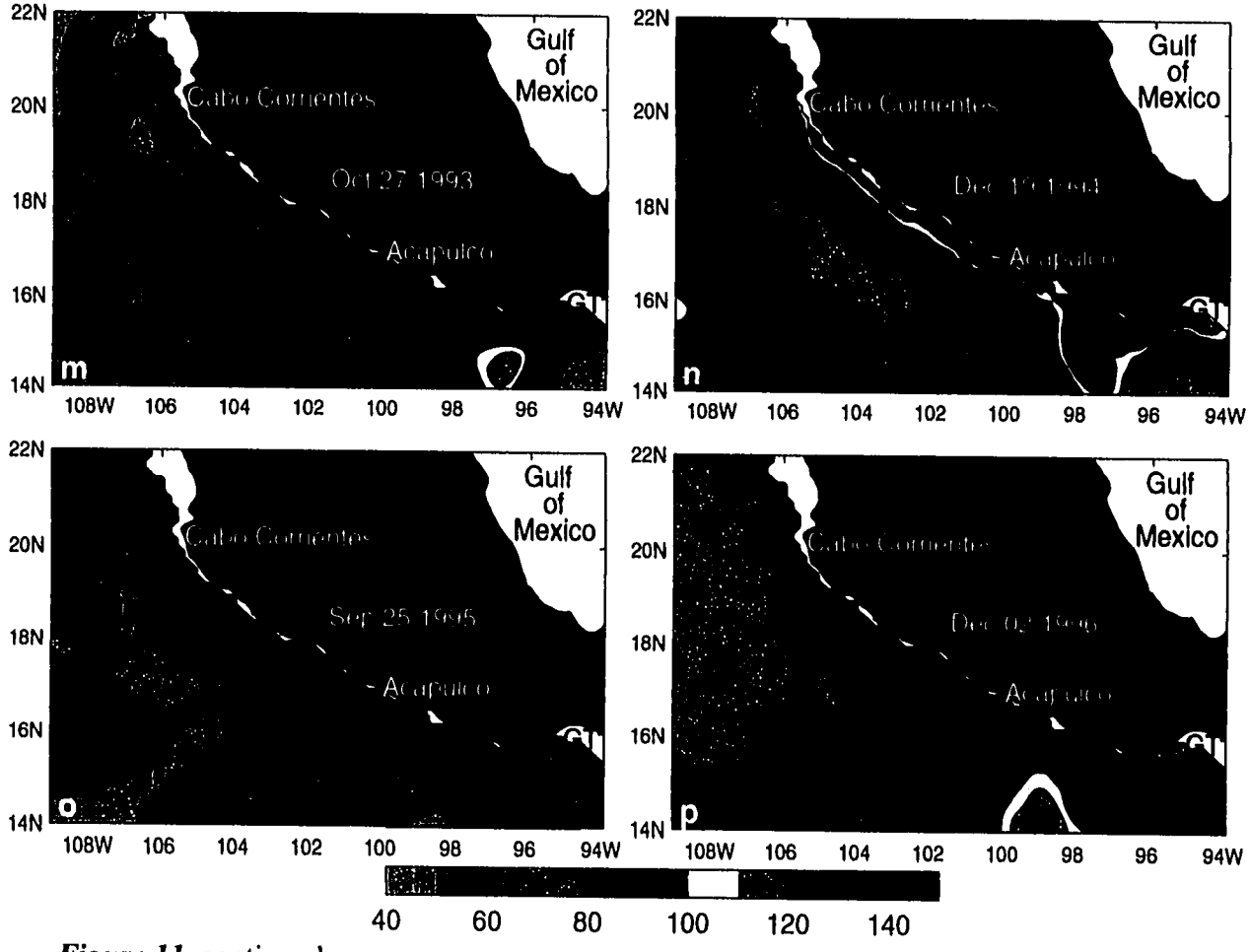

Figure 11. continued

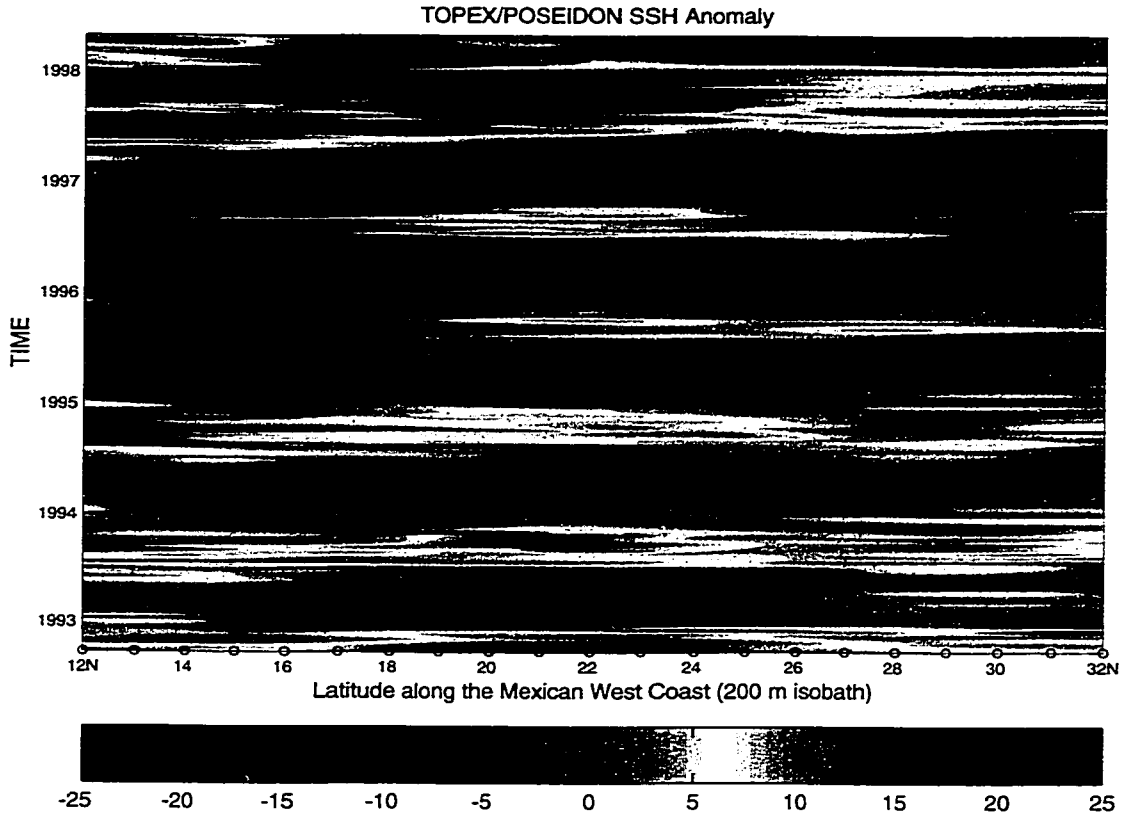

Figure 12. Latitude-time section of sea surface height anomaly (in centimeters) measured by TOPEX/Poseidon (T/P) along the 200 meter isobath along the west coast of Mexico. The latitudes of the T/P observations are indicated by the open circles.

distinctive features in Figure 12. To the best of the authors' knowledge, no eddy observations have been reported in the CZ. If our hypothesis is correct we would expect to observe anticyclonic eddies in the CZ in T/ERS measurements during the 1997-98 El Niño event. Figure 13 confirms this by showing a strong anticyclonic eddy centered at approximately the same position of the model eddy in Figure 10d. An exhaustive inspection of the T/ERS maps indicates that the anticyclonic eddy generation in the CZ is not limited to El Niño years. However, the strongest anticyclonic eddies are formed during El Niño events. There is no evidence of coastally generated eddies associated with the 1995-1996 strong negative anomaly event in the CZ. Overall, the satellite observations show the presence of cyclonic and anticyclonic eddies in the area; though, the cyclonic eddies are not detected at the coast.

3.3.2 The CZ and the Gulf of Alaska eddies

Analysis of the NLOM long term mean circulation of the upper layer of the ocean indicates that along the North America west coast, only the Gulf of Alaska (GOA) and the CZ are characterized by coastally attached northward-flowing currents[1] (Figure 14). Then, if the eddy generation mechanism is correct we would expect eddy activity in the GOA sometime after the CZ eddies are formed. Although the GOA is completely out of our area of study, timing the lag formation between the GOA eddies and the CZ eddies is instructive to emphasize into the oceanic teleconnections and the combination of two currents as an eddy generator mechanism.

[1] It is important to note that from 5°N to 15°N the CRCC flows northward but it is not completely attached to the coast.

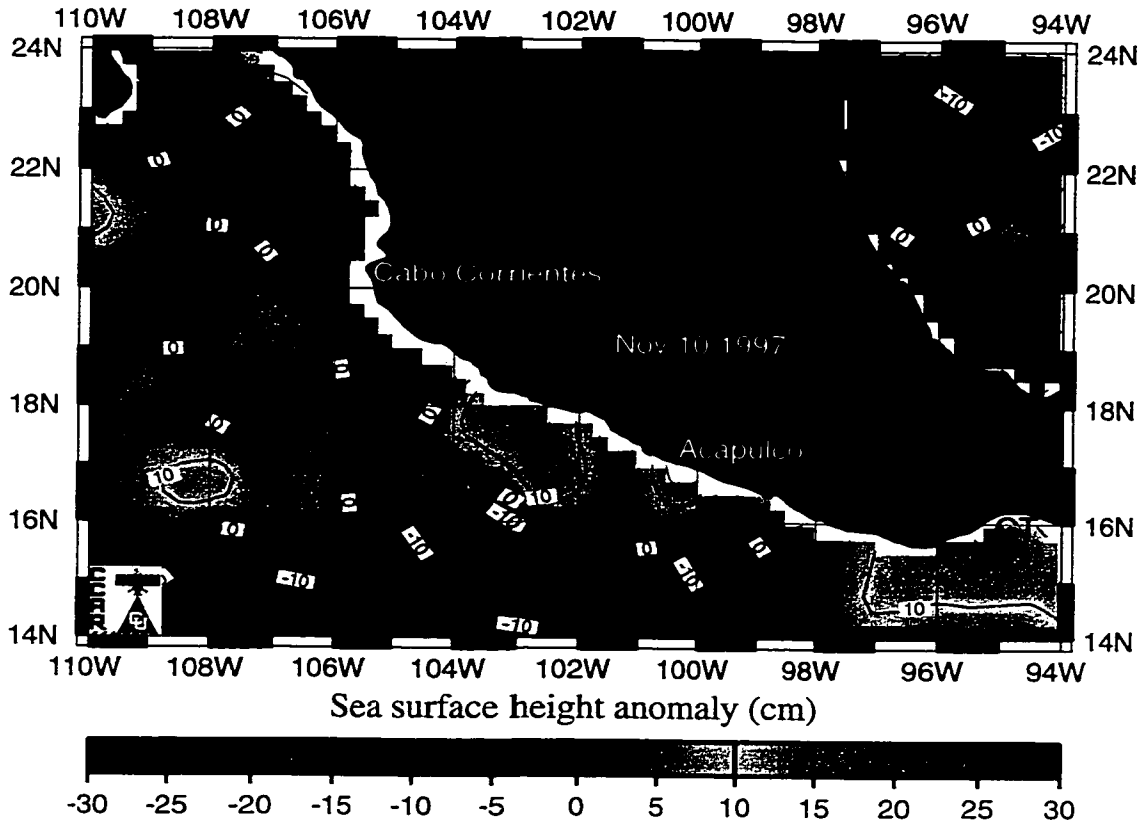

Figure 13. Sea surface height anomaly (color contours in centimeters) in November 1997 as determined from TOPEX/ERS 2 satellite altimeters. The reference level in this figure is a multiyear average. The position of the CZ anticyclonic eddy (CZE) is indicated. In addition, this picture includes cyclonic eddies offshore of the CZ and a Gulf of Tehuantepec (GT) anticyclonic eddy, which are due to different generation mechanisms. This map was obtained from the Colorado Center for Astrodynamics Research publicly accessible web site (http://www-ccar.colorado.edu/~realtime/global-historical_ssh).

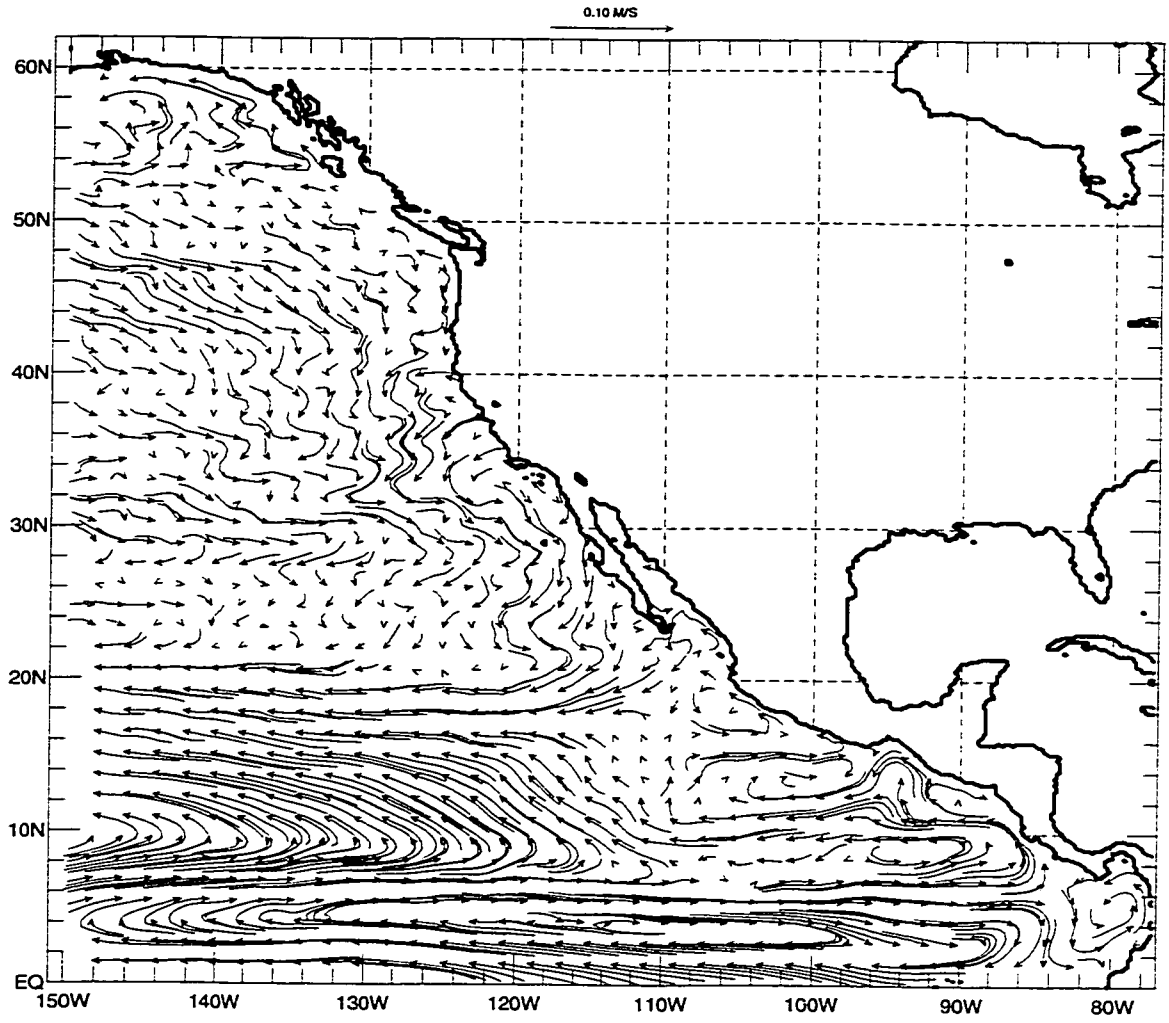

Figure 14. NLOM climatological mean currents (in m/s). The mean was calculated from an 11-year climatology. Note that only part of the southwest coast of Mexico and the Gulf of Alaska are characterized by coastally attached poleward-flowing currents.

The monthly eddy kinetic energy (EKE) maps indicate that the downwelling KW associated with the 1982-83 El Niño arrived at CZ in **August 1982** (Figure 15a). Eddy formation in the CZ is evident during **September and October of 1982.** However, the GOA does not show any eddy activity during those months. By **November**, the eddy activity in the CZ continues, some eddies have already separated from the coast, and it looks like the downwelling KW associated with the 1982-83 El Niño signal has arrived to the GOA during **November 1982.** By **December**, the eddy formation in the CZ has peaked and generates the largest and most energetic eddies. Eddy formation in the GOA starts to be clear at this time. By **January 1983** the eddies at the CZ are not as energetic as in December, the coastal separation processes are evident, and the eddies at the GOA have developed as a clear energetic signal. By **February** the eddies at the CZ have already started their open ocean journey and the eddies at the GOA have intensified. By **March** the eddies in the southeast GOA have separated from the coast. In summary, the EKE maps show eddy formation at the CZ and the GOA associated with the 1982-83 El Niño event. The maps suggest an eddy formation time lag of 2-3 months between those two coastal areas. Overall, without taking into account the Gulf of California, the sequence of maps indicates that the El Niño does not contribute to the eddy generation from 24°N to 45°N.

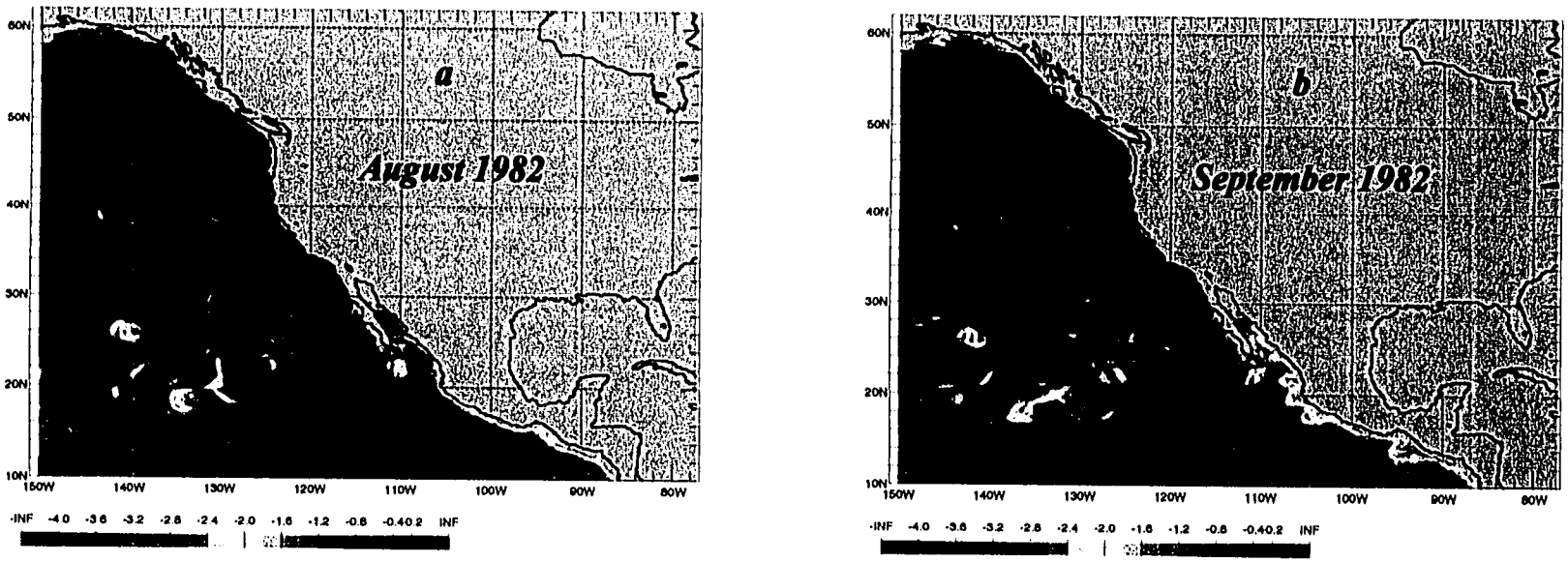

Figure 15. NLOM monthly mean eddy kinetic energy (in log (m^2/s^2)) for: (a) August 1982, (b) September 1982, (c) October 1982, (d) November 1982, (e) December 1982, (f) January 1983, (g) February 1983, and (h) March 1983.

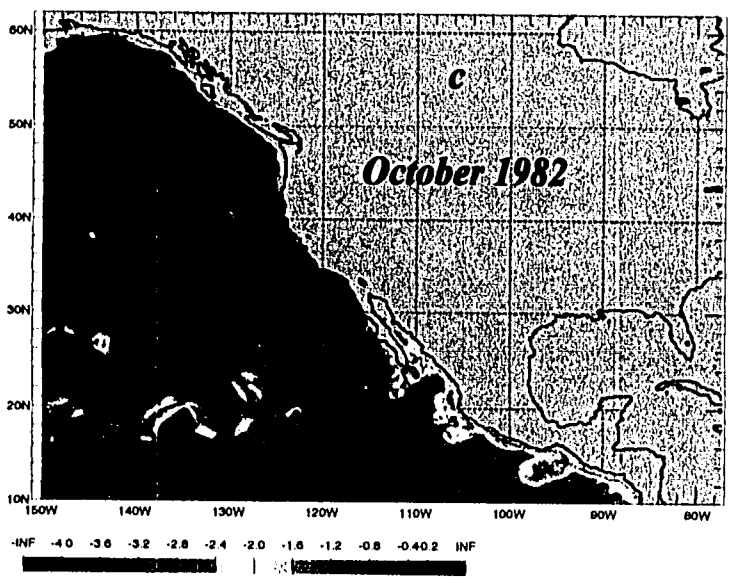

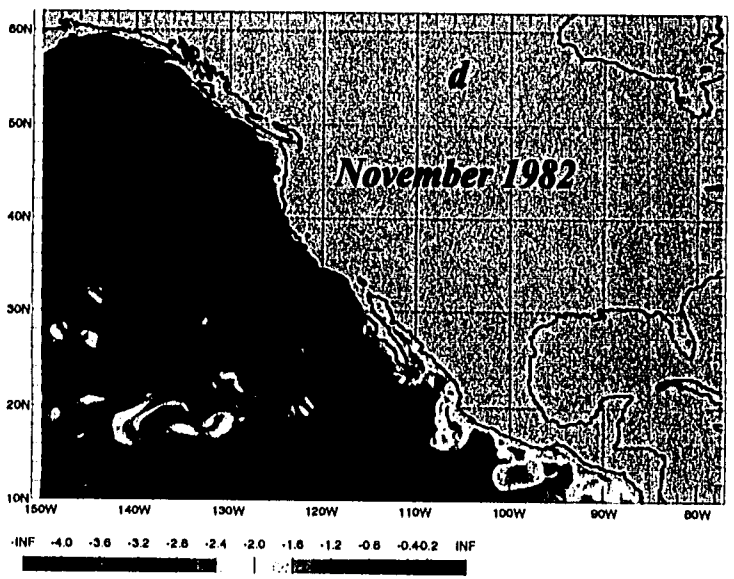

Figure 15.. continued

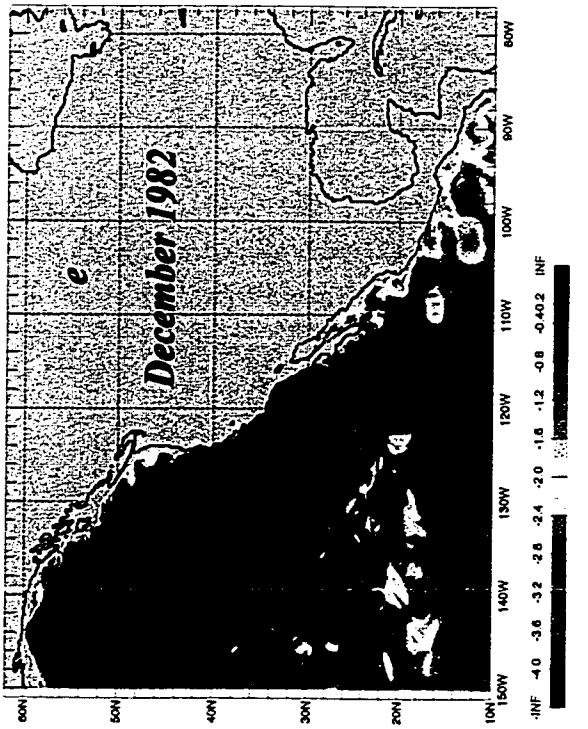

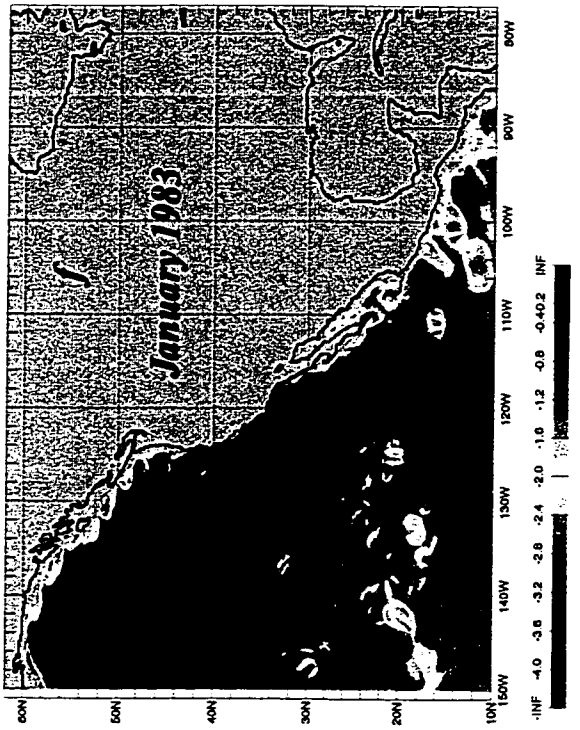

Figure 15. continued

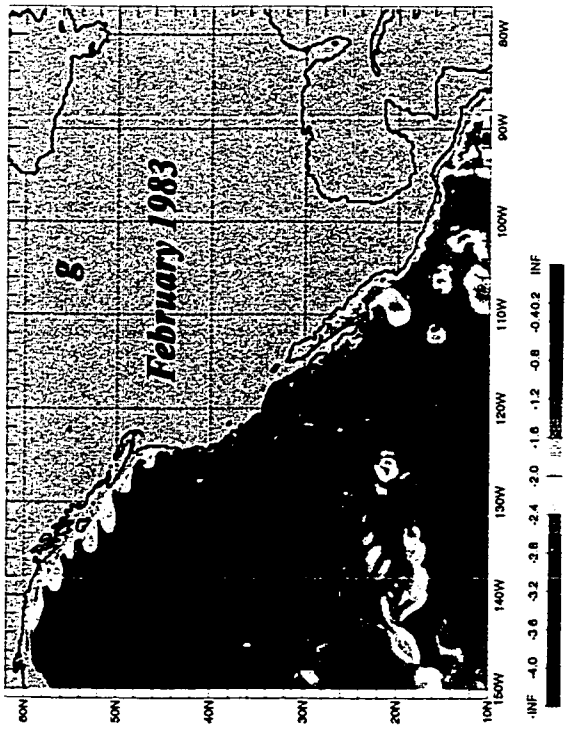

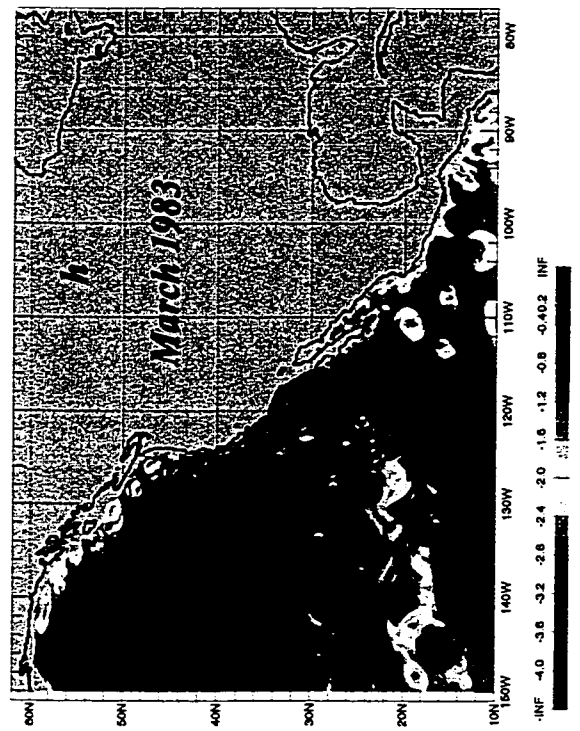

Figure 15. continued

3.4 Discussion

The results in the previous section describe the development of a jet along the southwest Mexican coast during El Niño events. However, no coastal jet is developed during La Niña events. To understand this, it is important to remember that downwelling (upwelling) KW induce a poleward (equatorward) circulation during their poleward propagation. Thus, the coastal jet genesis hypothesis can be understood as the combination of two currents flowing in the same direction. In our case these two currents are the surface intensified CRCC and the currents induced by the downwelling KW. In addition, the Florida State University (Stricherz, et al., 1992) and ECMWF/HR wind fields indicate that the local wind in the CZ is a weak upwelling favorable wind. Therefore, the influence of the local wind in the acceleration of the CRCC is negligible.

On the other hand, applying the same logic one could expect the formation of a southward jet during February-March-April of La Niña years. However, numerical and/or observational evidence of jet formation during La Niña years is lacking. An explanation is as follows. During its intensification the CC penetrates to ~15°N, but is not attached to the coast in the CZ, because the Baja California Peninsula redirects the CC seaward. Consequently, when the upwelling KW arrives at the CZ they do not find a distinct southward flow to be accelerated. In fact, north of 18°N the flow is poleward (Figure 8a). In addition, the observations reported by Wyrtki [1966] and the model results show a predominantly coastal poleward flow in the CZ.

The jet turns unstable when the wavelength of its oscillations becomes approximately 500 km. This number could suggest the existence of baroclinic

instabilities. The explanation is as follows. The jet dimensions allow us to approximate the offshore wave number as zero. Baroclinic instabilities criteria require the alongshore wavelength be approximately $2.6 \cdot \pi \cdot R_1$, where R_1 is the first baroclinic radius of deformation [Kundu, 1990]. In our study area, the model R_1 is ~37 km. Thus, perturbations of approximately 300 km can grow and destabilize the CZ jet. Nevertheless, Kundu [1990] shows that the $2.6 \cdot \pi \cdot R_1$ wavelength does not growth at the fastest rate. The wavelength with the fastest grow rate is $3.9 \cdot \pi \cdot R_1$, which is ~450 km in our area of study and is similar to the 500 km wavelength observed in the numerical simulations (Figure 10b).

In addition, following Tilburg [2000] we calculated instability growth rate diagrams for two different scenarios of the circulation along the southwest coast of Mexico. First, under only the presence of the CRCC no growth of any wave is recognized (Figure 16a). However, under the presence of both the CRCC and the coastal downwelling KW associated with the 1982-83 El Niño event, the growing of different waves is evident (Figure 16b). Also, to provide some insight about the origin of the instabilities a beta Rossby number (which is defined as the ratio of relative to planetary vorticity advection, $R_B = \upsilon / \beta r^2$) was calculated. υ is the maximum swirl velocity of an eddy averaged around the eddy, β is the meridional change of the Coriolis parameter, and r is the mean radius of the eddy. R_B of order 1 (10) suggest barotropic (baroclinic) instabilities involving the first baroclinic (barotropic) mode [McWilliams and Flierl, 1979; Hurlburt and Thompson, 1982, 1984; Murphy et al., 1999]. In the case reported here $\upsilon = 65\ cm/s$ and $r \approx 55$ km; therefore, $R_B \approx 9.8$,

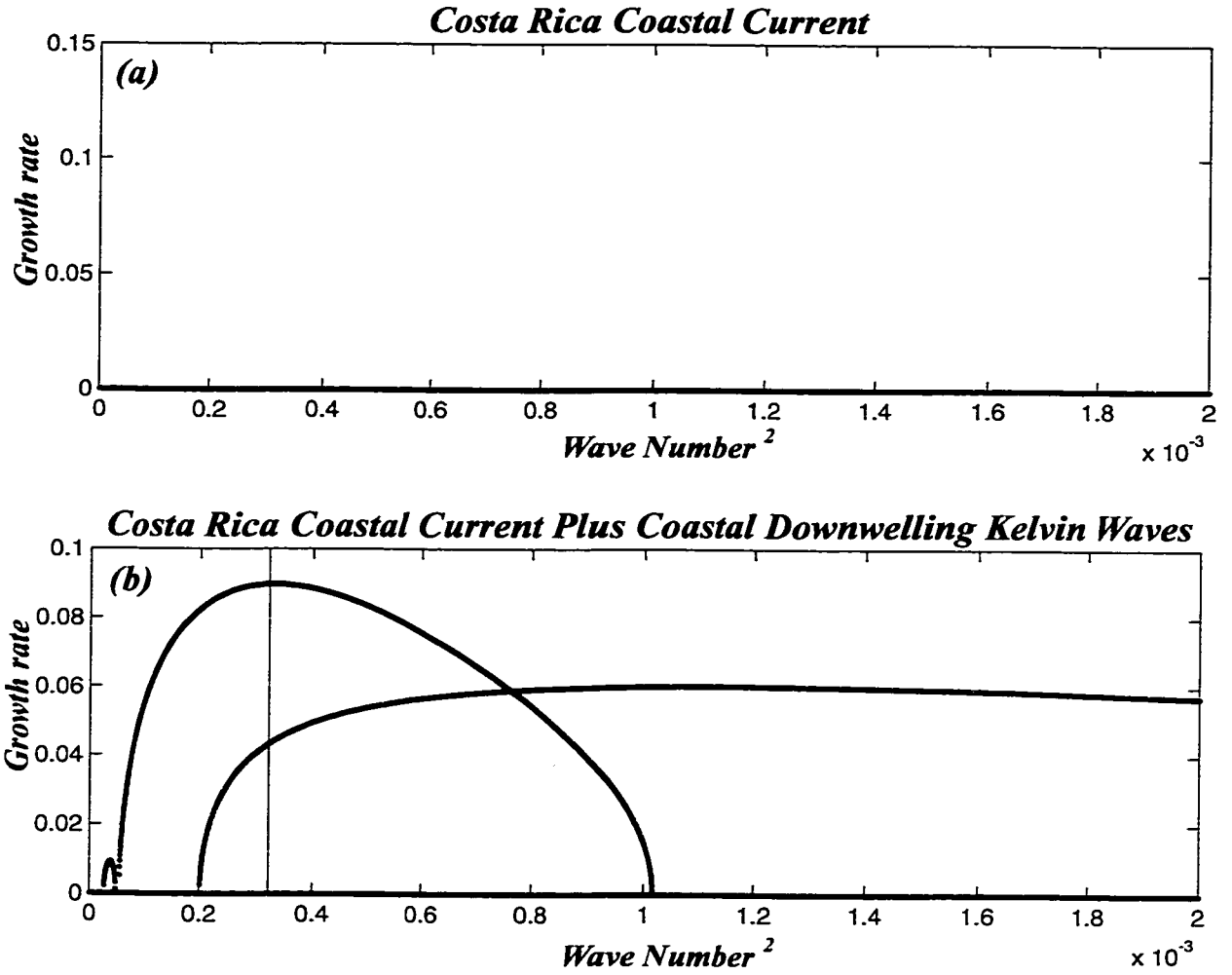

Figure 16. Baroclinic instability growth rate diagrams for the southwest coast of Mexico. (a) Only under the only influence of the Costa Rica Coastal Current (CRCC). (b) Under the influence of the CRCC and the Coastal downwelling Kelvin waves associated with the 1982-83 El Niño event. The black vertical line indicates the location of wavelengths of approximately 350 km.

which is order 10 and consequently suggests eddy formation as a result of baroclinic instabilities.

T/ERS observations include cyclonic and anticyclonic eddies in the area of study. However, strong cyclonic eddies are not very common in the model. Entrainment from the layer below is the reason why we cannot observe the strengthening of cyclonic eddies in the model. Entrainment in model layer 1 starts if its depth becomes less than 50 m. McCreary et al., [1989] and Trasviña et al., [1995] emphasized the relevance of the entrainment process in stopping the developing of cyclonic eddies in the Gulf of Tehuantepec.

Finally, the maximum SSH anomaly of the anticyclonic eddy observed by the altimeters in November of 1997 is ~20 cm. Assuming a 1.5 layers reduced gravity model the thermocline depth would be ~100 m. Although this is not the typical maximum layer 1 thickness of El Niño eddies in the model (~140 m), the eddies observed by the altimeters provide evidence supporting the eddy generation hypothesis.

3. 5. Summary and Conclusions

The process of formation and subsequent migration of ENSO related eddies along the southwest coast of Mexico are examined using the hydrodynamic Naval Research Laboratory Layered Ocean Model. Verification of the modeled eddies is based on TOPEX/Poseidon and ERS-2 sea surface height altimeter observations. Analysis suggests that the observed eddies form due to baroclinic instabilities within a surface-trapped narrow coastal jet. This jet is formed by the positive combination of the poleward circulation along the southwest coast of Mexico and the poleward currents induced by ENSO warm phase Kelvin waves.

4. TROPICAL WAVES INDUCE OCEAN EDDIES AT CABO CORRIENTES, MEXICO

4.1 Abstract.

The high resolution Naval Research Laboratory Layered Ocean Model is used to examine the generation of anticyclonic oceanic eddies near Cabo Corrientes, Mexico. Results indicate that the arrival of downwelling coastally trapped waves at Cabo Corrientes corresponds to the intensification of the local currents. The interaction of these intensified currents with the coastline geometry generates anticyclonic eddies. Comparison of different numerical simulations suggests that the bottom topography and the local wind are not responsible for the eddy generation. In fact, the coastline geometry, most notably the cape at Cabo Corrientes, causes the formation of eddies. The existence and timing of the modeled eddies is validated with sea surface height altimeter observations and temperature hydrographic data.

4.2 Introduction.

The formation of ocean eddies as a result of the interaction of coastal currents with capes is a well documented process and has been studied from several different points of view [Røed, 1980; D'asaro, 1988; Strub et al., 1991; Klinger, 1994; Pichevin and Nof, 1996; Cenedese and Whitehead, 2000]. The theories presented in these

studies have been used to explain the origin of the eddies observed near Cape St. Vincent (on the southwest coast of Portugal), Point Barrow (on the northeastern coast of Alaska), and the Capes Blanco and Mendocino (on the coasts of Oregon and California). However, so far as we are aware, no study has reported the existence and genesis of the anticyclonic ocean eddies observed by the satellite altimetry near Cabo Corrientes (on the Mexican West Coast) (Figure 17).

Bottom topography near Cabo Corrientes is characterized by an abrupt transition from a narrow to a wide shelf, while the coastline changes its orientation from northwest to approximately eastward, and the María Islands Archipelago works as an extension of the continental shelf (Figure 2). The mean surface ocean circulation at Cabo Corrientes is dominated by a poleward coastally-attached current known as the Costa Rica Coastal Current (CRCC) [Figure 18; Wyrtki, 1966; Badan et al., 1989; Zamudio et al., 2001]. The variability of the circulation at Cabo Corrientes is mainly dominated by equatorially generated (interannual and intraseasonal) and storm induced (higher frequency) coastally trapped waves[2] (CTW) [Chelton and Davies, 1982; Christensen et al., 1983; Enfield and Allen, 1983; Spillane et al., 1987; Enfield, 1987; Merrifield and Winant, 1989; Merrifield, 1992; Ramp et al., 1997].

Results from numerical simulations indicate that the mean poleward-flowing coastally trapped currents at Cabo Corrientes are characterized by a speed of ~8 cm/s, and an offshore extension of ~40 km (Figure 18). However, the arrival of downwelling CTW causes to increase the currents' speed to ~40 cm/s. The increased currents result

[2] The mathematical representation of these waves includes an exponential function that decays from the coast. Thus, in a general sense they are commonly known as coastally trapped waves.

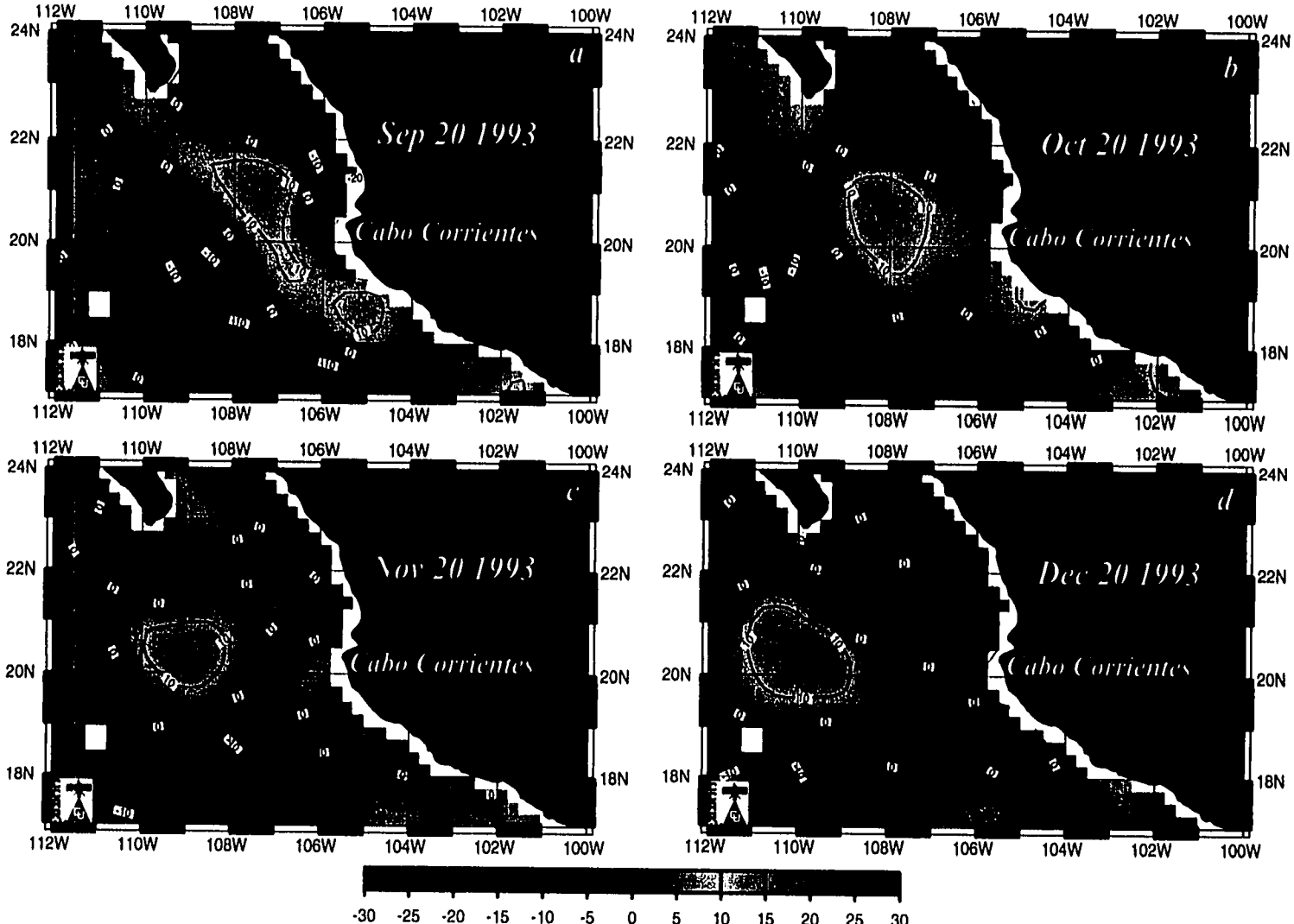

Figure 17. Sea surface height anomaly (color contours in centimeters) for four different dates in 1993 as determined from TOPEX/ERS-2 satellite altimeters. The most striking feature in the four different panels is the presence of the Cabo Corrientes eddy. These maps were designed to retain mesoscale sea surface height associated with fronts and eddies. They were obtained from the Colorado Center for Astrodynamics Research publicly accessible web site (http://www-ccar.colorado.edu/~realtime/global-historical_ssh).

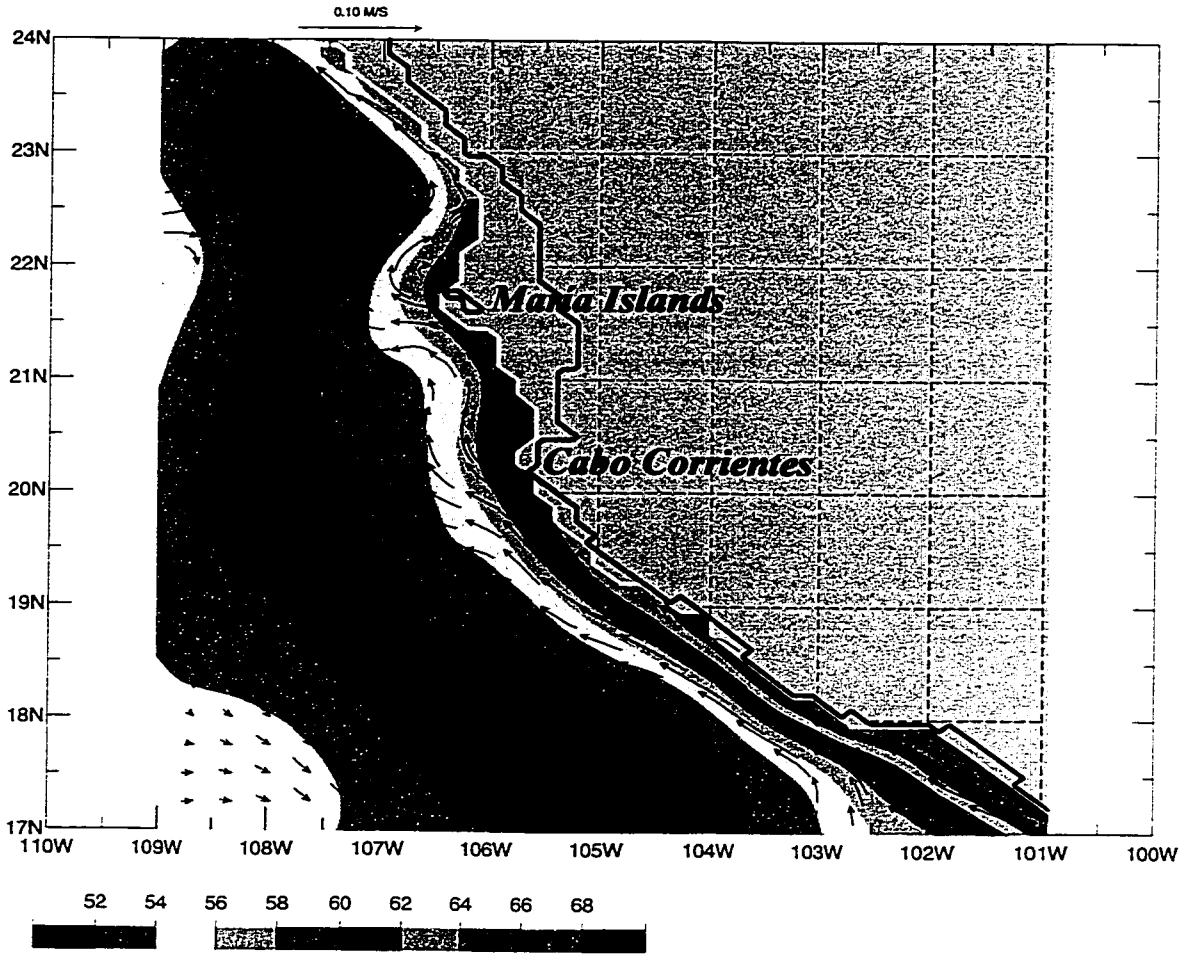

Figure 18. Mean layer 1 thickness (color contours in meters) and mean currents (vectors) from NLOM. The contour interval is 2 meters and the vectors represent the currents at the arrowhead. The means were calculated from an 11-year climatology. The solid black line represents the real coastline. Note that the orientation of Cabo Corrientes and the María Islands forces the CRCC to separate from the coast. The layer 1 thickness is at maximum near the coast and decays northward and offshore.

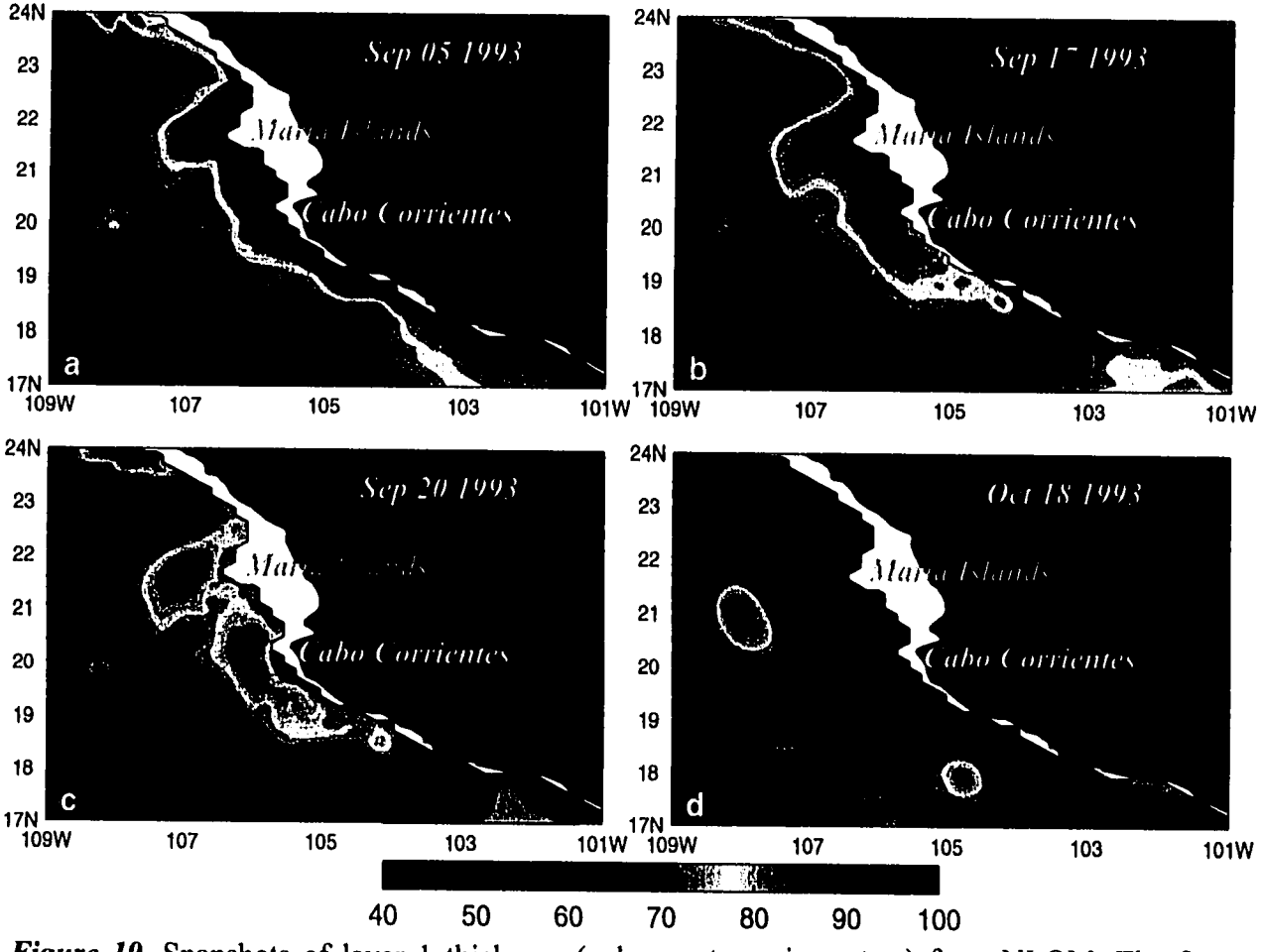

Figure 19. Snapshots of layer 1 thickness (color contours in meters) from NLOM. The four different panels indicate: (a) the arriving of the coastal trapped waves to Cabo Corrientes and María Islands area, (b) the eddies formation, (c) the eddies separation from the coast, (d) and the eddies westward and southwestward drifting.

in the formation of anticyclonic eddies (Figure 19). To determine the physical mechanisms responsible for the generation of these observed eddies, we analyzed 16 years (1981-1996) of data from several different simulations of the Naval Research Laboratory Layered Ocean Model (NLOM). The model results are validated with Sea Surface Height (SSH) satellite altimeter observations and hydrographic data.

4.3 Numerical experiments

We have used a suite of numerical simulations to examine the generation of the Cabo Corrientes' eddies. The simulations were performed using a hydrodynamic version of NLOM on a Pacific Ocean domain with a latitudinal extension (20°S-62°N) that allows equatorially generated signals (i.e. CTW) to influence the circulation of the Northeastern Pacific Ocean, most notably the Cabo Corrientes' circulation. All simulations include non-linearities, free surface, and a no slip boundary conditions. The only external forcing included in the simulations reported here is the ECMWF/HR hybrid wind stress described in section 2. We evaluate the effects of: (i) **Resolution**, 1/4° versus 1/16°. (ii) **Bottom topography**, realistic bottom topography versus flat bottom. (iii) **External forcing**, a downwelling CTW versus local wind stress. CTW are surface intensified. Thus, the rest of this section is focused to the analysis of the behavior of the model layer 1.

4.4. Model results

In this subsection the results of the basic simulation are described and in the discussion subsection the results differences between the different simulations are

pointed out. The model long-term mean circulation (Figure 18) indicates that when the CRCC arrives at Cabo Corrientes it rounds the cape to continue its advance. After crossing the cape the CRCC reattaches to the coast and continues its poleward route until it encounters the María Islands Archipelago, where again the CRCC rounds the Islands and reattaches to the coast. In addition, the vector velocity shows a reduction of the CRCC's speed and a weak anticyclonic circulation right at the North sides of Cabo Corrientes and the María Islands but not evidence of eddy activity.

Snapshots of model results (Figure 19) corresponding to the arrival and interaction of CTW with Cabo Corrientes do show eddies. At the time of the arrival of the downwelling CTW (Figure 19a) the upper layer's thickness is ~120 m, the coastally-attached poleward current speed is ~ 40 cm/s, and the separation from the coast is much more pronounced than the mean (Figure 18). By September 17, 1993 (Figure 19b) eddies have formed downstream of Cabo Corrientes and the María Islands. Three days later (Figure 19c) the complete CTW has already crossed the area of study and the two anticyclonic eddies have begun to separate from the coast. These eddies are characterized by a layer 1 thickness of ~90 m at their core, a swirl velocity of ~50 cm/s, and a diameter of ~90 km. A month later (Figure 18d), the eddies have completely separated from the coast and have drifted westward and southwestward at a speed of ~7 cm/s.

The eddies' formation process documented in Figure 19 is just an example. Based on 16 years of data, the model indicates that on average the CTW generate four eddies per year. The eddies included in that average have similar or larger horizontal and vertical dimensions than those at Figure 19. General characteristics of the eddy

formation process are: (1) After the eddy formation and before the eddy separation, large velocities develop to the southeast of Cabo Corrientes and the María Islands. (2) When the eddies have separated from the coast a distance no larger than a radius of deformation and a new CTW arrives to the area, the eddy is reinforced and/or fused with a new eddy generated by the latest CTW. Thus, a packet of CTW arriving at Cabo Corrientes results in one large eddy with a diameter of 150 km or more. (3) The formation of eddies varies interannually. During 1988 (La Niña year, Figure 9), only one eddy was formed. In contrast, 1987 (El Niño year, Figure 9) was the most prolific year, during which eight anticyclonic eddies were generated. Some of them were characterized by a deeper core than the CRCC and the CTW where they originated. (4) El Niño seemed to intensify the eddies. The CTW associated with the 1982-83 El Niño event generated currents of ~100 cm/s and the anticyclonic eddies with the largest dimensions. (5) All downwelling CTW arriving at Cabo Corrientes generated eddies. (6) Upwelling CTW at Cabo Corrientes did not generate eddies.

4.5 Discussion

This subsection is divided in three parts. First, the differences in the simulations results are discussed. Second, the eddy generation process is discussed and finally the model results are compared with observations.

4.5.1 Comparison of the different numerical experiments

(i) Resolution. The eddies formed in the 1/4° experiment were less frequent than the eddies formed in the 1/16° experiment. This was an expected result because in the 1/16° experiment the currents find a sharper corner (and separate more from the coast)

than in the 1/4° experiment generating a more distinctive anticyclonic circulation at the north side of Cabo Corrientes. In addition, in the 1/4° experiment the grid size, ~27.5 km, is not adequate to resolve the model first baroclinic radius of deformation (~32 km). **(ii) Bottom Topography**. The reduced gravity and the flat bottom experiments include eddy formation at Cabo Corrientes. Consequently, the bottom topography can be ruled out as a main factor in the anticyclonic eddy formation. **(iii) Topographic β effect**. The flat bottom and the reduced gravity experiments, which did not involve a topographic β effect, include eddy formation and detachment, suggesting that the topographic β effect is not a crucial element in the detachment of the Cabo Corrientes eddies. **(iv) Local wind**. The results of a flat bottom simulation, which was forced by a CTW only (no wind), includes eddy generation and detachment at Cabo Corrientes. These results and the inspection of the ECMWF and FSU wind stress curl fields suggest that the local wind stress curl is not a main element in the eddy generation at Cabo Corrientes.

4.5.2 Eddies' formation

The model results described in subsection 4.4 include the generation of anticyclonic eddies associated with the arrival of downwelling CTW to Cabo Corrientes. Two questions immediately present themselves. Why does the CRCC not generate eddies at Cabo Corrientes by itself? Why are the eddies generated during the arrival of downwelling CTW but not upwelling CTW? The process of eddy formation at capes has already been discussed under the assumption of the presence of a steady current [Pichevin and Nof, 1996]. The main processes are summarized as follows.

Consider a steadily flowing coastally-attached current that encounters a cape and rounds it to continue its advance as a boundary current. If the radius of curvature of the cape is smaller than the inertial radius ($|\vec{u}|/f$, where $|\vec{u}|$ is the characteristic speed of the current in question and f is the Coriolis parameter) the current will separate from the coast [Bormans and Garret, 1989; Hughes, 1989; Klinger, 1994a, 1994b]. After the separation the current reattaches to the coast due to its finite offshore extension, which is proportional to the radius of deformation [Bormans and Garret, 1989]. The separation and reattachment of the current produces an unbalanced flow-force around the cape that is balanced with the formation and shedding of eddies[Pichevin and Nof, 1996]. In our particular case the Cabo Corrientes radius of curvature is ~5 km; but the mean currents have an inertial radius of only ~2 km and do not separate. However, the arrival of a downwelling CTW reinforces the mean current resulting in an inertial radius of ~8 km. Poleward-flowing upwelling CTW induce equatorward currents that debilitate, rather than strengthen, the CRCC.

In Cabo Corrientes and the María Islands scenario the eddy forcing is not a steady forcing. It is an intermittent forcing that appears with the arrival of downwelling CTW. Past Cabo Corrientes, the coastline veers to the northeast and the currents turns to the northwest. The combination of these directional changes produces an anticyclonic circulation pool at the north side of Cabo Corrientes. During its presence in the area the CTW strengthen the anticyclonic circulation in the pool, generating an anticyclonic eddy. The eddy remains attached to the coast, being reinforced by the CTW and debilitated by the lateral friction produced by the coast,

until the CTW cross the area. Then, the eddy is detached from the coast and starts its open ocean westward drifting. Thus, the longevity and the consecutive arrivals of downwelling CTW maintain the eddy in the coastal area for a long period of time, which during the eddy is reinforced. Note that in the hypothetical case of an infinite long CTW we would have the steady current, which would require of the eddy generation and the eddy shedding to balance the forces around the cape. Thus, the eddy generation at Cabo Corrientes can be basically explained with the Pichevin and Nof [1996] eddy cannon theory.

Why are the generation mechanisms of the Cabo Corrientes eddies and the eddies that shows up close to Acapulco during El Niño years [section 3; Zamudio et al., 2001] different if both eddies originate from the arrival of CTW? In the Cabo Corrientes case the coastline is the crucial element in the eddy formation, whereas for the generation of the Acapulco eddies, baroclinic instabilities are the key element.

4.5.3 Observed and modeled eddies

The model results show anticyclonic eddy formation each time a CTW arrives at Cabo Corrientes. If the model results are correct we would expect to observe anticyclonic eddies at Cabo Corrientes in TOPEX/ERS satellite altimeter mesurements. Examination of SSH altimeter observations during September 1993 (Figure 17a) reveals the presence of an anticyclonic eddy (positive SSH anomaly) near Cabo Corrientes. Comparison between satellite observations (Figures 17a and 17b) and model results (Figures 19c and 19d) indicates that the simulated eddies are co-located, in time and space, with the observed ones, suggesting that this altimeter observed eddy was generated by the CTW that arrived to Cabo Corrientes on early

September 1993 (Figure 19a). Several examples of eddy formation near Cabo Corrientes have been observed using the Colorado Center for Astrodynamics Research publicly accessible web site (http://www-ccar.colorado.edu/~realtime/global-historical_ssh).

To provide some insight about the model validation we compared model results with hydrographic data. Trasviña et al. [1999] using temperature hydrographic data reported the presence of an anticyclonic oceanic eddy located at ~500 km to the west of Cabo Corrientes (Figure 20). The model results (Figure 21) suggest that the eddy was not created near the location at which it was observed. In fact, they suggest that the eddy was created in mid March 1992 on the north side of the María Islands as a result of the arriving of a CTW (Figure 21b). Next, the eddy drifted westward (Figures 21c-21f), passed by the line where the hydrographic data were taken on May 1992 (Figure 21f) and generated a positive anomaly in the temperature field (Figure 20c).

4.6. Summary and Conclusions

The role of Cabo Corrientes coastline geometry and coastal trapped waves on the generation of anticyclonic oceanic eddies have been studied. A suite of numerical simulations from the Naval Research Laboratory Layered Ocean Model was utilized to examine the eddy generation processes. The poleward-flowing local current (which is known as the Costa Rica Coastal Current) does not generate eddies. The eddies are generated when downwelling coastal trapped waves (which originate at the equator) arrive at Cabo Corrientes and intensify the local current. These intensified currents

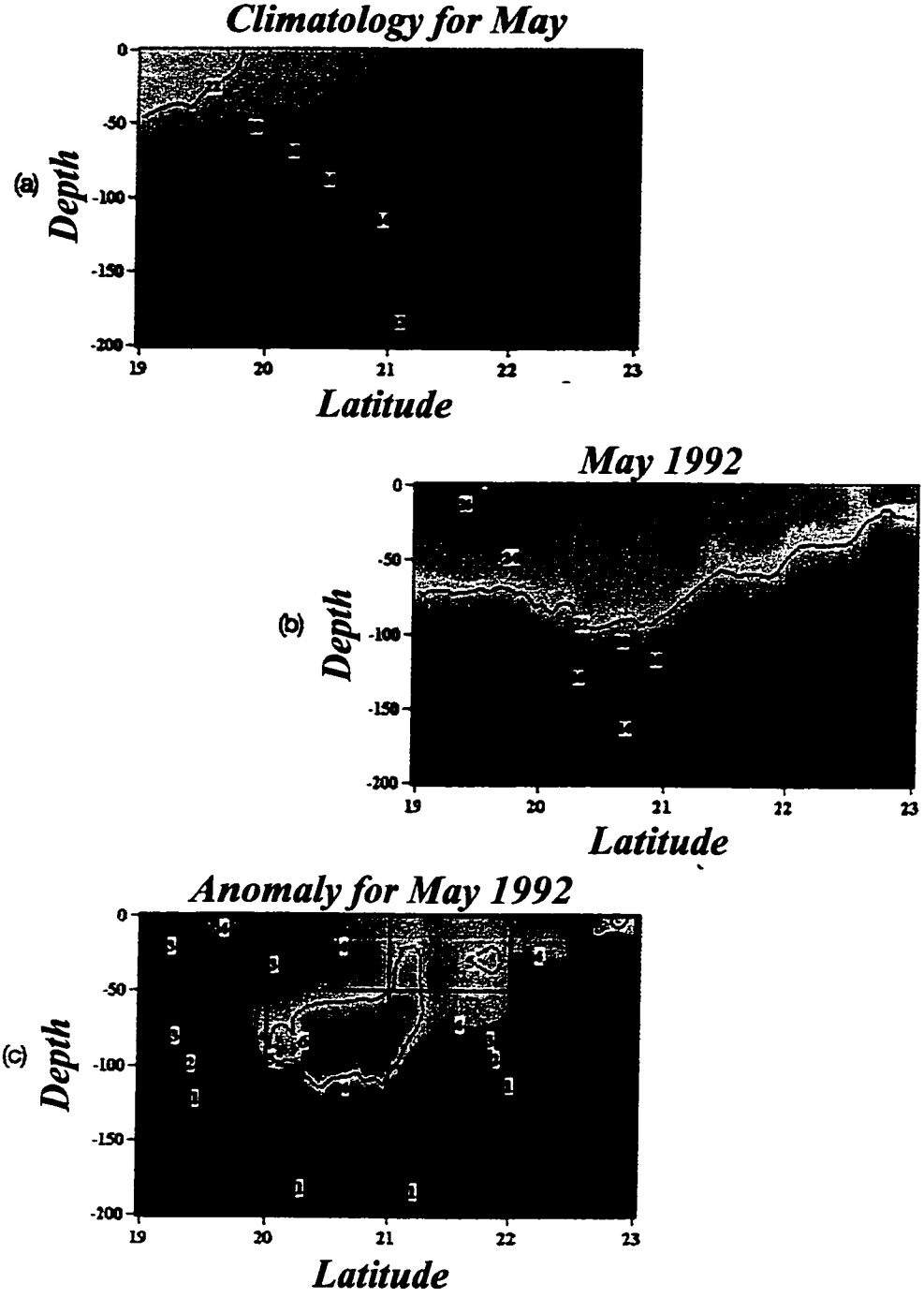

Figure 20. Latitude-depth sections of temperature (in °C) along the white line in Figure 21. (a) Climatology of the temperature for May. (b) Temperature field during May 1992. (c) Anomaly of the temperature for May 1992. From these transversal sections is not possible to conclude about a closed circulation. However, the downward bending of the isoterms in (b) (which reach a maximum depth between 20°N and 21°N) suggests the presence of an anticyclonic eddy in the area during May 1992. After Trasviña et al. [1999].

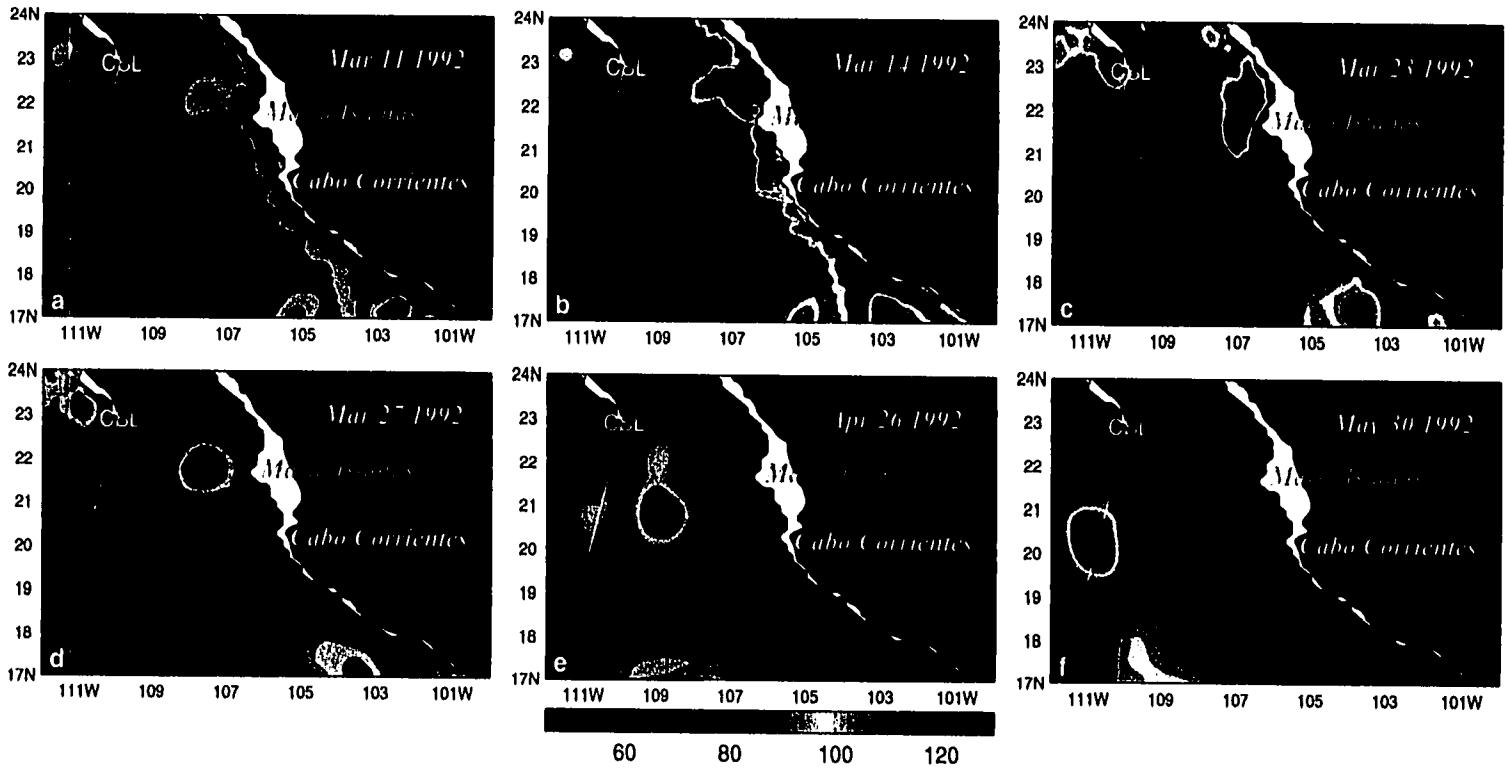

Figure 21. Snapshots of NLOM layer 1 thickness. The different panels indicate. (a) The arriving of the CTW to Cabo Corrientes and María Islands area. (b) The formation of anticyclonic eddies at the north sides of Cabo Corrientes and María Islands. (c) The two eddies have already fused and start the separation from the coast. (d)-(f) The eddy drifting westward. The white line represents the position of the hydrographic transect where the temperature field in Figure 20 was measured on May 1992. Note that the modeled eddy crossed the white line during May 1992.

interact with the cape and generate the anticyclonic eddies. The ability of the numerical model to isolate the dynamic effects allows us to rule out the local wind and the bottom topography as main factors in the eddy generation processes. Validation of the model simulated eddies is based on temperature hydrographic data and TOPEX/Poseidon and ERS-2 sea surface height altimeter observations.

5. ON THE INTERANNUAL VARIABILITY OF THE TEHUANTEPEC EDDIES

5.1 Abstract

TOPEX/Poseidon observations and the Naval Research Laboratory Layered Ocean Model are used to study the evolution of the oceanic eddies that are generated in the Gulf of Tehuantepec. The results reported in this section suggest that: (i) Outside of the equatorial region, the anticyclonic Tehuantepec eddies are the most energetic signal in the Eastern North Pacific Ocean. (ii) The interannual variability of the number and strength of the Tehuantepec eddies is directly related to El Niño-La Niña cycles. (iii) These eddies migrate ~5000 km, they weaken (decrease their maximum sea surface elevation) and disappear when they are exposed to the cyclonic shear between the North Equatorial Current and the North Equatorial Counter Current.

5.2 Introduction

It is well known that the position of the jet stream affects the day-to-day weather of North American cities. The geographical location of this jet is well correlated with the phases of the El Niño-La Niña cycle[3]. Normally, during El Niño

[3] By "El Niño (La Niña) phase" we mean a positive (negative) temperature's anomaly as shown in Figure 9.

(La Niña) phase the jet stream lies southward (northward) of its normal position (~45° N) (Figure 22), strengthening (weakening) the cold fronts that arrive at the Gulf of Mexico [Green et al., 1997; Smith et al., 1998]. Associated with the appearance of the cold fronts at the Gulf of Mexico is a high in the atmospheric pressure. This high, combined with the low atmospheric pressure in the Pacific Ocean, creates a pressure gradient that forces strong intermittent southward winds along the Isthmus of Tehuantepec during the boreal cold season (Figure 23a). Those winds reach the Pacific Ocean at the Gulf of Tehuantepec (Figures 4 and 23b) where they can have maximum gusts of 60 m/s [4] [Stumpf, 1975]. These winds, which mix the upper layers of the ocean and reduce the sea surface temperature (Figure 24), have been proposed as the physical mechanisms that generate anticyclonic oceanic eddies [Clarke, 1988; McCreary et al., 1989; Lavín et al., 1992]. Thus, the mechanism of generation of these eddies appears to be explained. However, their complete life cycle has not been reported yet.

In this section we use TOPEX/Poseidon sea surface height observations and the Naval Research Laboratory Layered Ocean Model to study the evolution of the Tehuantepec eddies. Special attention is given to life cycle, weakening and strengthening mechanisms, interannual variability and energetic characteristics.

[4] As a comparative example, hurricane Andrew was characterized by winds of 60-71 m/s during its landfall in Miami area in August 1992.

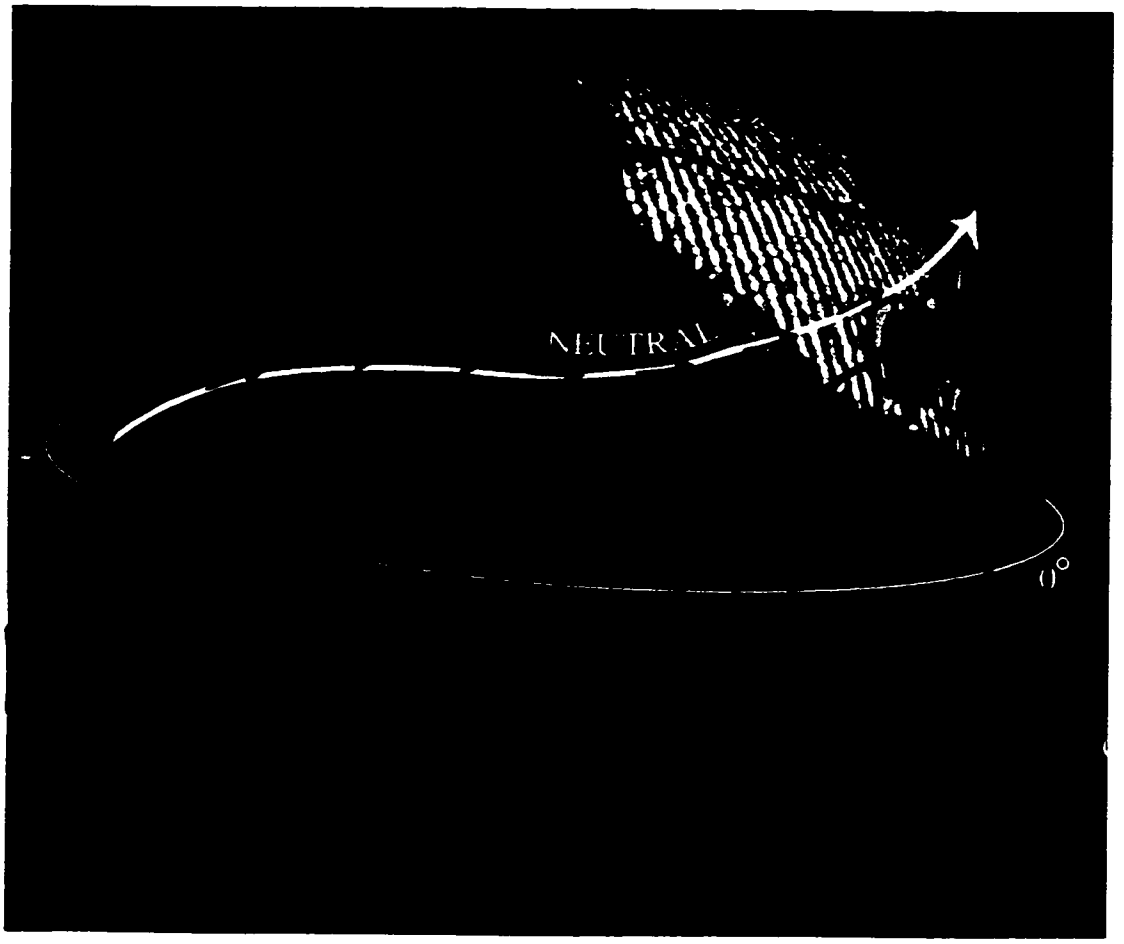

Figure 22. Conceptual portrayal of the jet stream's different positions during cold (blue), neutral (white) and warm (red) ENSO phases. After Green et al., [1997].

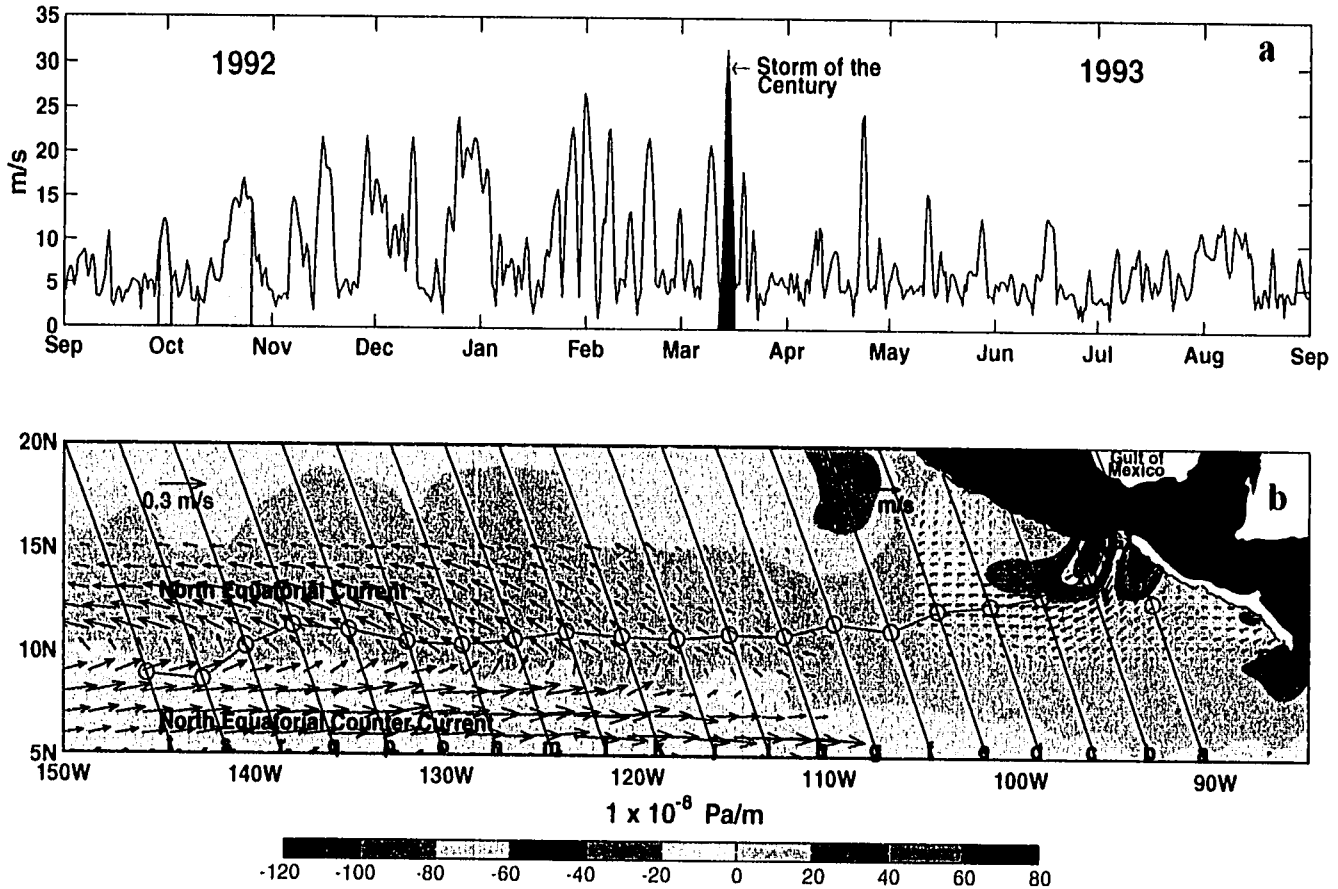

Figure 23. (a) Time series of European Center for Medium-Range Weather Forecasts (ECMWF) sea surface wind speed estimated at the center of the Gulf of Tehuantepec (GT). (b) Trajectory followed by an eddy generated at the GT as determined by the Topex/Poseidon (T/P) altimeter (magenta line). The yellow circles represent the position of the maximum altitude of the anticyclonic eddy shown in Figure 25. The white circle indicates the location of the minimum altitude of the cyclonic eddy shown in Figure 25a. Both eddies were generated during the wind event identified by the green shading in Figure 23a. The color contours (in 1 x 10^{-8} Pascals per meter) and the black arrows (in m/s) represent a 17 day average wind stress curl and wind field, respectively. Those 17 days (identified with yellow color in Figure 23a) are the period of time between the first and the second T/P measurement of the anticyclonic eddy. The red arrows represent the NLOM long term climatological mean ocean currents. Black lines identify the satellite tracks along which T/P detected the Tehuantepec eddies. The position of the Gulf of Papagayo (GP) is also indicated.

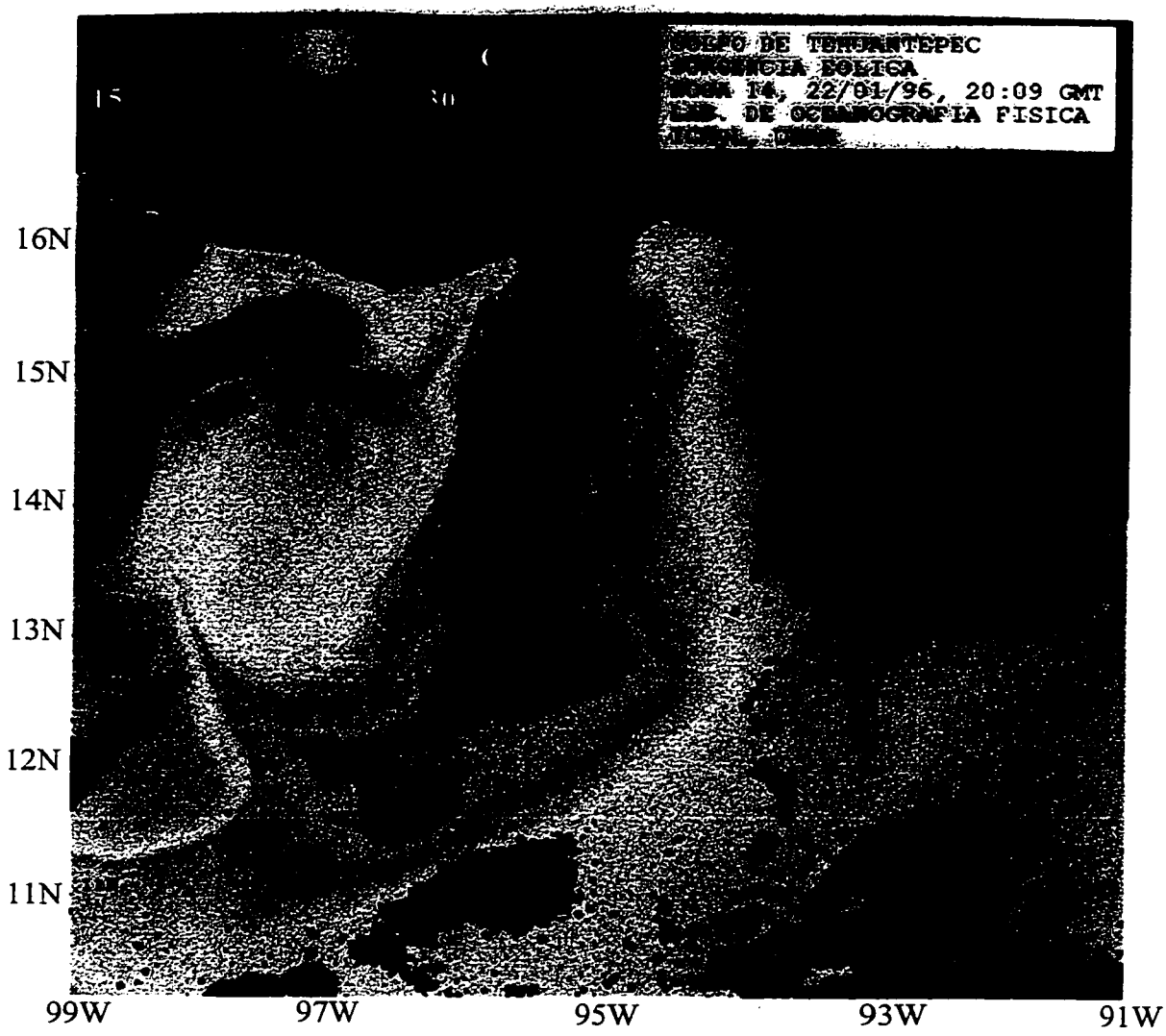

Figure 24. Sea surface temperature (in °C) for the Gulf of Tehuantepec for January 22, 1996. Note the strong zonal sea surface temperature gradient in the area and the coastal cold tongue of water from 96°W to 98°W characterized by yellow-green colors. Image processed by Agustin Fernandez (UNAM, Mexico).

5.3 Satellite observations

A peculiar characteristic of the warm-core Tehuantepec eddies is that they exist in a region where the surrounding water is also warm [Hansen and Maul, 1991]. However, during their formation and for a few days after that the eddies' thermal signature is clearly recognized in SST satellite images (Figure 24). This is possible thanks to the strong SST zonal gradient, which is created by the large SST reduction at the axes of the Gulf of Tehuantepec (GT) wind path. Nevertheless, the conditions at Figure 24 last just for a few days and after that the eddies' thermal signature is difficult to distinguish in SST images. Furthermore, thermal images are not able to track eddies for several months (the eddies' lifetime reported here is order 1 year) because the air-eddy interaction stimulates heat fluxes that eventually render the eddies undetectable in thermal images. In addition, the intrinsic cloud cover and persistent rain of this tropical area [Wents et al., 2000] make the eddy tracking difficult using passive satellite sensors. Thus, sea surface height (SSH) satellite altimeter observations are more useful for tracking eddies in that region of the ocean.

NASA Scatterometer (NSCAT) wind observations revealed several new attributes of the GT winds [Bourassa et al., 1999; Chelton et al., 2000a, 2000b]. Weak upwelling favorable winds were discovered to the west of the GT during the strong offshore wind events (Figure 4). The coastal upwelling favorable winds induce the transport of nutrient rich water to the surface (Figure 24). The anticyclonic eddies entrain some of this productive water into their domains. Thus, in addition to the physical intrigue of the problem by itself, it is interesting to study the evolution of the

Tehuantepec eddies for fisheries and the related biological processes [Blackburn, 1962; Robles-Jarero and Lara-Lara, 1993; Färber-Lorda et al., 1994].

5.4 The life cycle

The T/P satellite altimeter repeats an orbit every 10 days. It measures SSH every 6.2 km along satellite tracks (Figures 7 and 23). The distance between two continuous tracks is ~300 km in our area of study. This wide-track characteristic usually discourages the use of along track altimeter observations to track eddies. However, the large spatial extent of the Tehuantepec eddies, with horizontal dimensions of more than 300 km, and the high quality of T/P SSH measurements permits their use.

As soon as T/P altimeter became fully operational in October 1992 it detected the existence of the Tehuantepec eddies. The migration of an anticyclonic eddy generated by a wind event that occurred in the GT during the first week of October 1992 is documented in Figures 23b and 25. An initial southwestward drift and subsequent westward drift (which is mostly limited to 10°N–15°N) are some of the migration features in this example. Figure 25 includes T/P SSH measured along the tracks shown in Figure 23b. The dated along-track measurements represent the migration of a Tehuantepec anticyclonic eddy. This eddy migrated ~5000 km at an average speed of 17.5 cm/s during 335 days. It weakened (decreased its maximum sea surface elevation) and disappeared (Figures 25r-25t) when it crossed 10°N and was exposed to the cyclonic shear between the North Equatorial Current and the North

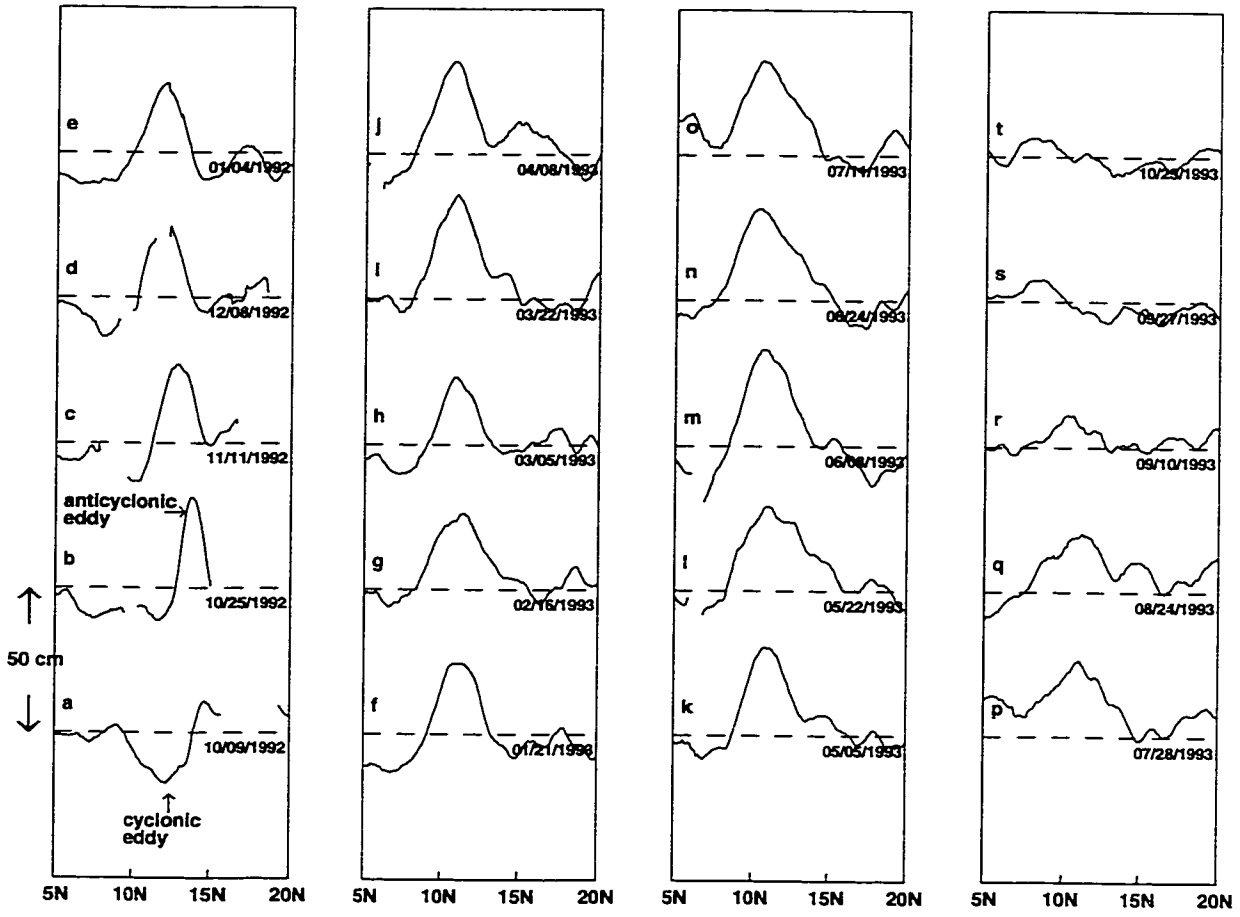

Figure 25. Sea surface height anomaly (in centimeters) measured by T/P along the different satellite tracks shown in Figure 22b. A southwestward migration of the anticyclonic eddy is evident in this example. The elevation and horizontal dimensions of this anticyclonic Tehuantepec eddy range from 21 to 36 cm and from 250 to 500 km, respectively. Note the presence of a cyclonic eddy in panel "a" (which is characterized by a SSH minimum of ~17 cm and a diameter of ~450 km) and how this eddy disappears in the rest of the panels.

Equatorial Counter Current (Figure 23b). The eddy strengthened when it was influenced by the negative GT wind stress curl (Figure 23b)[5]. Figures 23b and 25 document one example of a Tehuantepec eddy life cycle. The trajectory followed by this eddy as well as the eddy generated in the Gulf of Papagayo coincide with the areas of maximum SSH variability of the North Eastern Pacific Ocean (Figure 26). In addition to the examples shown in Figure 26, we have tracked several other Tehuantepec and Papagayo eddies, which were observed by the T/P during the period Oct 1992-April 2000. In general, the trajectory followed by those eddies and Figure 26 suggests that the Tehuantepec and Papagayo eddies are an important source of SSH variability on the North Eastern Pacific Ocean. Our observations agree with the results of Giese et al., [1995], who suggest that the eddies generated at the GT and the Gulf of Papagayo (Figure 26) are the source of a 50-60 day sea level variability out to 135° W, 11° N.

5.5 The strengthening and the weakening of the twin eddies

The NSCAT and the European Center for Medium-Range Weather Forecasts (ECMWF) wind fields [Bourassa et al., 1999; ECMWF, 1994] indicate the existence of atmospheric gyres at each side of the GT wind path (Figure 23b). Assuming that the Tehuantepec eddies are an oceanic response to the action of the strong winds, then we would expect oceanic gyres to form at each side of the wind path. Figures 25a and 25b

[5] NSCAT wind observations show that Tehuantepec winds affect an offshore region of at least 500 km [Figure 4, and Bourassa et al., 1999].

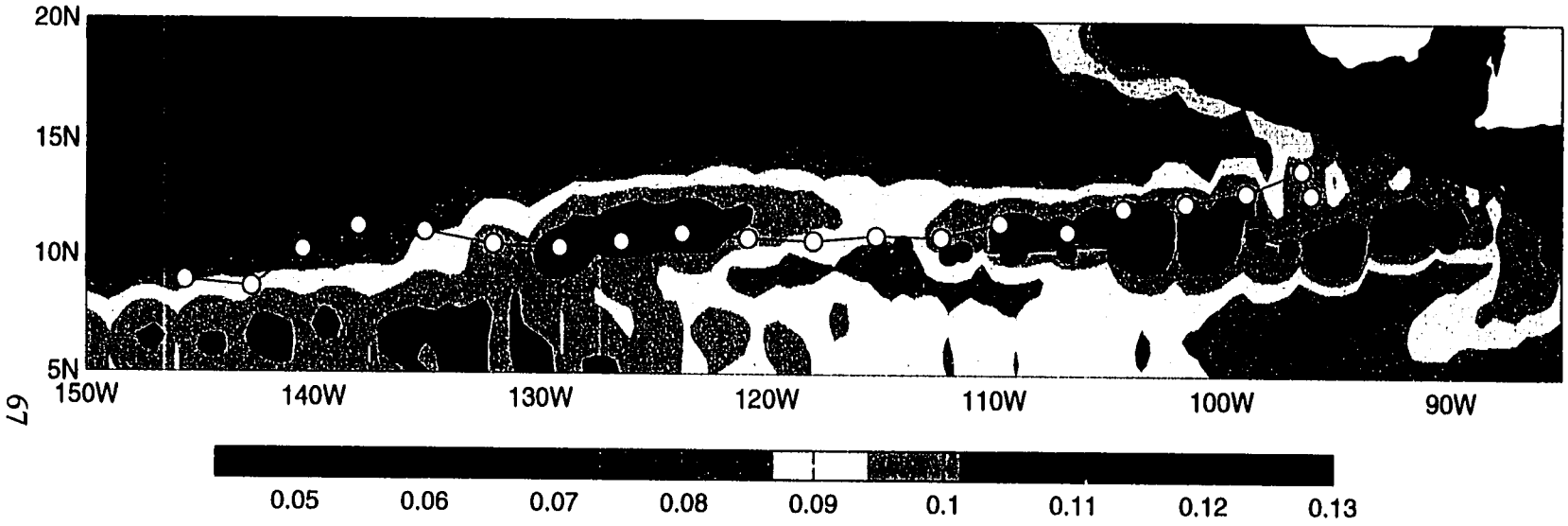

Figure 26. TOPEX/Poseidon (T/P) sea surface height standard deviation in meters for the period October 1992-April 2000. Note the location of the maximum standard deviation, which lies on the trajectory of the Tehuantpec (white circles) and Papagayo (green circles) eddies. This Tehuantepec eddy is the same as the one presented in Figures 23b and 25. The Papagayo eddy was measured by T/P during 1992-1993. The period of time between two white circles is indicated in Figure 25 and the one between two green circles is 10 days.

confirm this by showing an oceanic-twin-eddy, which is in concordance with the atmospheric-twin-gyre and reinforces the hypothesis that the Tehuantepec eddies are formed by the strong intermittent offshore GT winds [Clarke, 1988; McCreary et al., 1989; Lavín et al., 1992]. However, Figures 25a and 25b show the weakening of the cyclonic eddy. This behavior is partly due to the intermittence of the GT winds. After the first strong wind event (green shading in Figure 22a) the winds were relatively calm while the eddies migrated westward as indicated by the theory [Nof, 1981; Cushman-Roisin, 1986]. When the new GT wind event occurred in mid October 1992 (yellow shading in Figure 23a) the complete oceanic-twin-eddy had already migrated to the west side of the wind axis, and consequently was subjected to anticyclonic wind stress. Thus, both eddies received an anticyclonic wind stress spin injection, which reinforced the anticyclonic eddy and weakened the cyclonic one. This cyclonic eddy weakening mechanism complements the cool water entrainment mechanism that inhibits the development of the cyclonic eddies generated at the GT [McCreary et al., 1989; Trasviña et al., 1995]. The strengthening and weakening processes are summarized on the maps in Figure 27.

5.6 The interannual variability

The number of Tehuantepec eddies formed during a year depends on both the number and magnitude of the cold fronts arriving at the Gulf of Mexico. Hence, interannual variability is expected in eddy generation and strength. A multiyear space-time plot (Figure 28) shows T/P SSH positive anomaly signals radiating westward from the North America west coast during the northern hemisphere cold season.

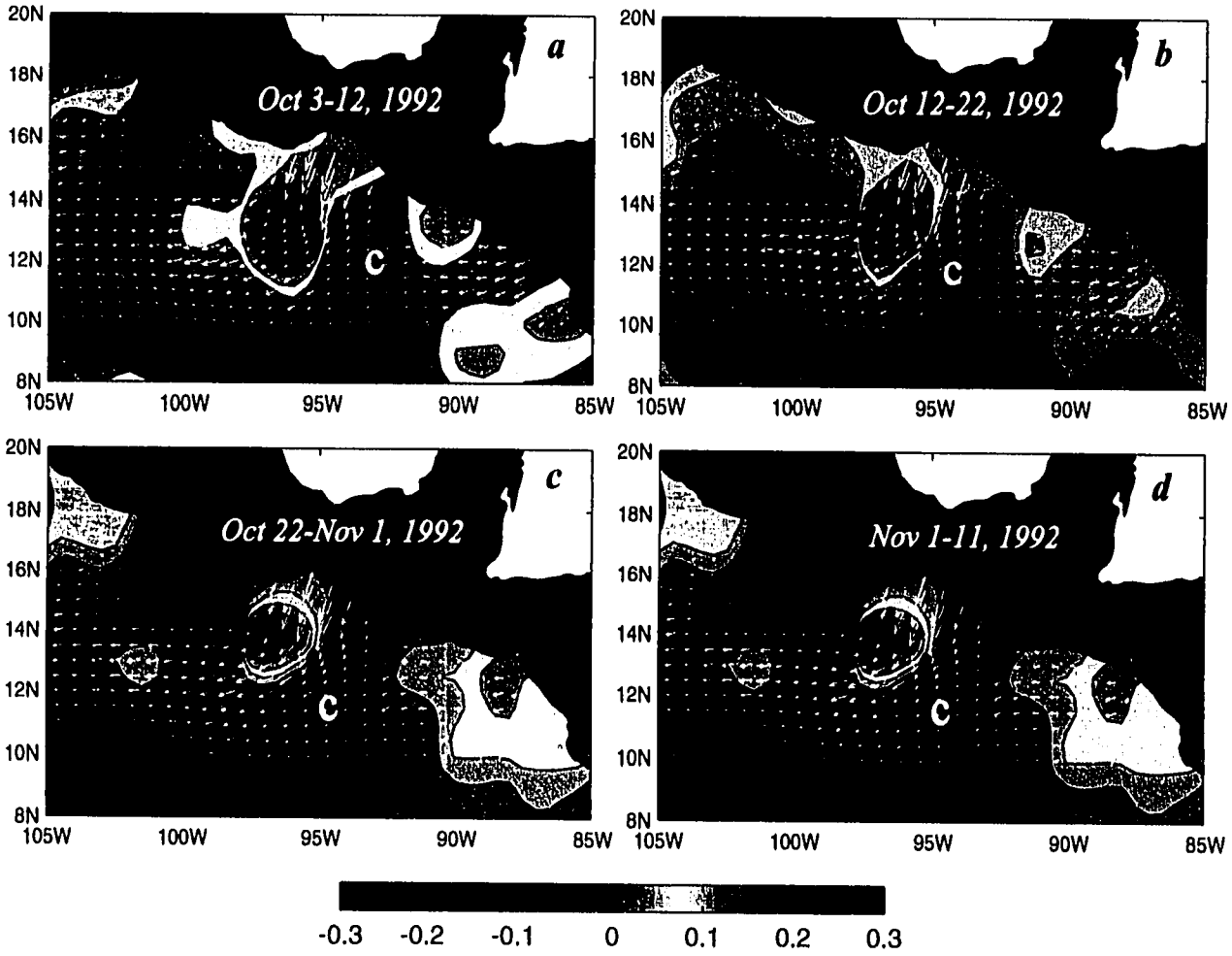

Figure 27. TOPEX/Poseidon sea surface height (SSH) anomaly (color contours in meters) for four different periods. The arrow vectors are the 17-day average ECMWF wind stress curl of Figure 23a. Note the westward drifting of the cyclonic eddy (minimum negative SSH anomaly identified with the letter "c") from panel (a) to panel (b) and how that eddy weakens (c) and disappears (d). In addition, the anticyclonic eddy (maximum positive SSH anomaly) is clearly recognized in the four panels.

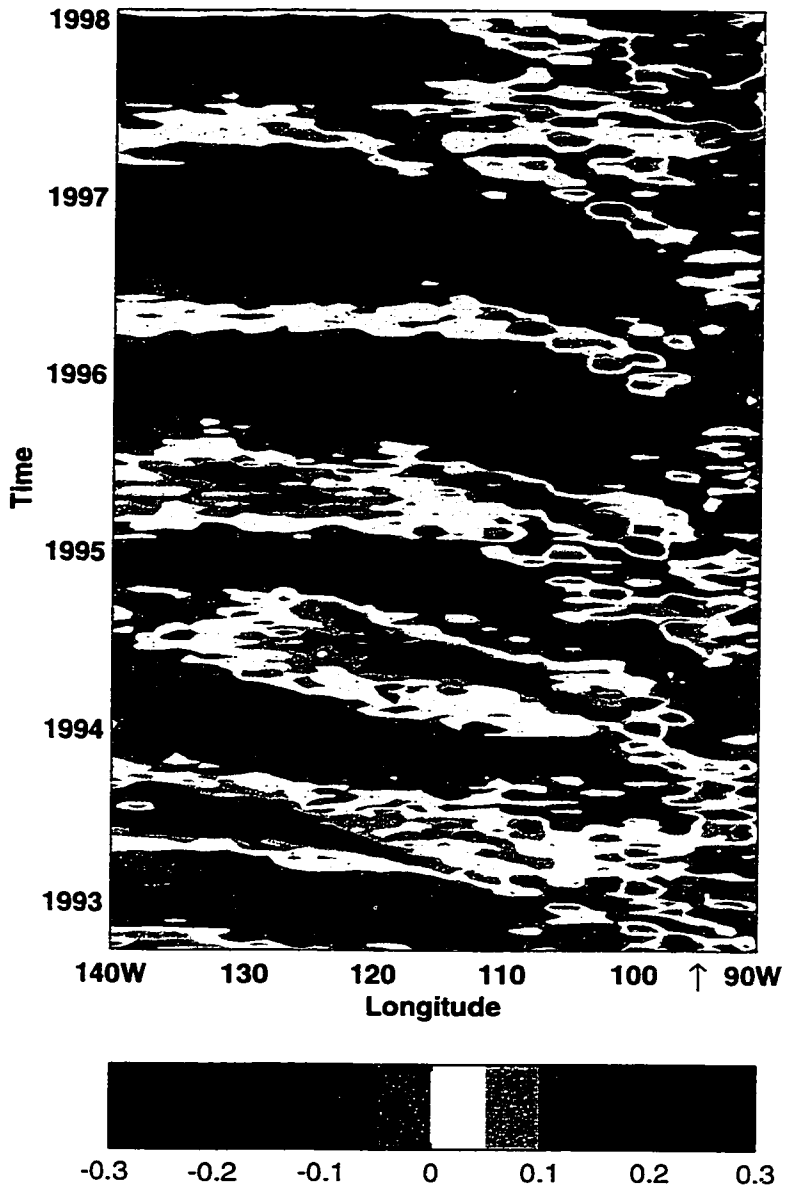

Figure 28. Longitude-time section of sea surface height anomaly (in meters) measured by T/P for the 10° N-15° N latitude band. The longitude of the center of the GT is indicated with a red arrow.

Analysis of the along track T/P observations and Figure 26 indicates that the anticyclonic eddies generated at the GT and the Gulf of Papagayo are the main sources of these positive SSH anomalies. Therefore, the westward propagating signals in Figure 28 are mainly due to the Tehuantepec and Papagayo anticyclonic eddies. The first three cold seasons, included in Figure 28, are characterized by strong positive SSH anomalies that propagate to ~140° W. The 1995-96 and 1996-97 winter seasons also include coastally generated anticyclonic eddies. Nevertheless, their SSH positive anomaly is not as strong as in the first three cold seasons.

To provide some insight about the Tehuantepec eddies interannual variability we constructed a T/P SSH anomaly time series for the period October 1992-April 2000 (Figure 29a). After the Tehuantepec eddies are generated, on the western side of the GT, they travel southwestward and are measured by T/P along the satellite track shown in Figure 29b. The anticyclonic Tehuantepec eddies are represented by the positive anomaly peaks in Figure 29a. Thus, we can recognize that during the first three cold seasons (1992-93, 1993-94, 1994-95) at least three anticyclonic Tehuantepec eddies were formed in each of them. The 1995-96 cold season was characterized by the formation of two anticyclonic Tehuantepec eddies. During the fall of 1996 no eddies were formed; however, during the 1996-97 winter season three eddies were formed. During the 1997-98 cold season at least seven anticyclonic Tehuantepec eddies were formed. Those eddies were characterized by the largest spatial dimensions. The 1998-99 cold season includes just one anticyclonic Tehuantepec eddy and the 1999-2000 cold season includes the formation of two anticyclonic Tehuantepec eddies.

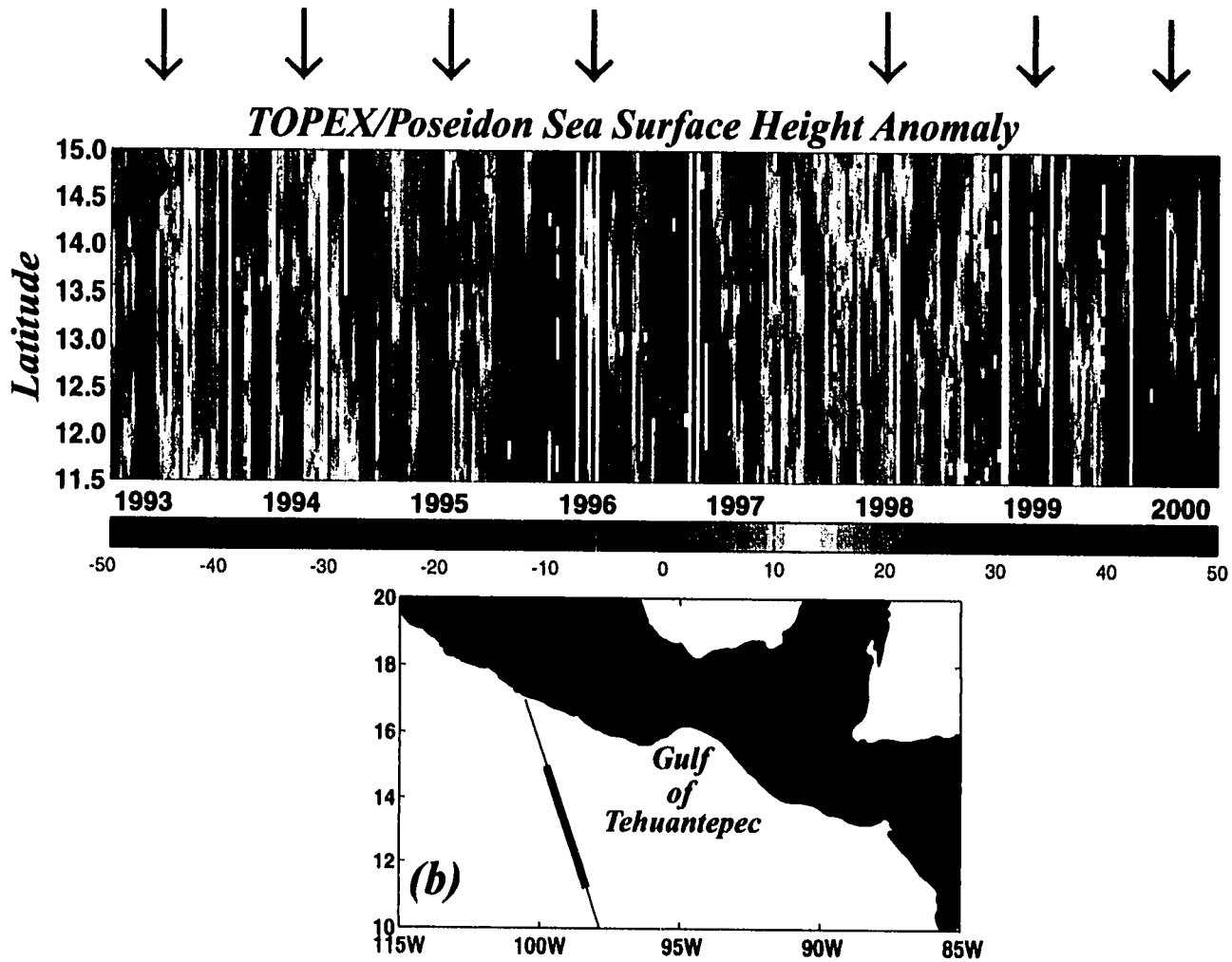

Figure 29. (a) TOPEX/Poseidon (T/P) sea surface height anomaly (in centimeters) time series measured along the red portion of the T/P satellite track shown in panel (b). The red (blue) arrows indicate positive (negative) sea surface temperature anomaly in the Japanese Meteorological Agency El Niño-La Niña index (Figure 9).

From Figures 28 and 29 we can recognize an interannual variability in the number and spatial dimensions of the anticyclonic Tehuantepec eddies. To understand this, it is important to remember that weak Tehuantepec eddies are caused by weak GT winds, which are associated with a weak atmospheric pressure gradient between the Gulf of Mexico and the Pacific Ocean and imply weaker than normal cold fronts arriving to the Gulf of Mexico. This is suggestive of an anomalously northern location of the jet stream and a possible La Niña phase. The JMA El Niño-La Niña index (Figure 9) and the SSH anomaly time series in Figures 28 and 29 indicate that the cold seasons characterized by the fewest and the smallest anticyclonic Tehuantepec eddies (1995-96, 1998-99, 1999-2000) occurred during the La Niña phase, whereas the cold seasons characterized by the largest (number and spatial dimensions) anticyclonic Tehuantepec eddies (1992-93, 1993-94, 1994-95, 1997-98) occurred during El Niño phase. This result is an interesting example of the existence of ocean-atmosphere teleconnections. The increase in the number of the Tehuantepec eddies suggests an increase in the number of the cold fronts arriving to the Gulf of Mexico, which suggests a change in the atmospheric pattern in mid-latitudes, which influences directly the tropical coastal waters of the Gulf of Tehuantepec.

5.7 The eddy train and the eddy kinetic energy

Satellite altimeter observations provide information about the behavior of the skin of the ocean. However, the Tehuantepec eddies' average depth is ~120 m [Barton et al., 1993]. Hence, satellite data need to be complemented with *in situ* hydrographic observations and/or numerical ocean model experiments. A numerical model permits exploration of time and space scales that are currently not possible observationally [Murphy et al., 1999], as well as the isolation of the physical mechanisms responsible for the genesis and evolution of the Tehuantepec eddies. Thus, we supplement the satellite observations with NLOM experiments described in section 2. Our premise is that the Tehuantepec eddies are a deterministic oceanic response to the atmospheric forcing. Then, it is expected that NLOM (which is forced only by ECMWF high frequency winds in this experiment) simulates the eddies detected by T/P. NLOM upper layer thickness and vector velocity snapshots are included in Figures 30a and 30b. The most striking features in these snapshots are the generation and migration of the Tehuantepec eddies. In the particular case of the eddy identified with the letter "A", it was generated by the wind event that occurred in the GT in early October 1992 (green shading in Figure 23a) and corresponds to the first eddy observed by T/P (Figures 23b and 25). Note the layer 1 thickness maximum of ~115 m at the core of the eddy and the eddy elongated shape while drifting inside of the area influenced by the wind (Figure 30a). In four months the eddy drifts more than 1000 km. As it drifts westward its shape becomes circular and its layer 1 thickness increases by ~15 m (Figure 30b).

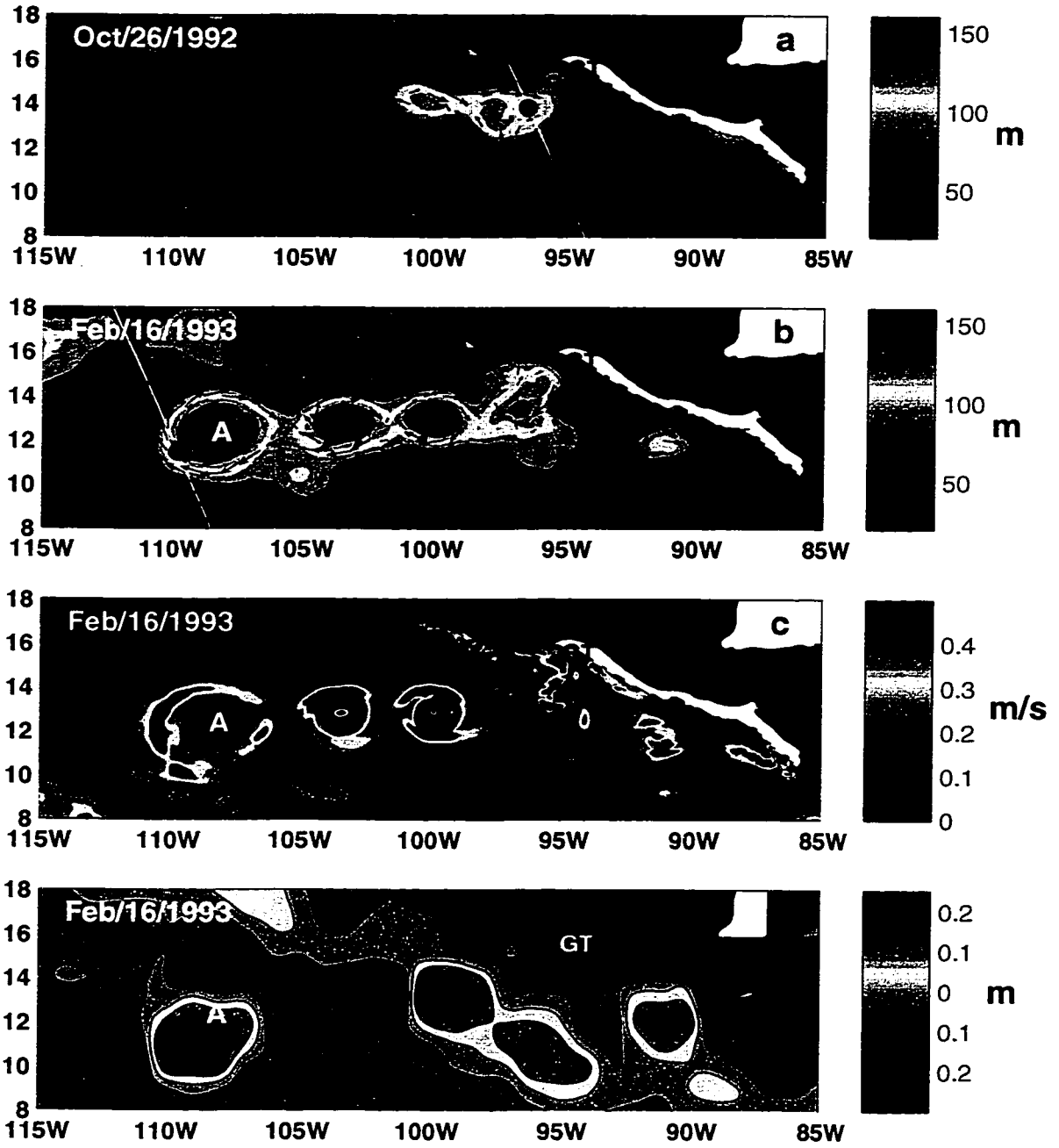

Figure 30. (a)-(b) NLOM snapshots of layer 1 thickness (in meters). T/P tracks are indicated with a white line and the green circles represent the location of maximum elevation of the anticyclonic eddy shown in the (b) and (g) panels of Figure 25. (c) Magnitude of the vectorial velocity difference of layer 1 minus layer 2 (color contours in m/s). (d) Sea surface height anomaly (color contours in meters) as determined by T/P.

If a new wind event develops after the eddies migrate out of the area influenced by the strong winds (Figure 23b), then a new eddy will be formed. Thus, it is common to observe the migration of a train of eddies emanating from the GT (Figures 30b-d). These eddies are characterized by a strong vertical velocity shear between the two uppermost layers of the ocean, which can easily reach values of 0.5 m/s (Figure 30c). The similarity of Figure 30c with a weather map that includes cyclones and anticyclones is not a pure coincidence: ocean eddies are the "storm systems" of the ocean [Robinson, 1983]. A qualitative comparison between model results (Figures 30b and 30c) and T/P observations (Figure 30d) indicates that the NLOM simulation includes most of the eddy characteristics observed by T/P (migration speed, location and spatial dimensions).

The high eddy kinetic energy (EKE) values of the eddies formed at the western boundary currents (e.g., Gulf Stream, Kuroshio, Agulhas) have received the attention of numerous oceanographic studies. Nevertheless, the EKE of the Tehuantepec eddies is comparable in magnitude to the EKE of the eddies at the western boundary currents (Figure 31). Certainly, the EKE signature associated with the Tehuantepec eddies dominates the EKE field along the North America West Coast.

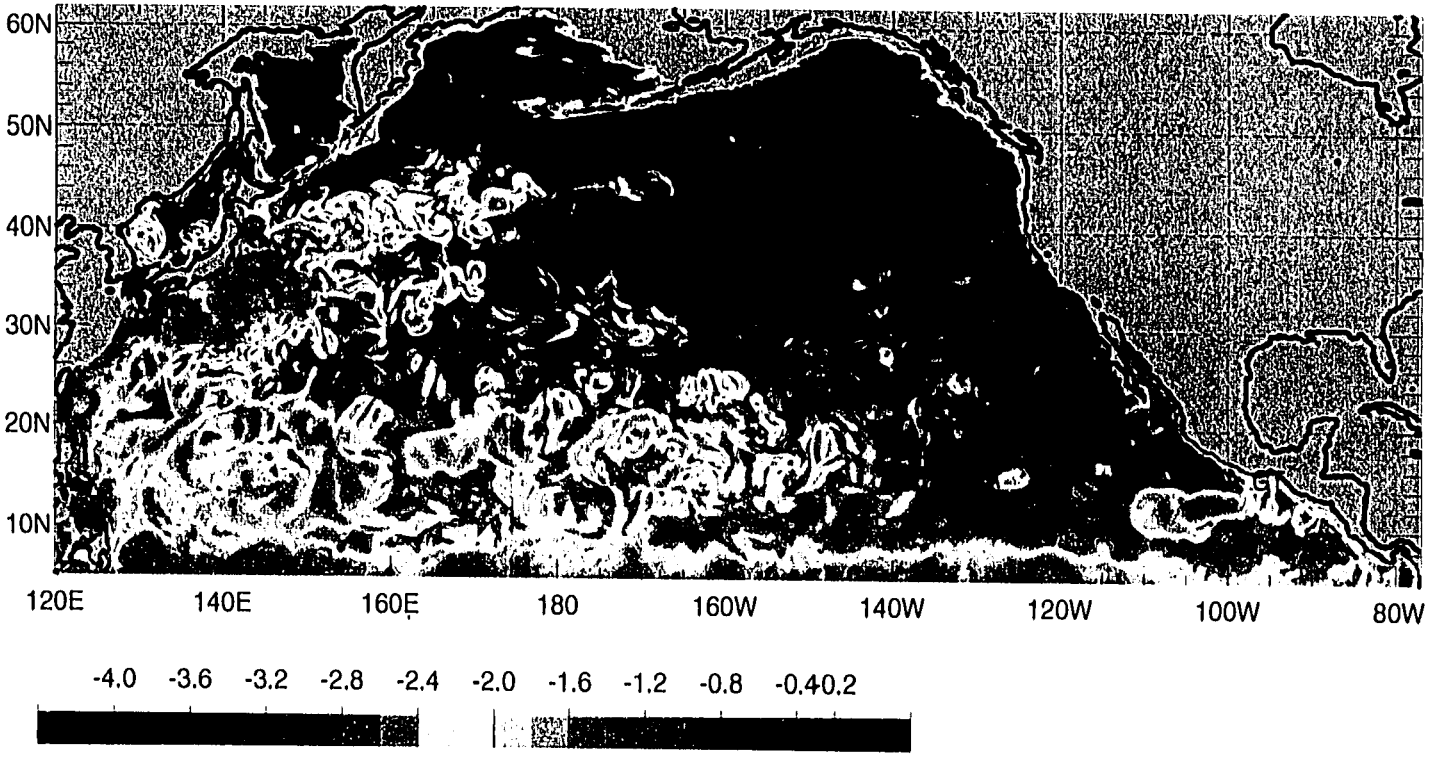

Figure 31. NLOM monthly mean eddy kinetic energy (in log (m^2/s^2)) for January 1993 for the shown region.

5.8 Summary and Conclusions

The Gulf of Tehuantepec strong and intermittent winds are responsible for the generation of long-lived and energetic eddies. This study represents the first time a Tehuantepec eddy has ever been tracked during its complete life cycle. This is also the first time the Tehuantepec eddies have been simulated using realistic high frequency variability winds. Analysis of their life cycle brings us to the following conclusions:

1. Satellite altimeter observations appear to be more useful than satellite temperature images to track the Tehuantepec eddies.

2. The Tehuantepec eddies are ~300 km of diameter with the ability to migrate for ~5000 km over ~1 year.

3. The cyclonic shear between the North Equatorial Current and the North Equatorial Counter Current appears to contribute to the weakening and disappearing of the anticyclonic Tehuantepec eddies.

4. The Gulf of Tehuantepec anticyclonic wind stress curl appears to contribute to the weakening of the cyclonic Tehuantpec eddies.

5. The strength and number of Tehuantepec eddies appears to be directly linked to the El Niño-La Niña cycle.

6. The Tehuantpec and Papagayo eddies appear to be an important source of SSH variability on the North Eastern Pacific.

7. The Tehuantpec eddies are the most energetic signal of the Northeast Pacific.

6. SUMMARY AND CONCLUDING REMARKS

Sea surface height altimetry observations and numerical ocean model simulations indicate that anticyclonic ocean eddies are an important source of mesoscale variability along the southwest coast of Mexico. Coastally trapped waves originating at the equator and strong intermittent winds originating from the arriving of cold fronts at the Gulf of Mexico are dominant physical mechanisms responsible for the eddies' formation (Figure 32). Three different eddy generation mechanisms are identified. First, the Acapulco eddies are due to baroclinic instabilities of a surface trapped narrow and elongated coastal jet. The appearance of the jet is due to the positive combination of the poleward flow along the southwest coast of Mexico and the poleward currents induced by strong warm ENSO events. Second, the eddies at Cabo Corrientes are due to the arriving of downwelling coastally trapped waves that intensify the northward-flowing local currents. The interaction of these intensified currents with the cape geometry generates anticyclonic eddies. A remarkable result of this section is how the model results concur in time and space with the existing hydrographic data and with the satellite observations. Third, the Gulf of Tehuantepec strong and intermittent winds generate anticyclonic eddies. For the first time ever a Tehuantepec eddy has been tracked during its complete life cycle. It has been possible due to the ability of the altimeter to observe sea surface height during all weather and

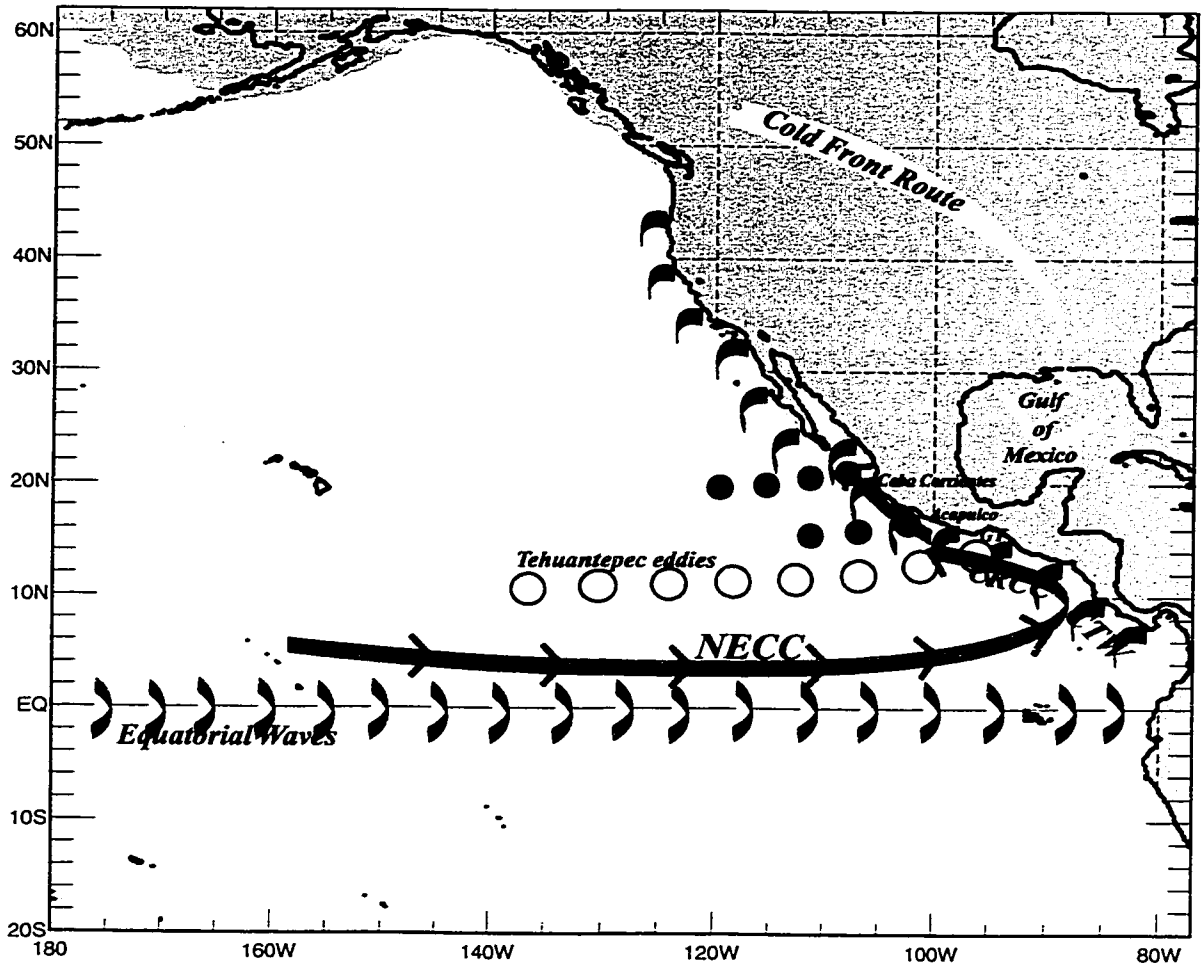

Figure 32. Conceptual portrayal including the equatorial return flow (the North Equatorial Counter Current (NECC) and the Costa Rica Coastal Current (CRCC)) and equatorially generated waves that travel eastward until the Americas west coast where they turn poleward and propagate as coastal trapped waves (CTW) passing by the southwest coast of Mexico. The positive combination of the CRCC and the currents generated by the CTW contributes to the formation of the Acapulco and Cabo Corrientes eddies (red circles), whereas the Tehuantepec eddies (yellow circles) are generated by the strong, intermittent, and offshore blowing Gulf of Tehuantepec (GT) winds, which appear after the arrival of cold fronts at the Gulf of Mexico.

all seasons. These eddies are characterized by a diameter of ~300 km, a life cycle of ~1 year, and a westward migration distance of ~5000 km. The eddy kinetic energy associated with the Tehuantepec eddies dominates the eddy kinetic energy field in the Eastern North Pacific. The interannual variability of the number and strength of the Tehuantepec eddies appears to be linked to the El Niño-La Niña cycle.

APPENDIX A

MODEL PARAMETERS AND NOTATION

Symbol Definition

$\bar{\nabla} = \hat{i}\frac{1}{a\cos(\theta)}\frac{\partial}{\partial\phi} + \hat{j}\frac{1}{a}\frac{\partial}{\partial\theta}$;

a radius of the Earth (6371 km);

A_H coefficient of isopycnal eddy viscosity;

C_b coefficient of bottom friction;

C_k coefficient of interfacial friction;

C_M coefficient of additional interfacial friction associated with entrainment;

$D(\phi,\theta)$ ocean depth at rest;

f coriolis parameter;

g acceleration due to gravity;

$G_{kl} = g \qquad l \geq k$;

$G_{kl} = g - g\left(\frac{\rho_k - \rho_l}{\rho_o}\right) \qquad l < k$;

h_k kth layer thickness;

h_k^+ kth layer thickness at which entrainment starts;

h_k^- kth layer thickness at which detrainment starts;

H_k kth layer thickness at rest;

$H_n = D(\phi,\theta) - \sum_{l=1}^{n-1} H_l$;

$\hat{i},\hat{j},\hat{k}$ unit vectors positive eastward, northward, and upward respectively;

t time;

$\vec{v}_k$ kth layer velocity;

$\vec{V}_k$ $h_k \vec{v}_k$;

θ latitude;

ϕ longitude;

ρ_k kth layer density (constant for space and time);

ρ_o reference density (constant);

$\vec{\tau}_w$ wind stress;

$\vec{\tau}_k = \vec{\tau}_w$ $k = 0$;

$\vec{\tau}_k = C_k \rho_o \left|\vec{v}_k - \vec{v}_{k+1}\right|\left(\vec{v}_k - \vec{v}_{k+1}\right)$ $k = 1...n-1$;

$\vec{\tau}_k = C_b \rho \left|\vec{v}_n\right| \vec{v}_n$ $k = n$;

$\omega_k = 0$ $k = 0, n$;

$\omega_k = \omega_k^+ - \omega_k^- - \Omega_k \hat{\omega}_k$ $k = 1...n-1$;

$$\omega_k^+ = \tilde{\omega}_k \left[\frac{\max\left(0, h_k^+ - h_k\right)}{h_k^+} \right]^2;$$

$$\omega_k^- = \tilde{\omega}_k \left[\frac{\max\left(0, h_k - h_k^-\right)}{h_k^+} \right]^2;$$

$$\hat{\omega}_k = \frac{\iint\left(\omega_k^+ - \omega_k^-\right)}{\iint \Omega_k};$$

$\tilde{\omega}_k$ kth interfase reference diapycnal mixing velocity

$\Omega_k(\phi,\theta)$ kth interface weighting factor for mass conservation

Parameter	Definition	Value
C_b	Coefficient of bottom friction	2×10^{-3}
C_d	Drag coefficient	1.5×10^{-3}
C_k	Coefficient of interfacial friction	0
g	Acceleration due to gravity	$9.8 m/s^2$
h_k^+	k-th layer thickness at which entrainment starts	50 m (k= 1,2) 40 m (k=3-6)
h_k^-	k-th layer thickness at which detrainment starts	Set to large and unreachable number

		(9999.0 m)
$\tilde{\omega}_k$	k-th interface reference vertical mixing velocity	0.04 m/s
TOPAMP	Bathymetry reduction factor	0.80
ρ_{air}	Sea-level air density	$1.2 kg / m^3$
ρ_k	Density of layer k (Sigma-T)	$23.95 kgm^{-3} (k = 1)$ $25.92 kgm^{-3} (k = 2)$ $26.83 kgm^{-3} (k = 3)$ $27.18 kgm^{-3} (k = 4)$ $27.39 kgm^{-3} (k = 5)$ $27.77 kgm^{-3} (k = 6)$
$\sum_{i=1}^{k} H_k$	Rest depth at base of layer k	135 m (k = 1) 320 m (k = 2) 550 m (k = 3) 800 m (k = 4) 1050 m (k = 5) 6500 m (k = 6)

REFERENCES

Badan-Dangon, A., J. M. Robles and J. García, Poleward flows off Mexico's Pacific Coast, in Poleward Flows Along Eastern Ocean Boundaries, edited by S. J. Neshyba, C. N. K. Mooers, R. L. Smith and R. T. Barber, pp. 176-201, Springer-Verlag, New York, 1989.

Badan-Dangon, A., Coastal Circulation from the Galápagos to the Gulf of California, in the SEA, The Global Coastal Ocean, Regional Studies and Syntheses, Volume 11, edited by A. R. Robinson and K. H. Brink, pp. 315-343, John Wiley & Sons, Inc., New York, 1998.

Barton, E. D., M. L. Argote, J. Brown, P. M. Kosro, M. Lavín, J. M. Robles, R. L. Smith, A. Trasviña, and H. S. Velez, Supersquirt: Dynamics of the Gulf of Tehuantepec, Mexico, Oceanography, 6, 23-30, 1993.

Blackburn, M., An oceanography study of the Gulf of Tehuantepec, Spec. Sci. Rep. Fish., 404, 28 pp., U.S. Fish and Wildlife Serv., Washington, D.C., 1962.

Bormans, M., and C. Garret, A simple criterion for gyre formation by the surface outflow from a strait, with application to the Alboran Sea, J. Geophys. Res., 94, 12,637-12,644, 1989.

Bourassa, M. A., L. Zamudio, and J. J. O'Brien, Noninertial flow in NSCAT observations of Tehuantepec winds, J. Geophys. Res., 104, 11,311-11,319, 1999.

Busalacchi, J. A., and J. J. O'Brien, Interanual Variability of the Equatorial Pacific in the 1960's, J. Geophys. Res., 86, 10,901-10,907, 1981.

Cane, M. A., and E. S. Sarachik, Forced baroclinic ocean motions. II. The linear equatorial bounded case, J. Mar. Res., 35, 395-432, 1977.

Cenedese, C., and J. A. Whitehead, Eddy Sheding from a Boundary Current around a Cape over a Sloping Bottom, J. Phys. Oceanogr., 30, 1514-1531, 2000.

Chelton, D. B., and R. E. Davis, Monthly mean sea level variability along the west coast of North America, J. Phys. Oceanogr., 12, 757-784, 1982.

Chelton, D. B., M. H. Freilich, and S. K. Esbensen, Satellite Observations of the Wind Jets off the Pacific Coast of Central America. Part I: Case Studies and Statistical Characteristics, Mon. Weather Rev., 128, 1993-2018, 2000.

Chelton, D. B. M. H. Freilich, and S. K. Esbensen, Satellite Observations of the Wind Jets off the Pacific Coast of Central America. Part II: Regional Relationships and Dynamical Considerations, Mon. Weather Rev., 128, 2019-2043, 2000.

Christensen, N., Jr., R. de la Paz, and G. Gutierrez, A study of sub-inertial waves off the west coast of Mexico, Deep-Sea Res., 30, 835-850, 1983.

Clarke, A. J. Inertial wind path and sea surface temperature patterns near the Gulf of Tehuantepec and Gulf of Papagayo, J. Geophys. Res., 93, 15,491-15,501, 1988.

Clarke, A. J. Low-Frequency Reflection from a Nonmeridional Eastern Ocean Boundary and the Use of Coastal Sea Level to Monitor Eastern Pacific Equatorial Kelvin Waves, J. Phys. Oceanogr., 22, 163-183, 1992.

Cushman-Roisin, B., Frontal geostrophic dynamics, J. Phys. Oceanogr., 16, 132-143, 1986.

D'Asaro, E. Generation of submesoscale vortices: A new mechanism, J. Geophys. Res., 93, 6685-6694, 1988.

Donohue, K. A., M. Wimbush, X. Zhu, S. M. Chiswell, R. Lukas, L. Miller, and H. E. Hurlburt, Five years' central Pacific sea level from in-situ array, satellite altimeter, and numerical model, Atmos.-Ocean, 32, 495-506, 1994.

Enfield, D. B., and J. S. Allen, The generation and propagation of sea level variability along the Pacific coast of Mexico, J Phys. Oceanogr., 13, 1012-1033, 1983.

Enfield, D. B., The intraseasonal oscillation in Eastern Pacific sea levels: How is it forced?, J. Phys. Oceanogr., 17, 1860-1876, 1987.

European Center for Medium-range Weather Forecasts (ECMWF), The description of the ECMWF/WCRP level III –A global atmospheric data archive, report, 72 pp., Reading, England, 1994.

Färber-Lorda, J., M. F. Lavín, M. A. Zapatero, J. M. Robles, Deep-Sea Res., Distribution and abundance of euphasiids in the Gulf of Tehuantepec during wind forcing, 41, 359-367, 1994.

Fiedler, P. C., Seasonal and interannual variability of coastal zone color scanner phytoplankton pigments and winds in the eastern tropical Pacific, J. Geophys. Res., 99, 18,371-18,384, 1994.

Giese, B. S., J. A. Carton, and L. J. Holl, Sea level variability in the eastern tropical Pacific as observed by TOPEX and Tropical Ocean-Global Atmosphere Tropical Atmosphere-Ocean Experiment, J. Geophys. Res., 99, 24,739-24,748, 1994.

Green, P. M., D. M. Legler, C. J. Miranda, and J. J. O'Brien, The North American Climate Patterns Associated with El Niño-Southern Oscillation, COAPS Project Report Series 97-1, Florida State University, Tallahassee, 10 pp., 1997.

Hansen, D. V., and G. A. Maul, Anticyclonic Current Rings in the Eastern Tropical Pacific Ocean, J. Geophys. Res., 96, 6965-6979, 1991.

Hellerman, S. and M. Rosenstein, Normal monthly wind stress over the world ocean with error estimates, J. Phys. Oceanogr., 13, 1093-1104, 1983.

Hogan, P. J., H. E. Hurlburt, G. A. Jacobs, A. J. Wallcraft, W. J. Teague, and J. L. Pringle, Simulation of GEOSAT, TOPEX/Poseidon, and ERS-1 altimeter data from a 1/8° Pacific Ocean Model: Effects of space-time resolution on mesoscale sea surface height variability, J. Mar. Technol. Soc., 26, 98-107, 1992.

Hughes, R. L., The hydraulics of local separation in a coastal current with application to the Kuroshio Meander, J. Phys. Oceanogr., 19, 1809-1820, 1989.

Hurd, W. E., Northers of the Gulf of Tehuantepec, Mon. Weather Rev., 57, 192-194, 1929.

Hurlburt, H. E., and J. D. Thompson, The dynamics of the Loop Current and shed eddies in a numerical model of the Gulf of Mexico, in Hydrodynamics of Semi-Enclosed Seas, edited by J. C. J. Nihoul, pp. 243-297, Elsevier Sci., New York, 1982.

Hurlburt, H. E., and J. D. Thompson, Preliminary results from a numerical study of the New England Seamount Chain influenced on the Gulf Stream, in Predictability of Fluid Motions, edited by G. Holloway and B. J. West, pp. 489-504, Am. Inst. of Phys., College Park, Md., 1984.

Hurlburt, H. E., A. J. Wallcraft, Z. Sirkes, and E. J. Metzger, Modeling of the Global and Pacific Oceans: On the path to eddy-resolving ocean prediction, Oceanography, 5, 9-18, 1992.

Hurlburt, H. E., P. J. Hogan, E. J. Metzger, W. J. Schmitz, and A. J. Wallcraft, Dynamics of the Kuroshio/Oyashio current system using eddy-resolving models of the North Pacific Ocean, J. Geophys. Res., 101, 941-976, 1996.

Hurlburt, H. E., and E. J. Metzger, Bifurcation of the Kuroshio Extension at the Shatsky Rise, J. Geophys. Res., 103, 7549-7566, 1998.

Jacobs, G. A., H. E. Hurlburt, J. C. Kindle, E. J. Metzger, J. L. Mitchell, W. J. Teague, and A. J. Wallcraft, Decade-Scale trans-Pacific propagation and warming effects of an El Niño anomaly, Nature, 370, 360-363, 1994.

Japanese Meteorological Agency, Climate charts of sea surface temperatures of the western North Pacific and the Global Ocean. Japan Meteorological Agency Marine Division, 51 pp., 1991.

Kindle, J. C., and P. A. Phoebus, The ocean response to operational westerly wind burts during the 1991-1992 El Niño, J. Geophys. Res., 100, 4893-4920, 1995.

Klinger, B., Gyre formation at a corner by rotating barotropic coastal flows along a slope, Dyn. Atmos. Oceans, 19, 27-64, 1993.

Klinger, B., Baroclinic eddy generation at a sharp corner in a rotating system, J. Geophys. Res., 99, 12,515-12,531, 1994a.

Klinger, B., Inviscid current separation from rounded capes, J. Phys. Oceanogr., 24, 1805-1811, 1994b.

Kundu, P. K., Fluid Mechanics, 638 pp., Academic Press, Orlando, Florida, 1990.

Lavín, M. F., J. M. Robles, M. L. Argote, E. D. Barton, R. Smith, J. Brown, M. Kosro, A. Trasviña, H. S. Vélez Muñoz, and J. García, Física del Golfo de Tehuantepec, Cienc. Desarrollo XVIII, 103, 97-108, 1992.

Leonardi, A. P., H. E. Hurlburt, E. J. Metzger, and J. J. O'Brien, Dynamics of the North Hawaiian Ridge Current, submitted to J. Phys. Oceanogr., 1999.

Levitus, S., Climatological atlas of the World Ocean, NOAA Professional Paper-13, 173 pp., U.S. Govt. Print. Off., Washington, D. C., 1982.

McCreary, J. P. Jr., H. S. Lee, and D. B. Enfield, The response of the coastal ocean to strong offshore winds: With application to the Gulfs of Tehuantepec and Papagayo, J. Mar. Res., 47, 81-109, 1989.

McWilliams, J. C., and G. R. Flierl, On the evolution of isolated nonlinear vortices, J. Phys. Oceanogr., 9, 1155-1182.

Melsom, A., S. D. Meyers, H. E. Hurlburt, E. J. Metzger, and J. J. O'Brien, ENSO effects on Gulf of Alaska eddies. Earth Inter., 3, pap. 001 (Available at http://EarthInteractions.org), 1999.

Merrifield, M. A., and C. D. Winant, Shelf Circulation in the Gulf of California: a description of the variability, J. Geophys. Res., 94, 18,133-18,160, 1989.

Merrifield, M. A., A comparison of long coastal-trapped wave theory with remote-storm-generated wave events in the Gulf of California, J. Phys. Oceanogr., 22, 5-18, 1992.

Metzger, E. J., H. E. Hurlburt, G. A. Jacobs, and J. C. Kindle, Hindcasting Wind-Driven Anomalies Using Reduced-Gravity Global Ocean Models with 1/2° and 1/4° Resolution, NRL Tech. Rep. 9444, 21 pp., Naval Research Laboratory, Stennis Space Center, Miss., 1994.

Metzger, E. J., and H. E. Hurlburt, Coupled dynamics of the South China Sea, the Sulu Sea and the Pacific Ocean, J. Geophys. Res., 101, 12,331-12,352, 1996.

Mitchell, J. L., W. J. Teague, G. A. Jacobs, and H. E. Hurlburt, Kuroshio Extension dynamics from satellite altimetry and a model simulation, J. Geophys. Res., 101, 1045-1058, 1996.

Mitchum, G. T., The source of 90-day oscillations at wake Island, J. Geophys. Res., 100, 2459-2475, 1995.

Moore, D. W., Planetary-gravity waves in an equatorial ocean, Ph.D. dissertation, 201 pp., Harvard University, 1968.

Murphy, S. J., H. E. Hurlburt, and J. J. O'Brien, The connectivity of eddy variability in the Caribbean Sea, the Gulf of Mexico, and the Atlantic Ocean, J. Geophys. Res., 104, 1431-1453, 1999.

NOAA, ETOPO5 digital relief of the surface of the earth, National Geophysical Data Center, Washington, D. C., Data Announcement 86-MGG-07, 1986.

Nof, D., On the β-induced movement of isolated baroclinic eddies, J. Phys. Oceanogr., 11, 1662-1672, 1981.

Pichevin, T., and D. Nof, The eddy cannon, Deep-Sea Res., 43, 1475-1507, 1996.

Pichevin, T., D. Nof, and J. Lutjeharms, Why are there Agulhas rings?, J. Phys. Oceanogr., 29, 693-707, 1999.

Ramp, S. R., J. L. McClean, C. A. Collins, A. J. Semtner, and K. A. S. Hays, Observations and Modeling of the 1991-1992 El Niño signal off Central California, J. Geophys. Res., 102, 5553-5582, 1997.

Ripa, P., Ondas y Dinámica Oceánica, in Contribuciones a la Oceanografía Física en México, edited by M. F. Lavín, pp. 75-98, Unión Geofísica Mexicana (Monografía No. 3), Ensenada, B. C., México, 1997.

Ripa, P., and A. C. Carrasco, Ray Theory and Scattering of Topographic Rossby Waves by an Abrupt Change of Shelf Width and Coastline, J. Geophys. Res., 98, 22,693-22,705, 1993.

Robinson, A. R. (Ed.), Eddies in Marine Science, 609 pp., Springer-Verlag, Berlin, 1983.

Robles-Jarero, E. G., and J. R. Lara-Lara, Phytoplankton biomass and primary productivity by size classes in the Gulf of Tehuantepec, Mexico, J. Plankton Res., 15, 1341-1358, 1993.

Roden, G. I., On the wind-driven circulation in the Gulf of Tehuantepec and its effect upon surface temperatures, Geofis. Int., 1, 55-72, 1961.

Røed, L. P., Curvature effects on hydraulically driven inertial boundary currents, J. Fluid Mechanics, 90, 395-412, 1980.

Shriver, J. F., and H. E. Hurlburt, The contribution of the global thermohaline circulation to the Pacific to the Indian Ocean throughflow via Indonesia, J. Geophys. Res., 102, 5491-5511, 1997.

Smith, S. R., P. M. Green, A. P. Leonardi, and J. J. O'Brien, Role of Multiple-Level Tropospheric Circulations in Forcing ENSO Winter Precipitation Anomalies, Mon. Weather Rev., 126, 3102-3116, 1998.

Spillane, M. C., D. B. Enfield and J. S. Allen, Intraseasonal Oscillations in Sea Level along the West Coast of the Americas, J. Phys. Oceanogr., 17, 313-325, 1987.

Stricherz, J. N., J. J. O'Brien and D. M. Legler, Atlas of Florida State University Tropical Pacific Winds for TOGA 1966-1985, Florida State University, Tallahassee, 275 pp., 1992.

Strub, P. T., P. M. Kosro, and A. Huyer, The Nature of the Cold Filaments in the California Current System, 96, 14,743-14,768, 1991.

Stumpf, H. G., Satellite detection of upwelling in the Gulf of Tehuantepec, Mexico, J. Phys. Oceanogr., 5, 383-388, 1975.

Stumpf, H. G., and R. V. Legeckis, Satellite observations of mesoscale eddy dynamics in the eastern tropical Pacific Ocean, J. Phys. Oceanogr., 7, 648-658, 1977.

Tilburg, C. E., Ocean Dynamics Around New Zealand, Ph. D. dissertation, 106 pp., Florida State University, 2000.

Trasviña, A., E. D. Barton, J. Brown, H. S. Velez, P. M. Kosro, and R. L. Smith, Offshore wind forcing in the Gulf of Tehuantepec, Mexico: The asymmetric circulation, J. Geophys. Res., 100, 20,649-20,663, 1995.

Trasviña, A., D. L. Cota, A. E. Filonov, and A. Gallegos, Oceanografía y El Niño, in Los Impactos de El Niño en México, edited by V. O. Magaña, pp. 69-101, UNAM, México, 1999.

Wentz, F. J., C. Gentemann, D. Smith, and D. Chelton, Satellite measurements of sea surface temperature through clouds, Science, 288, 847-850, 2000.

Wallcraft, A. J., The Navy Layered Ocean Models users guide, NOARL Rep. 35, 21 pp., Nav. Res. Lab., Stennis Space Center, Miss., 1991.

Wyrtki, K., Oceanography of the eastern equatorial Pacific Ocean. Mar. Biol. Annu. Rev., 4, 33-68, 1966.

Zamudio, L., A. P. Leonardi, S. D. Meyers, and J. J. O'Brien, ENSO and Eddies on the Southwest Coast of Mexico, Geophysical Res. Letters, 28, 13-16, 2001.

BIOGRAPHICAL SKETCH

Name: Luis-Fernando Zamudio-López.
Date of Birth: December 5, 1963.
Citizenship: Mexican.
Marital Status: Married.
E-mail: zamudi@coaps.fsu.edu

Degrees:

Centro de Investigación Científica y Educación Superior de Ensenada. (CICESE), **MS., Physical Oceanography**, 1992.
Thesis Title: "On the Effect of the Alongshore Pressure Gradient on a Coastal Circulation Model over the Continental Shelf" (In Spanish).

Autonomous University of Baja California, **BS., Oceanology**, 1987.
Thesis Title: "Evolution of Sediment Dispersion Using Ray Theory" (In Spanish).

Awards and Honors:

Fulbright, Graduate student scholarship 1995-98.
Autonomous University of Baja California, **Teaching award** 1994-95.
Centro de Investigación Científica y Educación Superior de Ensenada, **Graduate student scholarship** 1992.
CONACYT, Mexico, **Graduate student scholarship** 1989-91.
Autonomous University of Baja California, **Undergraduate student scholarship** 1985-87.

Professional Experience:

(a) Publications:

Refereed:

Zamudio, L., A. P. Leonardi, S. Meyers, and J. J. O'Brien, 2001: **ENSO and Eddies on the Southwest Coast of Mexico.** Geophysical Research Letters, 28, 13-16.

Zamudio, L., and J. J. O'Brien, 2000: **On the interannual variability of the Tehuantepec eddies.** Submitted to Science.

Bourassa, M. A., L. Zamudio, and J. J. O'Brien, 1999: **Noninertial flow in NSCAT observations of Tehuantepec winds.** J. Geophys. Res., 104, 11,311-11,319.

Zamudio, L. and M. López, 1994: **On the Effect of the Alongshore Pressure Gradient on Numerical Simulations over the Northern California Continental Shelf.** J. Geophys. Res., 99, 16,117-16,129.

Other publications: Zamudio, L. and J. J. O'Brien 2001: **Tropical Waves Induce Mesoscale Variability along the Southwest Coast of Mexico.** Research Activities in Atmospheric and Oceanic Modeling, H. Ritchie, Editor. Report (2001).

Zamudio, L., J. J. O'Brien, and B. Subrahmanyam, 2000: **Tracking Coastally Generated Eddies in the East Tropical Pacific.** Research Activities in Atmospheric and Oceanic Modeling, H. Ritchie, Editor. Report (2000).

Zamudio, L. and M. López, 1994: **On the Effect of the Alongshore Pressure Gradient on a Coastal Circulation Model over the Continental Shelf.** Geos, Bull. Mexican Geophysical Union. 11, 17-21. (In Spanish).

Zamudio, L. and M. López, 1991: **Modelling Wind-Driven Currents over the Continental Shelf.** Geos, Bull. Mexican Geophysical Union. 11, 14-17. (In Spanish).

Mejía, A., E. Pavía, E. García, J. García, L. Zamudio and S. Reyes, 1988: **Application of the Hurran Technique to Eastern Pacific Ocean.** Technical Report OC8802, CICESE.

Zamudio, L., and J. Ochoa, 1987: **Ray Theory Applied to Sediment Dispersion** (In Spanish). Memories of the VII National Oceanologic Congress, Ensenada, B. C.

(b) Meetings: AGU Fall Meeting, San Francisco, California, 2000.
Topic Title: **"On the interannual variability of the Tehuantepec eddies".**
Luis Zamudio and James J. O'Brien.

ENSO Colloquium, NCAR. 1997.

WOCE Pacific Workshop, California. 1996

Mexican Geophysical Union, Puerto Vallarta, Jalisco. 1993. Topic Title: **"On the Effect of the Alongshore Pressure Gradient on a Coastal Circulation Model over the Continental Shelf"** (In Spanish). Luis Zamudio and Manuel López.

Mexican Geophysical Union, Puerto Vallarta, Jalisco. 1991. Topic Title: **"Modelling Wind-Driven Currents over the Continental Shelf"** (In Spanish). Luis Zamudio and Manuel López.

VII National Oceanologic Congress, Ensenada, B. C. 1987. Topic Title: **"Ray Theory Applied to Sediment Dispersion"** (In Spanish). Luis Zamudio and José Ochoa.

(c) Teaching: 1991-1995 **Full time teaching position,** School of Marine Sciences, Autonomous University of Baja California, Mexico. **BS level courses in:** Mathematics, Calculus, Differential Equations, Vector Analysis, Oceanography Data Processing, Mathematical Methods, Fluid Mechanics, and Dynamical Oceanography.

1994-1995 **Head of the Mathematics Department**, School of Marine Sciences, University of Baja California, Mexico.

(d) Oceanographic Campaign: Participation aboard "EL PUMA" ship in the CICESE-8511 Oceanographic Campaign in the Gulf of California.